



Sfax University
Faculty of Sciences of Sfax
Stability and Control Systems
and Non Linear PDE Laboratory



Paul Sabatier University
Mathematics Institute of Toulouse
UMR 5219 IMT

Doctorate Thesis in Mathematics

(COTUTELLE)

by

Ameni GARGOURI

**On the perturbations theory of the Duffing oscillator
in a complex domain**

Defended on December 10, 2015

Committee

Pr. Mokhless HAMMAMI	Sfax University	Chairman
Pr. Smaïl DJEBALI	E. N. S-Kouba-Algiers University	Referee
Pr. Jean-Pierre FRANÇOISE	P. M. Curie, Paris 6 University	Referee
Pr. Lubomir GAVRILOV	Paul Sabatier University-ToulouseIII	Supervisor
Pr. Mohamed Ali HAMMAMI	Sfax University	Supervisor
Pr. Bassem BEN HAMED	Sfax University	Member
Pr. Martine KLUGHERTZ	Paul Sabatier University-ToulouseIII	Member

Academic year 2015/2016

Dedication

I dedicate this dissertation work to my family and my friends

My dear husband, for his support and his love during this accomplishment of this thesis.

My beloved children, for their inspiration that gave me courage, strength and hope during this thesis.

My parents father and mother, for their generosity and their deepness patience and for all the sacrifices that made for me.

My brothers and their wives, and my sisters for their endless love and their affection.

My special thanks to my uncle "Abdelwaheb" and his wife "Najia" for their support and tenderness.

My cousins for their moral support and their love.

Finally, for all my friends and colleague who shared with me all the good souvenirs.

Ameni

Ameni Gargouri

Acknowledgement

I express my deep gratitude and my sincere thanks to my supervisors Professor **Lubomir Gavrilov**, from Paul Sabatier University of Toulouse III, and my Professor **Mohamed Ali Hammami**, from Sfax University and special thanks to Professor **Bassem Ben Hamed**, from Sfax University as my Co-supervisor.

I appreciate them for their patience, their valuable advices and their availability through the preparation of this thesis in according their confidence with giving me a such precious subject.

All my respect and appreciation to Professor **Martine Klughertz**, from Paul Sabatier University of Toulouse III, Professor **Smaïl Djebali**, from E. N. S - Kouba - Algiers University and Professor **Jean-Pierre Françoise**, from P. M. Curie, Paris 6 University for their agreeing to be the referees of my thesis and their suggestions and comments that led to significant improvement in the thesis. I specially thank Professor **Martine Klughertz** for their presence during the realization of my thesis.

I appreciate Professor **Mokless Hammami**, from Sfax University, for agreeing to judge my work with the jury as a chairman.

I would like to express my gratitude to all the members of the research unit of Stability and Control Systems and Non Linear PDE laboratory, and mathematics laboratory Emile Picard for their sympathy. They made those three years very enjoyable.

I also would like to express my deep thanks to all my Professors of the Faculty of Sciences of Sfax who provided the knowledge that allowed me to achieve at this stage.

Ameni Gargouri

Contents

Dedication	1
Acknowledgement	3
List of Figures	7
Introduction	9
1 Qualitative theory of dynamical systems in the plane	15
1.1 Saddles, Nodes, Foci and Centers	15
1.1.1 Linear Systems in \mathbb{R}^2	15
1.1.2 Nonlinear Systems	19
1.1.3 Hamiltonian Systems	21
1.2 Dynamical Systems and Limit Cycles	23
1.2.1 Limit Set and Attractors	24
1.2.2 Periodic Orbits and Limit Cycles	26
1.2.3 The Poincaré Map	28
1.2.4 Melnikov's Functions	33
1.3 Principalization of the Bautin ideal	38
2 Special cubic perturbations of $\ddot{x} = x - x^3$	41
2.1 Generalities about the Duffing oscillator	41
2.2 Introduction	42
2.3 Picard-Fuchs equations	45
2.4 The monodromy of Abelian integrals	50
2.5 The zeros of the principal part of the displacement map in a complex domain .	52
2.6 The bifurcation diagram of the zeros of the Abelian integrals in a complex domain	54
2.6.1 The first Melnikov function M_1	54
2.6.2 The principal part M_k of the displacement map	56

3	General Cubic Perturbations of $\ddot{x} = x - x^3$	59
3.1	Introduction	59
3.2	Computation of Melnikov Functions	60
3.2.1	Computation of M_1	61
3.2.1.1	The interior Duffing oscillator	61
3.2.1.2	The exterior Duffing oscillator	63
3.2.2	Computation of M_2	63
3.2.2.1	The interior Duffing oscillator	64
3.2.2.2	The exterior Duffing oscillator	65
3.3	Picards-Fuchs equations	68
3.4	Zeros of Abelian integrals in a complex domain	68
3.4.1	The interior eight-loop case	69
3.4.1.1	The monodromy of Abelian integrals	69
3.4.1.2	Zeros of the first return map in a complex domain	70
3.4.2	The exterior eight-loop case	72
3.4.2.1	The monodromy of Abelian integrals	73
4	Study of the Duffing oscillator near a eight-loop	77
4.1	Introduction	77
4.2	The Petrov trick and the Dulac map	78
4.3	Cyclicity of eight-loop	80
4.3.1	The case $M_1 \neq 0$	83
4.3.2	The case $M_1 = 0$	84
4.4	Detecting alien limit cycles near a eight-loop	85
	Bibliography	89

List of Figures

1	A bifurcation generating a cycle.	14
2	A bifurcation killing a cycle.	14
1.1	A Saddle at the origin	16
1.2	A stable node at the origin	17
1.3	A stable focus at the origin	18
1.4	A center at the origin	19
1.5	The trajectory Γ of (1.3) which approaches a ω -limit point \mathbf{p}	25
1.6	A stable limit cycle Γ_0 which is an attractor of (1.6)	27
1.7	The Poincaré map	29
1.8	The Poincaré map for the system in example 1.2.18	30
1.9	The straight line Σ normal to Γ at 0	31
1.10	The straight line normal to γ_ϵ	35
1.11	Limit cycle of Van der Pol oscillator	37
2.1	The shape of $E(t)$ and schematic trajectories of the Duffing oscillator in the $(x, \dot{x}, E(t))$	42
2.2	Phase portrait of X_0 on the (x, y) -plane and the graph of $h = -\frac{x^2}{2} + \frac{x^4}{4}$	43
2.3	The vanishing cycles $\delta_0(h), \delta_1(h), \delta_{-1}(h)$ for $-\frac{1}{4} < h < 0$	50
2.4	The analytic continuation of a cycle $\gamma(h_0)$ in the domain \mathcal{D}	52
2.5	Bifurcation diagram of the zeros of the first Melnikov function M_1 in the complex domain \mathcal{D}	55
2.6	Bifurcation diagram of the zeros of $M_k, k \geq 2$, in the complex domain \mathcal{D}	56
3.1	Phase portrait of X_h where $-\frac{1}{4} < h < 0$; and the graph of $-\frac{x^2}{2} + \frac{x^4}{4}$	69
3.2	The analytic continuation of a cycle $\gamma(h)$ in the domain $\mathcal{D} = \mathbb{C} \setminus [0, +\infty)$	70
3.3	The analytic continuation of a cycle $\gamma(h)$ in the domain $\mathcal{D} = \mathbb{C} \setminus [0, -\infty)$	74
4.1	Monodromic eight-loop and the Dulac map d_ϵ^\pm	79
4.2	The domain \mathcal{D}_ϵ	79
4.3	Non symmetric perturbation of the eight-loop.	87

4.4 Bifurcation diagram of the first Melnikov function, containing an eight-loop.
The domain 14 has two limit cycles. 88

Introduction

This thesis focuses on the qualitative or geometrical theory of nonlinear systems of differential equations originated by Henri Poincaré in his work on differential equations at the end of the nineteenth century as well as on the functional properties inherent in the solution set of a system of nonlinear differential equations embodied in the more recent concept of a dynamical system .

The phenomenon of limit cycles was first discovered and studied by Poincaré [47] who presented the breakthrough qualitative theory of differential equations, and denotes an isolated periodic orbit.

Limit cycles are a common phenomenon, existing in almost all disciplines of science and engineering, including applied mathematics, physics, chemistry, mechanics, electrical circuits, control systems, economics, financial systems, ecological systems, etc. In fact, most early history in the theory of limit cycles was stimulated by practical problems displaying periodic behavior. Limit cycles are generated through bifurcations in many different ways, though mainly via Hopf bifurcation from a center or a focus, Poincaré bifurcation from closed orbits, or separatrix cycle bifurcation from homoclinic or heteroclinic orbits, especially for our part the limit cycles are generated through the bifurcations from the separatrix eight-loop. Computing limit cycles and determining their stability is not only theoretically significant, but also practically important.

Related to limit cycle theory, the well-known 23 mathematical problems proposed by Hilbert in 1900 [30], have had a significant impact on mathematics in the 20th century. Two of the 23 problems remain unsolved, one of which is the 16th problem. This problem has two parts: the first is about the relative positions of separate branches of algebraic curves, and the second is about the upper bound of the number of limit cycles and their relative locations in polynomial vector fields.

A general result concerning these configurations was obtained in [42]. To day, " Hilbert's 16th problem" usually refers to the second part. Many, many studies have been made of this problem, especially for quadratic and cubic systems; see [2, 14, 13].

Although the problem is still far from being completely solved, research on it has made great progress with significant contributions to the development of modern mathematics.

To state Hilbert's 16th problem more precisely, consider the planar vector field, described by the polynomial differential equations

$$\begin{cases} \dot{x} = P_n(x, y) \\ \dot{y} = Q_n(x, y) \end{cases}, \quad (1)$$

where $P_n(x, y)$ and $Q_n(x, y)$ denote n th-degree polynomials in x and y . The second part of Hilbert's 16th problem is to find the upper bound on the number of limit cycles that the system can have, which is denoted by $H(n)$, known as the Hilbert number. In general, this is a very difficult problem, and it is not known whether $H(n)$ is finite. Of course, $H(1) = 0$, but the finiteness of $H(n)$ with $n \geq 2$ is still an open problem. Although it has not been possible to obtain a uniform upper bound for $H(n)$, a great deal of effort has been made in finding the maximal number of limit cycles and raising the lower bound of the Hilbert number, $H(n)$, for general planar polynomial systems or for some specific system of a certain degree, hoping to be close to the real upper bound of $H(n)$.

In 1980, after two famous counter-examples of H.Dulac (any polynomial system has a finite number of limit cycles) and Petrovskii-Landis (any quadratic system has at most three limit cycles), it was observed the quasi-absence progress in the 16th Hilbert problem.

Dulac theorem has finally been proved independently by Yu.I.Lyashenko en Russie and by J.Ecalle en France.

In Spite of this the problem is very far from being resolved even in the simplest case , $n = 2$.

One direction of research on Hilbert 's 16th problem is to study the weakened Hilbert 16th problem, introduced by Arnold [1].

The weakened problem is also called the infinitesimal Hilbert 16th problem and it can be formulated as follows:

"Find an upper bound to the number of limit cycles of a polynomial vector field of degree n "

We refer to [29] for the detailed description of the weak Hilbert 16th problem .

In perturbation from a period annulus, limit cycles can be created from the exterior, boundary or from the interior.

INTRODUCTION

In any case, all limit cycles under consideration coincide with fixed points of the Poincaré return map which is an analytic function near any periodic orbit in the period annulus. The perturbation problem can be reduced to the perturbation from an analytic Hamiltonian system with Hamiltonian H :

$$X_\epsilon : \begin{cases} \dot{x} &= H_y + \epsilon P_n(x, y) \\ \dot{y} &= -H_x + \epsilon Q_n(x, y) \end{cases} \quad (2)$$

Using 1-forms the above system can be written as the equivalent Pfaffian equation $dH + \epsilon\omega = 0$ with $\omega = Q_n dx - P_n dy$.

So that the issue of finding the number of limit cycles is transformed into finding the roots of Abelian integrals or Melnikov functions:

$$M(h) = \int_{H=h} Q_n dx - P_n dy$$

Therefore in the literature it appears under different names: Pontryagin integral, Poincaré-Pontryagin integral, Melnikov integral.

The weakened Hilbert 16th problem with Abelian integrals and Melnikov functions will be discussed in more detail in the second and third parts of this thesis (see Chap. 2, 3).

Then, probably, the most basic tool for studying the stability and bifurcations of periodic orbits is the Poincaré map or first return map, defined by Henri Poincaré in 1881, see [43]. However, Melnikov's method which is presented in section 1.2.4 in this section gives us an excellent method for determining the number of limit cycles in a continuous band of cycles that are preserved under perturbation. In fact the number, positions, and multiplicities of perturbed planar differential equations for a small parameter $\epsilon \neq 0$ are determined by the number, positions, and multiplicities of the zeros of the generating functions. The Melnikov function is more precisely, called the first-order Melnikov function. If this function is identically equal zero across the continuous band of cycles, one computes the so-called "higher order Melnikov functions", and without more effort it is seen that properties 3.2.2 and 3.2.3 can be generalized in a straightforward way when the first-order Melnikov function is replaced by the first nonzero higher-order Melnikov function. Then a higher order analysis is necessary, which can be done by making use of the so called "the algorithm of Françoise", see [18] and the references given there.

However, the discussions and computation presented in this thesis are restricted not only to the first-order Melnikov function (see Chap. 2), but also to the second -order Melnikov functions (see Chap. 3).

As a part of Hilbert's 16th problem, many authors consider the least upper bound of the number of zeros of the abelian integrals associated with quadratic perturbations of quadratic Hamiltonian systems is almost finished, see [12, 21, 31, 38, 56] and their references.

In this case, Gavrilov in [21] proved that the number of zeroes is ≤ 2 (also around two foci).

In 1952, Bautin [5] proved that a quadratic planar polynomial vector field could have a maximum of 3 small limit cycles. Later, around the end of the 1970s, concrete examples were constructed to show the existence of 4 limit cycles [11, 49], i.e., $H(2) \geq 4$. In the past few years, great progress has been achieved in obtaining better estimates of the lower bounds of $H(n)$ for $n \geq 3$: $H(3) \geq 13$ [41], $H(4) \geq 20$ [28], $H(5) \geq 25$ [55], $H(6) \geq 35$ [52], $H(7) \geq 49$ [39], $H(9) \geq 80$ [54], and $H(11) \geq 121$ [53].

Most mathematicians working in the same problem for quadratic integrable but non-Hamiltonian systems, especially with two centers, may give the richest dynamical behavior, see [4] for instance. The exact upper bound of the number of limit cycle, the configurations of limit cycles, and the bifurcations diagrams for different range of parameter are given in [15].

The next natural step is to consider the same problem of Hilbert, precisely, for the symmetric planar polynomial Hamiltonian systems. This problem is stated by V.I. Arnold in 1977 and it is not solved completely, but there are many nice results concerning it.

Firstly, A. N. Varchenko and A. G. Khovanski proved the finiteness of the maximal number of limit cycles for polynomial Hamiltonian vector field (i.e. they are not accumulated by limit cycles), however they don't give any formula for this number. The proof of Varchenko is based on the methods developed in the book [51], (asymptotic expansions of integrals along cycles in complex algebraic curves), and some finiteness results from real analytic geometry.

Concrete estimates are given with some restrictions on the Hamiltonian function.

- The general results about finiteness of that number are due to Khovansky [36] and Varchenko [50].

Petrov in [44] considered the case of the elliptic cubic Hamiltonian: $y^2 + x^3 - x$ and proved that the number of zeros is ≤ 2

- In the case of a hyperelliptic Hamiltonian $y^2 + R(x)$ (with fixed polynomial R) Petrov [46] proved the linear estimate $\leq an + b$ for the number of zeroes of any form $Qdx - Pdy$ of degree n .

For our work, we study the families of symmetric elliptic Hamiltonians of degree four, presented in the second, third and four chapter. We will give a procedure to obtain more limit cycles for a perturbed polynomial Hamiltonian system of degree three by using the displacement function and Melnikov's functions .

INTRODUCTION

This tools will be useful to resolve the question proposed in the second, third and four chapter.

This thesis is organized into four chapters as follows:

In chapter1, we begin our study by constructing the various phase portraits of a dynamical linear and non linear systems. Next, we study limit sets and attractors of nonlinear systems case. The major part of this chapter discusses planar dynamical systems and the existence of limit cycles.

In general the cyclicity of the asymmetrically perturbed Duffing oscillator $x'' = x - x^3$ is a well known problem extensively studied in the literature.

In chapter 2, we are interested of the cyclicity of the exterior period annulus of the asymmetrically perturbed Duffing oscillator presented in the system (2.1), then, we provide a complete bifurcation diagram for the number of the zeros of the associated Melnikov function in a suitable complex domain (the argument principle) after the pioneering work by G. S. Petrov [45]. The so called Petrov trick has been used in a more general context in several papers which is based on the argument principle, e.g. [9, 8]. The result is summarized in theorem 2.6.2, and that the leading term of the displacement map is given by a function of the form 3.2 which completes the proof of theorem 2.2.2, see [40] for details. We give a geometric description of the monodromy group of $M(t)$, based on the classical Picard-Lefschetz theory is described in section 2.4 from which we deduce sufficient conditions for $M(t)$ to satisfy a differential equation of Picard- Fuchs type 2.3.

In chapter 3, we consider arbitrary one-parameter cubic deformations of the Duffing oscillator, take the functions $P_n(x, y, \epsilon)$ and $Q_n(x, y, \epsilon)$ in 2 which are polynomials in $x^i y^j$ and depend analytically on a small parameter ϵ , we prove in theorem 3.4.4 and 3.4.1 the maximal cyclicity of the interior and exterior eight loop especially for arbitrary cubic perturbations. In this chapter, we can first compute the first melnikov function M_1 in the interior and exterior cases, next, according to the Iliev formula [32] we can compute M_2 in the case when M_1 vanishes and by using Picard-Fuchs equations, see Proposition 3.2.2 and Proposition 3.2.3, after we study its zeros (see 3.4.2, 3.4.3, 3.4.6, 3.4.7) in a suitable complex domain in the same way of Iliev and Gavrilov in [27] for the four asymmetric Hamiltonian $H = \frac{1}{2}y^2 + \frac{1}{2}x^2 - \frac{1}{2}x^3 + \frac{a}{4}x^4$, $a \neq 0, \frac{8}{9}$.

In chapter 4, the goal is to determine the cyclicity of eight-loop, in the spirit of Gavrilov and Iliev [26].

It is well known in the first part as in the previous chapters that in a generic way, the study of the integral Abelian I is sufficient for a complete knowledge of the number of limit cycle and their bifurcations.

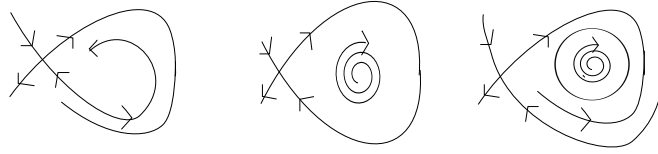


Figure 1: A bifurcation generating a cycle.

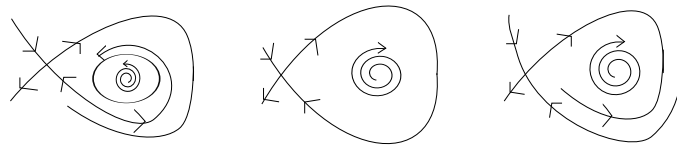


Figure 2: A bifurcation killing a cycle.

On the other hand, it is shown in second part, that after bifurcation of eight-loop can give rise to an alien limit cycle. This is a limit cycle that is not controlled by a zero of the related Abelian integral.

The missing "alien" limit cycle are a new phenomenon in the bifurcation theory of vector fields, discovered recently by Caubergh, Dumortier and Roussarie [10, 17]. To guarantee the existence of an alien limit cycle one can verify generic conditions on the Abelian integral and on the transition map associated to the connections of eight-loop, then under these conditions, the bifurcation diagram of limit cycle near the eight-loop (of the first Melnikov function) was computed (see fig. 4.4). It follows that the cyclicity of the eight-loop under the perturbation (4.1) is two (property 4.4.1).

The bifurcation diagram is based on the Hopf Poincaré-Bendixon theorem.

In fact, the birth or death of a cycle is accompanied by a loss of stability of the equilibrium state:

A soft loss of stability, when a stable cycle is born (see Fig.1).

A hard loss of stability when a dying unstable cycle gives its instability to the equilibrium state (see Fig.2).

Chapter 1

Qualitative theory of dynamical systems in the plane

This chapter is an introduction. The notations are the ones used by Perko in [43], we will give briefly the context. We begin by presenting the various phase portraits of a dynamical linear and non linear system. Than, we study limit sets and attractors of nonlinear systems case. The major part of this chapter discusses planar dynamical systems and the existence of limit cycles. We also present the map poincaré and the Melnikov's function. The tools proposed in this chapter will be useful to solve our problem.

1.1 Saddles, Nodes, Foci and Centers

1.1.1 Linear Systems in \mathbb{R}^2

In this section, we discuss the various phase portraits that are possible for the linear system

$$\mathbf{x}' = A\mathbf{x}, \quad (1.1)$$

when $\mathbf{x} \in \mathbb{R}^2$ and $A \in \mathcal{M}_2(\mathbb{R})$. We begin by describing the portraits for the linear system

$$\mathbf{x}' = B\mathbf{x}, \quad (1.2)$$

where the matrix $B = P^{-1}AP$; $P \in GL_2(\mathbb{R})$, has one of the follows forms:

$$B = \begin{pmatrix} \lambda & 0 \\ 0 & \mu \end{pmatrix}, B = \begin{pmatrix} \lambda & 1 \\ 0 & \lambda \end{pmatrix}, B = \begin{pmatrix} a & -b \\ b & a \end{pmatrix}.$$

The phase portrait for the linear system (1.1) above is then obtained from the phase portrait for (1.2) under the linear transformation coordinates $\mathbf{x} = P\mathbf{y}$.

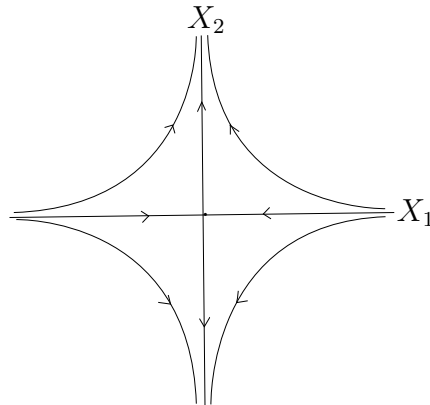


Figure 1.1: A Saddle at the origin

case I:

$$B = \begin{pmatrix} \lambda & 0 \\ 0 & \mu \end{pmatrix}, \lambda < 0 < \mu,$$

The phase portrait for the linear system (1.2) in this case is given in figure 1.1. Then the system (1.2) is said to have a saddle at the origin in this case.

Remark 1.1.1 *If $\mu < 0 < \lambda$, then the arrows in figure 1.1 are reversed.*

Case II :

$$B = \begin{pmatrix} \lambda & 0 \\ 0 & \mu \end{pmatrix}; \lambda \leq \mu < 0, \quad B = \begin{pmatrix} \lambda & 1 \\ 0 & \lambda \end{pmatrix}; \lambda < 0.$$

The phase portraits for the linear system (1.2) in these cases are given in figure 1.2. The origin is referred to as a stable node in each of these cases.

1.1 Saddles, Nodes, Foci and Centers

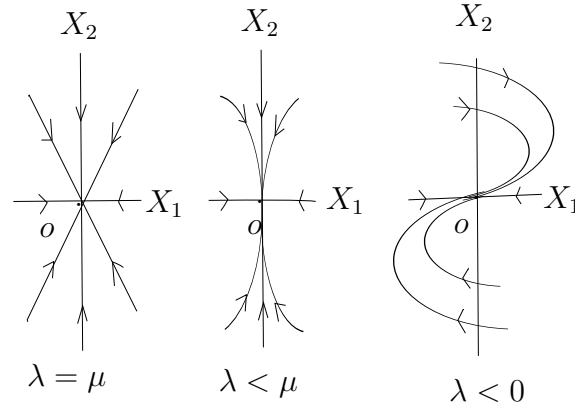


Figure 1.2: A stable node at the origin

- If $\lambda = \mu$ Then the origin is a proper node .
- If $\lambda < \mu$ or if $\lambda < 0$ Then the origin is an improper node in the other two cases. see fig. 1.2.

Remark 1.1.2 If $\lambda \geq \mu > 0$ or if $\lambda > 0$ in Case II, then the arrows in figure. 1.2 are reversed and the origin is referred to as an unstable node. Thus, Then the stability of the node is determined by the sign of the eigenvalues:

- If $\lambda \leq \mu < 0$ Then we have a stable node at the origin.
- If $\lambda \geq \mu > 0$ Then we have a unstable node at the origin.

Case III :

$$B = \begin{pmatrix} a & -b \\ b & a \end{pmatrix}, a < 0.$$

The phase portrait for the linear system (1.2) in this case is given in figure 1.3. The origin is referred to as a stable focus in these cases.

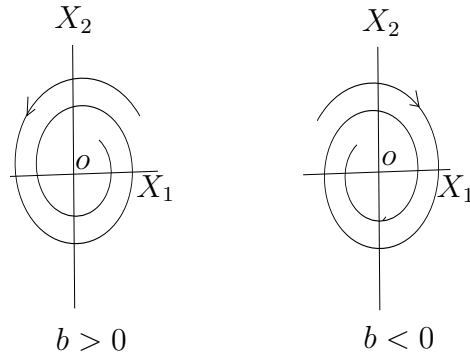


Figure 1.3: A stable focus at the origin

Remark 1.1.3 *If $a > 0$, the trajectories spiral away from the origin with increasing t and the origin is called an unstable focus.*

Cas IV :

$$B = \begin{pmatrix} 0 & -b \\ b & 0 \end{pmatrix}.$$

The phase portrait for the linear system (1.2) in this case is given in figure . 1.4. The system (1.2) is said to have a center at the origin in this case.

Definition 1.1.4 *The linear system (1.1) is said to have a saddle, a node, a focus or a center at the origin if the matrix A is similar to one of the matrices B in cases I, II, III, or IV respectively, i.e., if its phase portrait is linearly equivalent to one of the phase portraits in figures 1.1, 1.2, 1.3 or 1.4.*

Pour $\det(A) \neq 0$, there is an easy method for determining if the linear system has a saddle, node, focus, or center at the origin. This is given in the next theorem. Note that if $\det(A) \neq 0$ then $A\mathbf{x} = 0$ iff $\mathbf{x} = 0$; i.e., the origin is the only equilibrium point of the linear system (1.1) when $\det(A) \neq 0$

Theorem 1.1.5 *Let $\delta = \det(A)$ and $\tau = \text{tr}(A)$ and consider the linear system (1.1).*

(a) *If $\delta < 0$ then (1.1) has a saddle at the origin.*

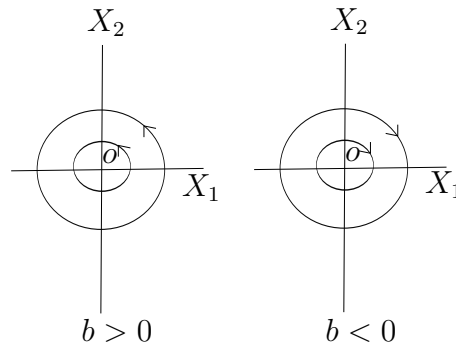


Figure 1.4: A center at the origin

(b) If $\delta > 0$ and $\tau^2 - 4\delta \geq 0$ then (1.1) has a node at the origin; it is stable if $\tau < 0$ and unstable if $\tau > 0$.

(c) If $\delta > 0$, $\tau^2 - 4\delta < 0$ and $\tau \neq 0$ then (1.1) has a focus at the origin; it is stable if $\tau < 0$ and unstable if $\tau > 0$.

(d) If $\delta > 0$ and $\tau = 0$ then (1.1) has a center at the origin.

Note that in case (b), $\tau^2 \geq 4|\delta| > 0$; i.e $\tau \neq 0$.

Proof See [43, p. 25-26].

Definition 1.1.6 A stable node or focus of (1.1) is called a sink of the linear system and unstable node or focus of (1.1) is called a source of the linear system.

1.1.2 Nonlinear Systems

In this subsection, we begin our study of non linear system of differential equations

$$\mathbf{x}' = \mathbf{f}(\mathbf{x}), \tag{1.3}$$

where $\mathbf{f} : E \rightarrow \mathbb{R}^n$ is a continuous map and E is an open subset of \mathbb{R}^n . We will see also the local behavior of the nonlinear system (1.3) near an equilibrium hyperbolic point \mathbf{x}_0 where $\mathbf{f}(\mathbf{x}_0) = \mathbf{0}$ is typically determined by the behavior of the linear system (1.1) near the origin when the matrix $A = D\mathbf{f}(\mathbf{x}_0)$ the derivate of \mathbf{f} at \mathbf{x}_0 .

Definition 1.1.7 A point $\mathbf{x}_0 \in \mathbb{R}^n$ is called an equilibrium point or critical point of (1.3) if $\mathbf{f}(\mathbf{x}_0) = 0$. An equilibrium point is called a hyperbolic equilibrium point of (1.3) if none of the eigenvalues of the matrix $D\mathbf{f}(\mathbf{x}_0)$ have zero real part. The linear system (1.1) with the matrix $A = D\mathbf{f}(\mathbf{x}_0)$ is called the linearisation of (1.3) at \mathbf{x}_0 .

If $\mathbf{x}_0 = 0$ is an equilibrium point of (1.3) then $\mathbf{f}(0) = 0$ and, by Taylor's Theorem,

$$\mathbf{f}(\mathbf{x}) = D\mathbf{f}(0)\mathbf{x} + \frac{1}{2}D^2\mathbf{f}(0)(\mathbf{x}, \mathbf{x}) + \dots$$

It follows that the linear function $D\mathbf{f}(0)\mathbf{x}$ is a good first approximation to the nonlinear function $\mathbf{f}(\mathbf{x})$ near $\mathbf{x} = 0$ and it is reasonable to expect that the behavior of the nonlinear system (1.3) near the point $\mathbf{x} = 0$ will be approximated by the behavior of its linearization at $\mathbf{x} = 0$.

Definition 1.1.8 1. An equilibrium point \mathbf{x}_0 of (1.3) is called a sink if all of the eigenvalues of the matrix $D\mathbf{f}(\mathbf{x}_0)$ have negative real part.

2. It is called a source if all of the eigenvalues of $D\mathbf{f}(\mathbf{x}_0)$ have positive real part.

3. It is called a saddle if it is a hyperbolic equilibrium point and $D\mathbf{f}(\mathbf{x}_0)$ has at least one eigenvalue with a positive real part and at least one with a negative real part.

Theorem 1.1.9 Let E be an open subset of \mathbb{R}^2 containing the origin, let $\mathbf{f} \in C^1(E)$. If the origin is a hyperbolic equilibrium point of the nonlinear system (1.3), then the origin is topological saddle for (1.3) if and only if the origin is a saddle for the linear system (1.1) with $A = D\mathbf{f}(0)$.

Example 1.1.10 According to the above theorem, we consider The nonlinear system

$$\begin{cases} x' = x + 2y + x^2 - y^2 \\ y' = 3x + 4y - 2xy \end{cases}.$$

This system has the form: $\mathbf{x}' = A\mathbf{x} + \mathbf{g}(\mathbf{x})$ with $\mathbf{x} = (x, y)^\top$ and $A = D\mathbf{f}(0) = \begin{pmatrix} 1 & 2 \\ 3 & 4 \end{pmatrix}$.

Thus, $\delta = \det(A) = -2 < 0$. Then the origin is a topological saddle for (1.1) and saddle for the nonlinear system (1.3).

Theorem 1.1.11 Let E be an open subset of \mathbb{R}^2 containing the origin and let $\mathbf{f} \in C^2(E)$. suppose that the origin is a hyperbolic critical point of the nonlinear system (1.3). Then

- The origin is a stable (or unstable) node for the nonlinear system (1.3) if and only if it is a stable (or unstable) node for the linear system (or unstable) (1.1) with $A = D\mathbf{f}(0)$.

1.1 Saddles, Nodes, Foci and Centers

- The origin is a stable (or unstable) focus for the nonlinear system (1.3) if and only if it is a stable (or unstable) focus for the linear system (1.1) with $A = D\mathbf{f}(0)$.

Theorem 1.1.12 Let E be an open subset of \mathbb{R}^2 containing the origin and let $\mathbf{f} \in C^1(E)$ with $\mathbf{f}(0) = 0$. If the origin is a center for the linear system (1.1) with $A = D\mathbf{f}(0)$. Then the origin is either a center or a focus for the nonlinear system (1.3).

1.1.3 Hamiltonian Systems

In this subsection, we study two interesting types of systems which arise in physical problems and from which we draw a wealth of examples of the general theory.

Definition 1.1.13 (Hamiltonian systems) E be an open subset of \mathbb{R}^{2n} and let $H \in C^2(E)$ where $H = H(\mathbf{x}, \mathbf{y})$ with $\mathbf{x}, \mathbf{y} \in \mathbb{R}^n$. A system of the form

$$\begin{cases} \mathbf{x}' = \frac{\partial H}{\partial \mathbf{y}} \\ \mathbf{y}' = -\frac{\partial H}{\partial \mathbf{x}} \end{cases}, \quad (1.4)$$

where

$$\frac{\partial H}{\partial \mathbf{x}} = \left(\frac{\partial H}{\partial x_1}, \dots, \frac{\partial H}{\partial x_n} \right)^\top, \quad \frac{\partial H}{\partial \mathbf{y}} = \left(\frac{\partial H}{\partial y_1}, \dots, \frac{\partial H}{\partial y_n} \right)^\top,$$

is called a Hamiltonian system with n degrees of freedom on E .

Theorem 1.1.14 (Conservation of Energy) The total energy $H(\mathbf{x}, \mathbf{y})$ of the Hamiltonian system (1.4) remains constant along trajectories of the system.

We next establish some very specific results about the nature of the critical points of Hamiltonian system with one degree of freedom. Note that the equilibrium points or critical points of the system (1.4) correspond to the critical points of the Hamiltonian function $H(\mathbf{x}, \mathbf{y})$ where $\frac{\partial H}{\partial \mathbf{x}} = \frac{\partial H}{\partial \mathbf{y}} = 0$. assume that the critical point in question has been translated to the origin.

Lemma 1.1.15 If the origin is a focus of the Hamiltonian system

$$\begin{cases} x' = H_y(x, y) \\ y' = -H_x(x, y) \end{cases}, \quad (1.5)$$

then the origin is not a strict local maximum or minimum of the Hamiltonian function $H(x, y)$.

Definition 1.1.16 A Critical point of the system (1.3) at which $D\mathbf{f}(\mathbf{x}_0)$ has no zeros eigenvalues is called a nondegenerate critical point of the system, otherwise, it is called a degenerate critical point of the system.

Note that any nondegenerate critical point of a planar system is either a hyperbolic critical point of the system or a center of the linearized system.

Theorem 1.1.17 *Any nondegenerate critical point of an analytic Hamiltonian system (1.5) is either a topological saddle or a center; furthermore, (x_0, y_0) is a topological saddle for (1.5) iff it is a saddle of the Hamiltonian $H(x, y)$, and (1.5).*

Proof We assume that the critical point is at the origin. Thus, $H_x(0, 0) = H_y(0, 0) = 0$ and the linearization of (1.5) at the origin is

$$\mathbf{x}' = A\mathbf{x}, \tag{1.1}$$

where

$$A = \begin{pmatrix} H_{yx}(0, 0) & H_{yy}(0, 0) \\ -H_{xx}(0, 0) & -H_{xy}(0, 0) \end{pmatrix}.$$

We see that $\tau = \text{tr}(A) = 0$ and the $\delta = \det(A) = H_{xx}(0, 0)H_{yy}(0, 0) - H_{xy}^2(0, 0)$. Thus, the critical point at the origin is a saddle of the function $H(x, y)$ if and only if $\det(A) < 0$, then it is a saddle for the linear system (1.1), according to the theorem 1.1.5, it is a topological saddle for the Hamiltonian system (1.5). Also, if $\text{tr}(A) = 0$ and $\det(A) > 0$ then the origin is a center for the linear system (1.1), according to the theorem 1.1.12, is either a center or a focus for (1.5). Thus, if the non degenerate critical point $(0, 0)$ is a strict local maximum or minimum of the function $H(x, y)$ then $\det(A) > 0$, and the origin is not a focus for (1.5); i.e., the origin is a center for the Hamiltonian system (1.5).

Example 1.1.18 *According to the above theorem, we consider The Duffing oscillator's equation:*

$$\ddot{x} = x - x^3$$

which can be written as:

$$\begin{cases} x' = y \\ y' = x - x^3 \end{cases}.$$

This system has three critical points at $(0, 0)$ and at $(\pm 1, 0)$

- The linearization of this system at the origin is:

$$\mathbf{x}' = A\mathbf{x} \text{ with } \mathbf{x} = (x, y)^\top \text{ and } A = D\mathbf{f}(0) = \begin{pmatrix} 0 & 1 \\ 1 & 0 \end{pmatrix}.$$

We see that: $\tau = \text{tr}A = 0$ and $\delta = \det(A) = -1 < 0$. Then the origin is a saddle for the linear system (1.1) and it is a topological saddle for the Hamiltonian system (1.5).

1.2 Dynamical Systems and Limit Cycles

• The linearization of this system at $(\pm 1, 0)$ is:

$\mathbf{x}' = A\mathbf{x}$ with $A = D\mathbf{f}(\pm 1, 0) = \begin{pmatrix} 0 & 1 \\ -2 & 0 \end{pmatrix}$, $\tau = \text{tr}A = 0$ and $\delta = \det(A) = 2 > 0$, then $(\pm 1, 0)$ is a center for the linear system (1.1) and it is a topological center for the Hamiltonian system (1.5).

1.2 Dynamical Systems and Limit Cycles

A dynamical system gives a functional description of the solution of a physical problem or of the mathematical model describing the physical problem. Mathematically speaking, a dynamical system is a function $\phi(t, \mathbf{x})$, defined for all $t \in \mathbb{R}$ and $\mathbf{x} \in E \subset \mathbb{R}^n$, which describes how points $\mathbf{x} \in E$ move with respect to time. We require that the family of maps $\phi_t(\mathbf{x}) = \phi(t, \mathbf{x})$ have the properties of a flow.

Definition 1.2.1 A dynamical system on E is a \mathcal{C}^1 -map

$$\phi : \mathbb{R} \times E \rightarrow E,$$

where E is an open subset of \mathbb{R}^n and if $\phi_t(\mathbf{x}) = \phi(t, \mathbf{x})$ then ϕ_t satisfies

1. $\phi_0(\mathbf{x}) = \mathbf{x}$, for all $\mathbf{x} \in E$.
2. $\phi_t \circ \phi_s(\mathbf{x}) = \phi_{t+s}(\mathbf{x})$, for all $t, s \in \mathbb{R}$ and $\mathbf{x} \in E$.

Remark 1.2.2 The family $(\phi_t)_{t \in \mathbb{R}}$ is a one-family of diffeomorphisms on E .

It is easy to see that if A is an $n \in \mathbb{N}^*$ matrix, then the function $\phi(t, \mathbf{x}) = \exp(tA)\mathbf{x}$ defined a dynamical system on \mathbb{R}^n , and also, for each $\mathbf{x}_0 \in \mathbb{R}^n$, $\phi(t, \mathbf{x}_0)$ is the solution of the initial value problem

$$\begin{cases} \mathbf{x}' = A\mathbf{x} \\ \mathbf{x}(0) = \mathbf{x}_0 \end{cases}.$$

In general, if $\phi(t, \mathbf{x})$ is a dynamical system on $E \subset \mathbb{R}^n$ then the function

$$\mathbf{f}(\mathbf{x}) = \left. \frac{d}{dt} \phi(t, \mathbf{x}) \right|_{t=0}$$

defines a \mathcal{C}^1 -vector field on E and for each $\mathbf{x}_0 \in \mathbb{R}^n$, $\phi(t, \mathbf{x}_0)$ is a solution of the initial value problem

$$\begin{cases} \mathbf{x}' = \mathbf{f}(\mathbf{x}) \\ \mathbf{x}(0) = \mathbf{x}_0 \end{cases}.$$

1.2.1 Limit Set and Attractors

Consider the autonomous system

$$\mathbf{x}' = \mathbf{f}(\mathbf{x}) \quad (1.3),$$

with $\mathbf{f} \in \mathcal{C}^1(E)$ where E is an open subset \mathbb{R}^n . We saw that there is no loss in generality in assuming that the system (1.3) defines a dynamical system $\phi(t, \mathbf{x})$ on E . For $\mathbf{x} \in E$, the function $\phi(\cdot, \mathbf{x}) : \mathbb{R} \rightarrow E$ defines a solution curve, trajectory, or orbit of (1.3) through the point \mathbf{x} in E . If we identify the function $\phi(\cdot, \mathbf{x})$ with its graph, we can think of a trajectory through the point \mathbf{x}_0 as a motion along the curve

$$\Gamma_{\mathbf{x}_0} = \{\mathbf{x} \in E : \mathbf{x} = \phi(t, \mathbf{x}_0), t \in \mathbb{R}\}$$

defined by (1.3). We shall also refer to $\Gamma_{\mathbf{x}_0}$ as the trajectory of (1.3) through the point \mathbf{x}_0 at time $t = 0$. By the positive half-trajectory through the point \mathbf{x}_0 , we mean the motion along the curve

$$\Gamma_{\mathbf{x}_0}^+ = \{\mathbf{x} \in E : \mathbf{x} = \phi(t, \mathbf{x}_0), t \geq 0\}$$

defined by (1.3), and the negative half-trajectory through the point \mathbf{x}_0 , $\Gamma_{\mathbf{x}_0}^-$, is similarly defined. Any trajectory $\Gamma_{\mathbf{x}_0} = \Gamma_{\mathbf{x}_0}^+ \cup \Gamma_{\mathbf{x}_0}^-$. If the point \mathbf{x}_0 plays no role in the discussion we simply denote the trajectory Γ by $\Gamma_{\mathbf{x}_0}$.

Definition 1.2.3 1. A point $\mathbf{p} \in E$ is an ω -limit of the trajectory $\phi(\cdot, \mathbf{x})$ of the system (1.3) if there is a sequence $(t_n) \rightarrow +\infty$ such that

$$\lim_{n \rightarrow +\infty} \phi(t_n, \mathbf{x}) = \mathbf{p}.$$

see figure 1.5.

2. Similarly, if there is a sequence $(t_n) \rightarrow -\infty$ such that

$$\lim_{n \rightarrow -\infty} \phi(t_n, \mathbf{x}) = \mathbf{q}.$$

and the point $\mathbf{q} \in E$ is called an α -limit of the trajectory $\phi(\cdot, \mathbf{x})$ of system (1.3).

3. The set of all α -limit points of a trajectory Γ is called α -limit set of Γ and it is denoted by $\alpha(\Gamma)$, and the set of all ω -limit points of a trajectory Γ is called ω -limit set of Γ and it is denoted by $\omega(\Gamma)$.

4. The set of all limit points $\alpha(\Gamma) \cup \omega(\Gamma)$ is called the limit set of Γ .

Theorem 1.2.4 The α and ω -limit set of a trajectory of (1.3); $\alpha(\Gamma)$ and $\omega(\Gamma)$; are closed subset of E , and if Γ is contained in a compact subset of \mathbb{R}^n , then $\alpha(\Gamma)$ and $\omega(\Gamma)$ are non-empty, connected, compact subsets of E .

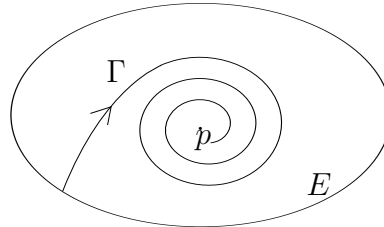


Figure 1.5: The trajectory Γ of (1.3) which approaches a ω -limit point \mathbf{p}

Theorem 1.2.5 *If \mathbf{p} is an ω -limit of a trajectory Γ of (1.3) then all other points of the trajectory $\phi(\cdot, \mathbf{p})$ of (1.3) through the point \mathbf{p} are also ω -limit points of Γ ; i.e., if $\mathbf{p} \in \omega(\Gamma)$ then $\Gamma_{\mathbf{p}} \subset \omega(\Gamma)$ and similarly if $\mathbf{q} \in \alpha(\Gamma)$ then $\Gamma_{\mathbf{q}} \subset \alpha(\Gamma)$.*

Proof By using the properties of the flow .

Corollary 1.2.6 *$\alpha(\Gamma)$ and $\omega(\Gamma)$ are invariant with respect to the flow ϕ_t of (1.3).*

In the next definition, a neighborhood of a set A is any open set U containing A , and we say that $\mathbf{x}(t) \rightarrow A$ as $t \rightarrow +\infty$ if the distance $d(\mathbf{x}(t), A) \rightarrow 0$ as $t \rightarrow +\infty$.

Definition 1.2.7 *A closed invariant set $A \subset E$ is called an attracting set of (1.3) if there is some neighborhood U of A such that, for all $\mathbf{x} \in U$, $\phi_t(\mathbf{x}) \in U$ for all $t \geq 0$ and $\phi_t(\mathbf{x}) \rightarrow A$ as $t \rightarrow +\infty$. An attractor of (1.3) is an attracting set which contains a dense orbit.*

Remarks 1.2.8 1. *If a trajectory Γ of (1.3) has a unique ω -limit point \mathbf{x}_0 , then by the corollary 1.2.6, this point is an equilibrium point of (1.3).*

2. *A stable node or focus, defined of planar system (1.3) is the ω -limit set of every trajectory in some neighborhood of the point; and a stable node or focus of (1.3) is an attractor of (1.3).*

3. If \mathbf{q} is any regular point in $\alpha(\Gamma)$ or $\omega(\Gamma)$ then the trajectory through \mathbf{q} is called a limit orbit of Γ . Thus, by the theorem 1.2.5, we see that $\alpha(\Gamma)$ et $\omega(\Gamma)$ consist of equilibrium points and limit orbit of (1.3).

We now consider the below example of limit set and attractors:

Example 1.2.9 Consider the system

$$\begin{cases} x' &= -y + x(1 - x^2 - y^2) \\ y' &= x + y(1 - x^2 - y^2) \end{cases} \quad (1.6)$$

In polar coordinates, we have

$$\begin{cases} rr' &= xx' + yy' \\ r^2\theta' &= xy' - yx' \end{cases} .$$

We have

$$\begin{cases} r' &= r(1 - r^2) \\ \theta' &= 1 \end{cases} .$$

Then $\theta(t) = \theta_0 + t$. We see that the origin is an equilibrium point of this system; the flow spirals around the origin in the counter-clockwise direction; and it spirals outwards for $0 < r < 1$ since $r' > 0$; and it spirals inward for $r > 1$ since $r' < 0$. The counter-clockwise flow on the unit circle describes a trajectory Γ_0 of (1.6) since $r' = 0$ on $r = 1$. The trajectory through the point $(\cos(\theta_0), \sin(\theta_0))$ on the unit circle at $t = 0$ is given by $(x(t), y(t)) = (\cos(t + \theta_0), \sin(t + \theta_0))$. The phase portrait for this system is shown in figure 1.6. The trajectory Γ_0 is called a stable limit cycle. A precise definition of a limit cycle is given in the next section.

The stable limit cycle Γ_0 of the system in (1.6), shown in figure 1.6, is the ω -limit of every trajectory of this system except the equilibrium point at the origin. Γ_0 is composed of one limit orbit and is its own α and ω -limit set.

1.2.2 Periodic Orbits and Limit Cycles

In this section, we discuss periodic orbits or cycles, limit cycles and separatrix cycles of a dynamical system $\phi(t, \mathbf{x})$ defined by (1.3).

Definition 1.2.10 A cycle periodic orbit of (1.3) is any closed solution curve of (1.3) which is not an equilibrium point of (1.3). A periodic orbit Γ is called stable if for each $\epsilon > 0$, there is a neighborhood U of Γ such that for all $\mathbf{x} \in U$, $d(\Gamma_{\mathbf{x}}^+, \Gamma) < \epsilon$; i.e., if for all $\mathbf{x} \in U$ and

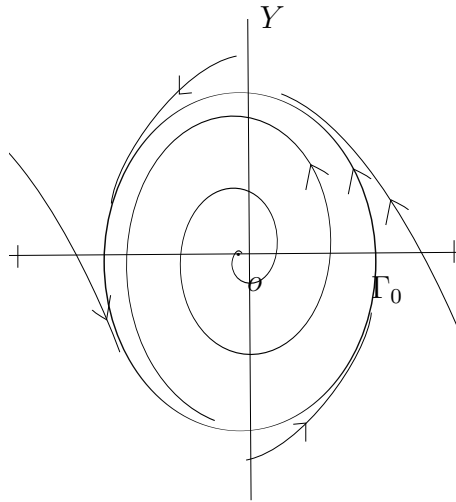


Figure 1.6: A stable limit cycle Γ_0 which is an attractor of (1.6)

$t \geq 0$, $d(\phi(t, \mathbf{x}), \Gamma) < \epsilon$. A periodic orbit Γ is called unstable if it is not stable; and Γ is called asymptotically stable if it is stable and if for all points $\mathbf{x} \in U$, of Γ

$$\lim_{t \rightarrow +\infty} d(\phi(t, \mathbf{x}), \Gamma) = 0.$$

We next consider periodic orbits of planar system, (1.3) with $\mathbf{x} \in \mathbb{R}^2$.

Definition 1.2.11 1. If a cycle Γ is the ω -limit set of every trajectory in some neighborhood of Γ , then Γ is called an ω -limit cycle or stable limit cycle.

2. If a cycle Γ is the α -limit set of every trajectory in some neighborhood of Γ , then Γ is called an α -limit cycle or unstable limit cycle.

3. If a cycle Γ is the ω -limit set of one trajectory other than Γ and the α -limit set of another trajectory other than Γ , then Γ is called a semi-stable limit cycle.

Theorem 1.2.12 If one trajectory in the exterior of a limit cycle Γ of a planar C^1 -system (1.3) has Γ as its ω -limit set, then every trajectory in some exterior neighborhood U of Γ has Γ as its ω -limit set. Moreover, any trajectory in U spirals around Γ as $t \rightarrow +\infty$ in the sense that it intersects any straight line perpendicular to Γ an infinite number of times at $t = t_n$ where $t_n \rightarrow +\infty$.

Example 1.2.13 Consider the system

$$\begin{cases} x' = -y + x(x^2 + y^2) \sin\left(\frac{1}{\sqrt{x^2 + y^2}}\right) \\ y' = x + y(x^2 + y^2) \sin\left(\frac{1}{\sqrt{x^2 + y^2}}\right) \end{cases}, \quad (1.7)$$

for $x^2 + y^2 \neq 0$ with $x' = y' = 0$ at $(0, 0)$ defines a C^1 -system on \mathbb{R}^2 which can be written in polar coordinates as

$$\begin{cases} r' = r^3 \sin\left(\frac{1}{r}\right) \\ \theta' = 1 \end{cases}.$$

The origin is an equilibrium point and there are limit cycle Γ_n lying on the circles $r = \frac{1}{n\pi}$. These limit cycles accumulate at the origin ; i.e.,

$$\lim_{n \rightarrow +\infty} d(\Gamma_n, \mathbf{0}) = 0.$$

Each of the limit cycles Γ_{2n} is stable while Γ_{2n+1} is unstable.

Theorem 1.2.14 (Dulac) In any bounded region of the plane, a planar analytic system (1.3) with $\mathbf{f}(\mathbf{x})$ analytic in \mathbb{R}^2 has at most a finite number of limit cycles. Any polynomial system has at most a finite number of limit cycles in \mathbb{R}^2 .

1.2.3 The Poincaré Map

The idea of the Poincaré map is quite simple: If Γ is a periodic orbit of the system (1.3) through the point \mathbf{x}_0 and Σ is an hyperplane perpendicular to Γ at \mathbf{x}_0 , then for any point $\mathbf{x} \in \Sigma$ sufficiently near \mathbf{x}_0 , the solution of (1.3) through \mathbf{x} at $t = 0$, $\phi_t(\mathbf{x})$ will cross Σ again at a point $P(\mathbf{x})$ near \mathbf{x}_0 ; cf. figure 1.7. The mapping $\mathbf{x} \mapsto P(\mathbf{x})$ is called the Poincaré map. The next theorem establishes the existence and continuity of the Poincaré map $P(\mathbf{x})$, and of its first derivative $DP(\mathbf{x})$.

Theorem 1.2.15 Let E be an open subset of \mathbb{R}^n and let $\mathbf{f} \in C^1(E)$. Suppose that $\phi_t(\mathbf{x}_0)$ is a periodic solution of (1.3) of period T and that the cycle

$$\Gamma = \{\mathbf{x} \in \mathbb{R}^n : \mathbf{x} = \phi_t(\mathbf{x}_0), 0 \leq t \leq T\}$$

is contained in E . Let Σ be an hyperplane orthogonal to Γ at \mathbf{x}_0 ; i.e., let

$$\Sigma = \{\mathbf{x} \in \mathbb{R}^n : (\mathbf{x} - \mathbf{x}_0) \cdot \mathbf{f}(\mathbf{x}_0) = 0\}.$$

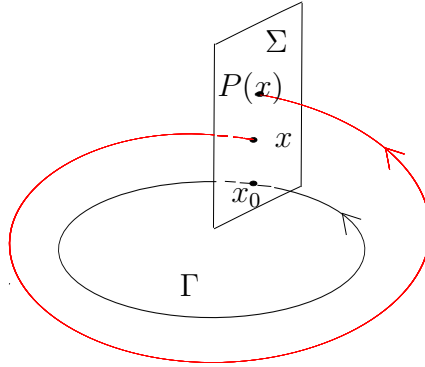


Figure 1.7: The Poincaré map

Then there is a $\delta > 0$ and a unique function $\tau(\mathbf{x})$ defined and continuously differentiable for $\mathbf{x} \in N_\delta(\mathbf{x}_0)$, such that $\tau(\mathbf{x}_0) = T$ and

$$\phi_{\tau(\mathbf{x})}(\mathbf{x}) \in \Sigma, \forall \mathbf{x} \in N_\delta(\mathbf{x}_0).$$

Definition 1.2.16 Let Γ , Σ , δ and $\tau(\mathbf{x})$ be defined as in theorem 1.2.15. Then for $\mathbf{x} \in N_\delta(\mathbf{x}_0) \cap \Sigma$, the function $P(\mathbf{x}) = \phi_{\tau(\mathbf{x})}(\mathbf{x})$ is called the Poincaré map for Γ at \mathbf{x}_0 .

Remark 1.2.17 It follows from theorem 1.2.15, that: $P \in \mathcal{C}^1(U)$ where $U = N_\delta(\mathbf{x}_0) \cap \Sigma$.

Example 1.2.18 On consider the system

$$\begin{cases} x' &= -y + x(1 - x^2 - y^2) \\ y' &= x + y(1 - x^2 - y^2) \end{cases} \quad (1.6)$$

It was shown that the system 1.2.9, had a limit cycle Γ represented by $\gamma(t) = (\cos(t), \sin(t))^T$. The Poincaré map for Γ can be found by solving this system written in polar coordinates:

$$\begin{cases} r' &= r(1 - r^2) \\ \theta' &= 1 \end{cases}, \text{ where } r(0) = r_0 \text{ and } \theta(0) = \theta_0.$$

The first equation $r' = r - r^3$, can be solved either as a separable differential equation or as a Bernoulli equation; if $r^3 \neq 0$ then

$$\frac{r'}{r^3} - \frac{1}{r^2} = -1.$$

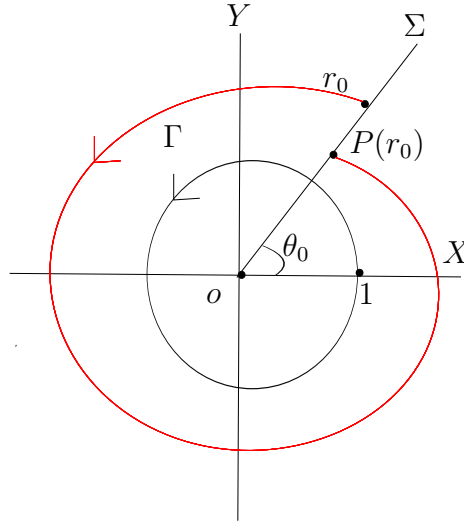


Figure 1.8: The Poincaré map for the system in example 1.2.18

Suppose that $z(t) = \frac{1}{r^2}$, we have

$$\frac{1}{2}z'(t) + z(t) = 1.$$

Thus $z(t) = \left(\frac{1}{r_0^2} - 1\right) \exp(-2t) + 1$. The solution is given by

$$\begin{cases} r(t, r_0) = \left(\left(\frac{1}{r_0^2} - 1\right) \exp(-2t) + 1\right)^{-\frac{1}{2}} \\ \theta(t, \theta_0) = \theta_0 + t \end{cases}.$$

If Σ is the ray $\theta = \theta_0$ through the origin, then Σ is perpendicular to Γ and the trajectory through the point $(r_0, \theta_0) \in \Sigma \cap \Gamma$ at $t = 0$ intersects the ray $\theta = \theta_0$ again at $t = 2\pi$ cf. figure 1.8.

It follows that Poincaré map is given by

$$\begin{aligned} P(r_0) &= \left(\left(\frac{1}{r_0^2} - 1\right) \exp(-4\pi) + 1\right)^{-\frac{1}{2}} \\ P(1) &= 1. \end{aligned}$$

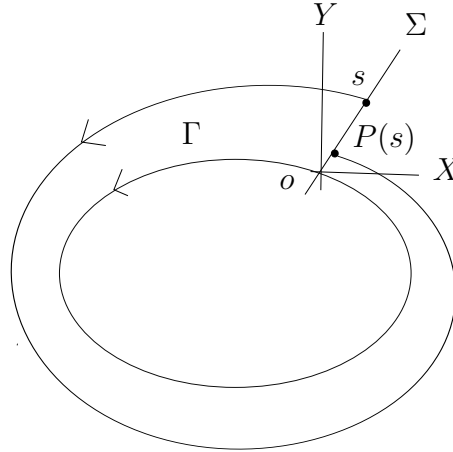


Figure 1.9: The straight line Σ normal to Γ at 0

Clearly $P(1) = 1$ corresponding to the cycle Γ and we see that

$$P'(r_0) = \exp(-4\pi)r_0^{-3} \left(\left(\frac{1}{r_0^2} - 1 \right) \exp(-4\pi) + 1 \right)^{-\frac{3}{2}}$$

$$P'(1) = \frac{\exp(-4\pi)}{\sqrt{2}} < 1.$$

We next cite some specific results for the Poincaré map of planar systems. If we translate the origin to the point $\mathbf{x}_0 \in \Gamma \cap \Sigma$, the normal line Σ will be a line through the origin ; cf.figure 1.9.

The point $\mathbf{0} \in \Gamma \cap \Sigma$ divides the line Σ into two open segments Σ^+ and Σ^- where Σ^+ lies entirely in the exterior of Γ . Let s be the signed distance along Σ^+ with $s > 0$ for points in Σ^+ and $s < 0$ for points in Σ^- . According to theorem 1.2.15, The Poincaré map is then defined for $|s| < \delta$ and we have : $P(0) = 0$. In order to see how the stability of the cycle Γ is determined by $P'(0)$, let us introduce the displacement function

$$d(s) = P(s) - s.$$

Then $d(0) = 0$ and $d'(s) = P'(s) - 1$; and it is follows from the mean value theorem that for $|s| < \delta$

$$d(s) = d'(\sigma)s,$$

for some $\sigma \in (0, s)$. Since $d'(s)$ is continuous, the sign of $d'(s)$ will be the same as the sign of $d'(0)$ for $|s|$ sufficiently small as long as $d'(0) \neq 0$. Thus, if $d'(0) < 0$ then $d(s) < 0$ for $s > 0$ and that $d(s) > 0$ for $s < 0$; i.e., the cycle Γ is a stable limit cycle or an ω -limit cycle. cf. figure 1.9. Similarly, if $d'(0) > 0$ then Γ is an unstable limit cycle or an α -limit cycle.

We have the corresponding results that if $P(0) = 0$ and $P'(0) < 1$, then Γ is a stable limit cycle and if $P(0) = 0$ and $P'(0) > 1$ then Γ is an unstable limit cycle. Thus, the stability of Γ is determined by the derivative of the Poincaré map.

Theorem 1.2.19 *Let E be an open subset of \mathbb{R}^2 and suppose that $\mathbf{f} \in \mathcal{C}^1(E)$. Let $\gamma(t)$ be a periodic solution of (1.3) of period T . Then the derivative of the Poincaré map $P(s)$ along a straight line Σ normal to*

$$\Gamma = \{\mathbf{x} \in \mathbb{R}^2 : \mathbf{x} = \gamma(t) - \gamma(0), 0 \leq t \leq T\}$$

at point $\mathbf{x} = \mathbf{0}$ is given by

$$P'(0) = \exp\left(\int_0^T \nabla \cdot \mathbf{f}(\gamma(t)) dt\right).$$

Corollary 1.2.20 *Under the hypotheses of theorem 1.2.19, the periodic solution $\gamma(t)$ is a stable limit cycle if*

$$\int_0^T \nabla \cdot \mathbf{f}(\gamma(t)) dt < 0,$$

it is an unstable limit cycle if

$$\int_0^T \nabla \cdot \mathbf{f}(\gamma(t)) dt > 0,$$

and it may be semi-stable limit cycle if

$$\int_0^T \nabla \cdot \mathbf{f}(\gamma(t)) dt = 0.$$

Example 1.2.21 *For example 1.2.18 above, we have : $\gamma(t) = (\cos(t), \sin(t))^\top$, $\nabla \cdot \mathbf{f}(x, y) = 2 - 4x^2 - 4y^2$ and*

$$\int_0^{2\pi} \nabla \cdot \mathbf{f}(\gamma(t)) dt = \int_0^{2\pi} (2 - 4\cos^2(t) - 4\sin^2(t)) dt = -4\pi < 0.$$

Thus, with $s = r - 1$ then, it follows from 1.2.19 that

$$P'(0) = \exp(-4\pi)$$

which agrees with the result found in example 1.2.18. Since $P'(0) < 1$, the cycle $\gamma(t)$ is a stable limit cycle in this example.

Definition 1.2.22 Let $P(s)$ be the Poincaré map for a cycle Γ of a planar analytic system (1.3) and let $d(s) = P(s) - s$ be the displacement. Then, if

$$d(0) = d'(0) = \dots = d^{(k-1)}(0) = 0 \quad \text{and} \quad d^{(k)}(0) \neq 0,$$

Γ is called a multiple limit cycle of multiplicity k . If $k = 1$, then Γ is called a simple limit cycle.

We note that $\Gamma = \{\mathbf{x} \in \mathbb{R}^2 : \mathbf{x} = \gamma(t), 0 \leq t \leq T\}$ is a simple limit cycle if and only if

$$\int_0^T \nabla \cdot \mathbf{f}(\gamma(t)) dt \neq 0.$$

Furthermore, if Γ is a multiple limit cycle of multiplicity then k , then k limit cycles can be made to bifurcate from Γ under a suitable small perturbation of (1.3).

Theorem 1.2.23 (Poincaré) A planar analytic system (1.3) cannot have an infinite number of limit cycles which accumulate on a cycle (1.3).

1.2.4 Melnikov's Functions

In this section, consider the differential system can then be written as

$$\begin{cases} x' = P(x, y) \\ y' = Q(x, y) \end{cases}, \quad (1.8)$$

where P and Q are real polynomials of degree d . Denote

$$\omega_0 = P(x, y)dy - Q(x, y)dx$$

The 1-form associated with the system (1.8). Let U is an open subset of \mathbb{R}^2 and $t \mapsto (x(t), y(t))$ a solution of system (1.8). Denote

$$\Delta_{(x,y)}^U = \{t \in \mathbb{R} : (x(t), y(t)) \in U\}.$$

Definition 1.2.24 We call an integrant factor of system (1.8) on U associated with a first integral H , the map $\psi : U \rightarrow \mathbb{R}$ making the 1-form ω_0 exact and equal to dH , i.e.,

$$\psi\omega_0 = dH.$$

A usual technique for obtaining a differential system with limit cycles is to consider a polynomial system of type (1.8) having a center, and therefore integrable.

Let H a first integral of the system (1.8) and ψ it's an integrant factor. We perturbed this system by polynomials \bar{P} and \bar{Q} of the same degree as P and Q . Then the above system can be written

$$\begin{cases} x' &= P(x, y) + \epsilon\bar{P}(x, y) \\ y' &= Q(x, y) + \epsilon\bar{Q}(x, y) \end{cases}, \quad (1.9)$$

\bar{P} and \bar{Q} depend analytically on a small real parameter $\epsilon \neq 0$.

After perturbation usually there remain only a finite number of closed phase curves (the limit cycles). Our aim is to count their number correspond to the zeros of the displacement map:

$$d(\epsilon, s) = P_\epsilon(s) - s = \epsilon M_1(s) + \dots + \epsilon^k M_k(s) + o(\epsilon^{k+1}),$$

where the first return map P_ϵ is defined in figure 1.8, and $(M_i)_{i \geq 1}$ defined in Σ are called Melnikov's function.

In the present section we shall find the relations between these functions and the resolution of Hilbert's 16th problem :

- (i) The number of limit cycles bifurcating from a period annulus of (1.9) is given by the number of real zeros of the Melnikov function not identically zero. In the literature this function appears under different names: Poincaré-Pontryagin-Melnikov, Pontryagin integral, Melnikov integral, Pontryagin-Melnikov integral, generating function.
- (ii) An equilibrium point is a center if and only if the Poincaré map is the identity map in its neighborhood, or if and only if all the Melnikov functions are identically zero.

Therefore to compute the first non-zero derivative of the return map of a planar vector field, which can be done by making use of the so called " the algorithm of Françoise", see [18] and the references given there.

Lemma 1.2.25 *The expression of the first Melnikov function is given by the formula:*

$$\frac{\partial P_\epsilon}{\partial \epsilon} \Big|_{\epsilon=0} = M_1(s) = - \oint_{\{H=s\}} \omega, \quad \omega = \psi (\bar{P}dy - \bar{Q}dx).$$

Proof Let γ_ϵ be the arc of solution of $\omega_\epsilon = dH + \epsilon\omega = 0$; with $\omega = \bar{Q}dx - \bar{P}dy$ between the two points s and $P(s, \epsilon)$, see fig. 1.10.

We have: $dH + \epsilon\omega = 0$

Then

$$\begin{aligned} & \int_{\gamma_\epsilon} dH + \epsilon\omega = 0 \\ \Rightarrow & \int_{s \widehat{P(s, \epsilon)}} dH + \epsilon \int_{\gamma_\epsilon} \omega = 0 \end{aligned}$$

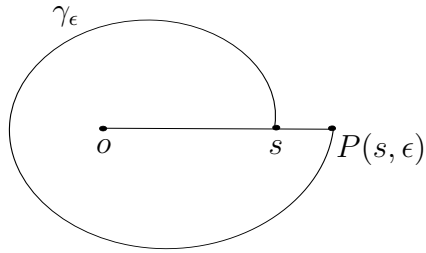


Figure 1.10: The straight line normal to γ_ϵ .

$$\Rightarrow H(P(s)) - H(s) + \epsilon \int_{\gamma_\epsilon} \omega = 0$$

Up to $O(\epsilon)$; γ_ϵ coincide with the closed curve $\{H = s\}$ and so we obtain

$$H(P(s)) - H(s) + \epsilon \int_{\{H=s\}} \omega \equiv 0 \quad [\epsilon^2] \tag{1.10}$$

or

$$\begin{aligned} H(P(s)) - H(s) &= \int_{sP(s,\epsilon)} dH \\ &= \int_{sP(s,\epsilon)} (H_x dx + H_y dy) \\ &= \epsilon \int_0^\tau (H_x \bar{P} + H_y \bar{Q}) dt \\ &= \epsilon F(h, \epsilon) \end{aligned}$$

obviously;

$$\begin{aligned}
 F(h, 0) &= \oint_{\{H=s\}} (H_x \bar{P} + H_y \bar{Q})|_{\epsilon=0} dt \\
 &= \oint_{\{H=s\}} (\bar{Q} dx - \bar{P} dy) \\
 &= \int \int_{H \leq s} (\bar{P}_x + \bar{Q}_y)|_{\epsilon=0} dx dy \\
 &= M_1(s)
 \end{aligned}$$

Returning to (1.10) we have

$$\epsilon M_1(s) + \epsilon \oint_{H=s} \omega = O(\epsilon^2)$$

Then

$$M_1(s) = - \oint_{H=s} \omega$$

□

Example 1.2.26 Consider van der Pol's equation

$$\ddot{x} + \epsilon(x^2 - 1)\dot{x} + x = 0$$

which can be written as

$$\begin{cases} x' = y \\ y' = -x - \epsilon(x^2 - 1)y \end{cases}, \quad (1.11)$$

For $\epsilon = 0$, (1.11) has periodic orbits $\Gamma_h : \frac{1}{2}(x^2 + y^2) = h; h > 0$. By lemma 1.2.25 we have

$$\begin{aligned}
 M(h) &= \int \int_{x^2 + y^2 \leq 2h} (1 - x^2) dx dy \\
 &= \frac{\pi}{4} \cdot h^2 (4 - h^2).
 \end{aligned}$$

The function M has a unique positive zero $h = 2$.

We have $\oint_{\Gamma_2} (1 - x^2) dt = M'(2) = -2\pi < 0$.

Hence, by 1.2.20, 1.11 has a unique limit cycle $\Gamma(\epsilon)$ which is stable, simple approaches the circle $x^2 + y^2 = 4$ as $\epsilon \rightarrow 0$.

Remark 1.2.27 It is said that the first integral H satisfies the condition of Françoise, if for all 1-form $\bar{\omega}$, the following assertions are equivalent

1.

$$\oint_{\{H=s\}} \bar{\omega} \equiv 0.$$

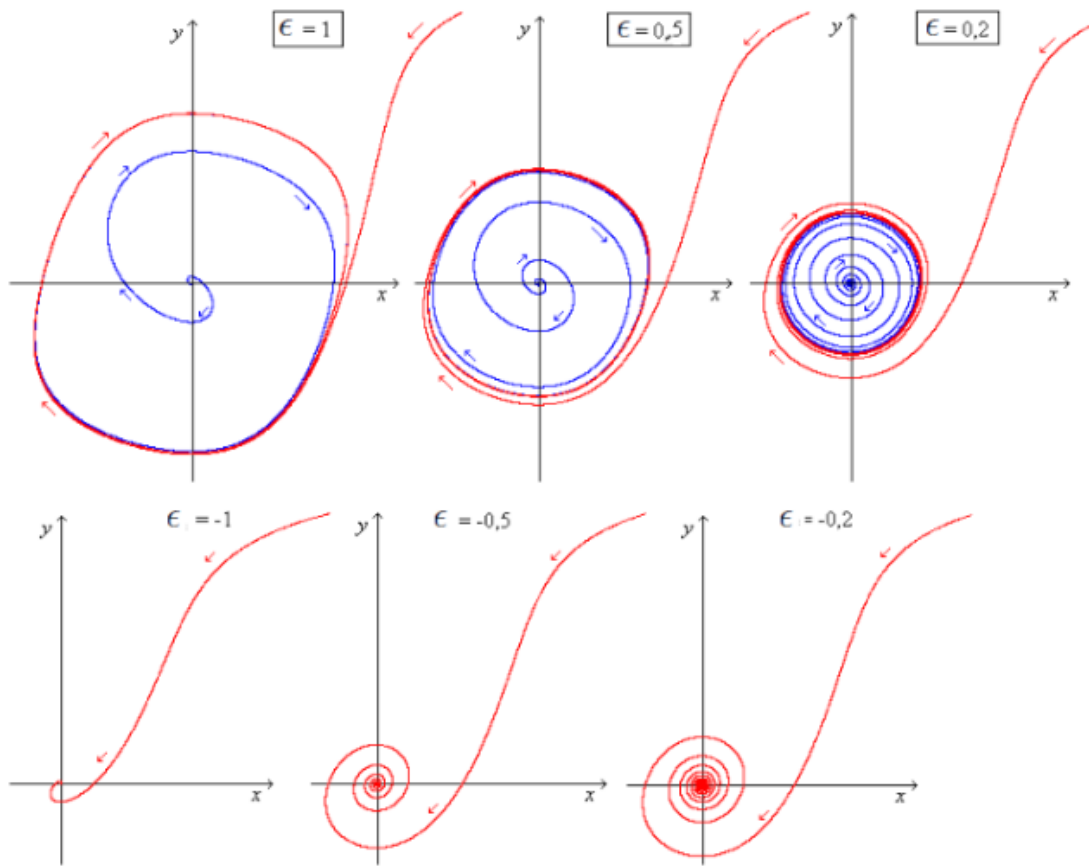


Figure 1.11: Limit cycle of Van der Pol oscillator

2. There exists analytic functions g and R such that $\bar{\omega} = g dH + dR$.

Françoise in [18] generalized the classical Melnikov function to any order, for the first nonzero derivative of a return mapping. (His method relied on the decomposition of a 1-form associated of the perturbed vector field (1.8)). This formula is given by the following theorem:

Theorem 1.2.28 (Françoise) *Suppose that H satisfy the condition of Françoise and consider the solutions of the equation differential $\omega_\epsilon = \frac{1}{\psi}(H + \epsilon\omega) = 0$. Suppose that $M_1(s) \equiv \dots \equiv M_k(s) \equiv 0$. Then there exists analytic functions $g_1, \dots, g_k, R_1, \dots, R_k$ such that*

$$\omega = g_1 dH + dR_1, \quad g_1 \omega = g_2 dH + dR_2, \quad \dots, \quad g_{k-1} \omega = g_k dH + dR_k,$$

and the $(k+1)^{ième}$ Melnikov function, is given by

$$\frac{\partial P_\epsilon^{k+1}}{\partial \epsilon^{k+1}} \Big|_{\epsilon=0} = M_{k+1}(s) = - \oint_{\{H=s\}} g_k \omega.$$

Theorem 1.2.29 (Gavrilov, [22]) *The generating function of limit cycles M_k satisfies a linear differential equation of Fuchs type:*

Recall that a ordinary differential equation

$$x^{(n)} + p_1(s)x^{(n-1)} + \dots + p_n(s)x = 0, \quad ' = \frac{d}{ds},$$

where $p_j, 1 \leq j \leq n$, are analytic in a domain D is called Fuchs type, if there are singular points $s_1, \dots, s_m, s_{m+1} = \infty$ such that

$$p_j(s) = \frac{a_j(s)}{\prod_{i=1}^m (s - s_i)^j}, \quad 1 \leq j \leq n,$$

where, for all $1 \leq j \leq n$, $a_j(s)$ is a polynomial of degree at most $j(m-1)$.

1.3 Principalization of the Bautin ideal

Let $h \mapsto P_\lambda(h)$ be the first return map associated to the deformed vector field X_λ and the period annulus of X_λ , bounded by Γ . Consider the Bautin ideal

$$\mathbf{B} = \langle a_k(\lambda) \rangle \subset \mathbb{C}[\lambda]$$

generated by the coefficients of the expansion

$$P_\lambda(h) - h = \sum_{k=0}^{\infty} a_k(\lambda) h^k.$$

1.3 Principalization of the Bautin ideal

Then $P(h) \equiv h \Leftrightarrow \langle a_k = 0 \rangle; a_k = a_k(\lambda_0, \lambda_1, \dots, \lambda_k) \Rightarrow \mathbf{I} = \langle a_k \rangle \subset P[\lambda_0, \lambda_1, \dots, \lambda_k]$: is an ideal of the period annulus of X_λ , or we recall that this ideal is generated by $\langle a_k \rangle = \langle f_1, f_2, \dots, f_k \rangle$.

Then each a_j is a linear combination of f_j , $a_j = M_1 f_1 + \dots + M_k f_k$.

Then $P(h) = h + \sum_{k=0}^{\infty} a_k(\lambda) h^k = h + M_1 f_1 + \dots + M_k f_k$: it is the general formula of the return map.

If we take $\epsilon \rightarrow \lambda_i = \lambda_i(\epsilon) \Rightarrow f_1 = \epsilon + \dots, f_2 = \epsilon^2 + \dots, f_k = \epsilon^k + \dots$

Then $P(h) = h + \epsilon M_1(h, \lambda) + \epsilon^2 M_2(h, \lambda) + \dots + \epsilon^k M_k(h, \lambda) + O(\epsilon^{k+1})$.

Therefore, the power series expansion of the first return map takes the form

$$P_\lambda(h) - h = \epsilon^k M_k(h) + O(\epsilon^{k+1}) \quad (1.12)$$

where M_k is the k-th order Melnikov function not identically zero, associated to P_λ . The function $O(\epsilon)$, by abuse of notation, depends on h, λ too, but it is of $O(\epsilon)$ type uniformly in h, λ , where h belongs to a compact complex domain in which the return map is regular.

The principality of the Bautin ideal is equivalent to the claim, that $M_k(h)$ is not identically zero.

Chapter 2

Special cubic perturbations of $\ddot{x} = x - x^3$

We are interested in this chapter of the cyclicity of the exterior period annulus of the asymmetrically perturbed Duffing oscillator, then, we provide a complete bifurcation diagram for the number of the zeros of the associated Melnikov function in a suitable complex domain.

2.1 Generalities about the Duffing oscillator

The **Duffing equation** (or **Duffing oscillator**) named after Georg Duffing, is a non-linear second-order differential equation used to model certain damped and driver oscillators.

The equation is given by

$$\ddot{x} + \delta\dot{x} + \beta x + \alpha x^3 = \gamma \cos(\omega t)$$

where the (unknown) function $x = x(t)$ is the displacement at time t , \dot{x} is the first derivative of x with respect to time and \ddot{x} is the second time derivative of x , i.e. acceleration. the numbers δ , α , β , γ and ω are given constants.

The Duffing equation is an example of dynamical system that exhibits chaotic behavior.

For $\beta > 0$, the Duffing oscillator can be interpreted as a forced oscillator with a spring whose restoring force is written as $F = -\beta x - \alpha x^3$.

For $\beta < 0$, the Duffing oscillator describes the dynamics of a point mass in a double well potential, and it can be regarded as a model of a periodically forced steel beam which is deflected toward the two magnets.

In this thesis, the dynamics of the unforced system ($\gamma = 0$) is examined when there is no damping ($\delta = 0$), the Duffing equation can be integrated as $E(t) = \frac{1}{2}\dot{x}^2 + \frac{1}{2}\beta x^2 + \frac{1}{4}\alpha x^4 = \text{const.}$

Therefore in this case, the Duffing equation is Hamiltonian system .

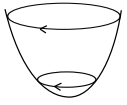
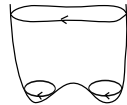
$\alpha > 0$	$\delta = 0$
$\beta > 0$	
$\beta < 0$	

Figure 2.1: The shape of $E(t)$ and schematic trajectories of the Duffing oscillator in the $(x, \dot{x}, E(t))$

We are interestingly in the rest of this thesis with the special case $\delta = 0$, $\alpha = 1$, $\beta = -1$ with no forcing;

$$\begin{cases} \dot{x} = y \\ \dot{y} = x - x^3 \end{cases}$$

2.2 Introduction

Consider the asymmetrically perturbed Duffing oscillator

$$X_{\lambda, \nu} : \begin{cases} \dot{x} = y \\ \dot{y} = x - x^3 + \nu x^2 + \lambda_0 y + \lambda_1 x y + \lambda_2 x^2 y \end{cases} \quad (2.1)$$

in which ν, λ_i are small real parameters. For $\nu = \lambda_0 = \lambda_1 = \lambda_2 = 0$ the system is integrable, with a first integral

$$H = \frac{y^2}{2} - \frac{x^2}{2} + \frac{x^4}{4} \quad (2.2)$$

and its phase portrait is shown on fig.2.2. Alternatively, the system (2.1) defines a real plane foliation by the formula

$$d\left(H - \nu \frac{x^3}{3}\right) + (\lambda_0 + \lambda_1 x + \lambda_2 x^2) y dx = 0 \quad (2.3)$$

2.2 Introduction

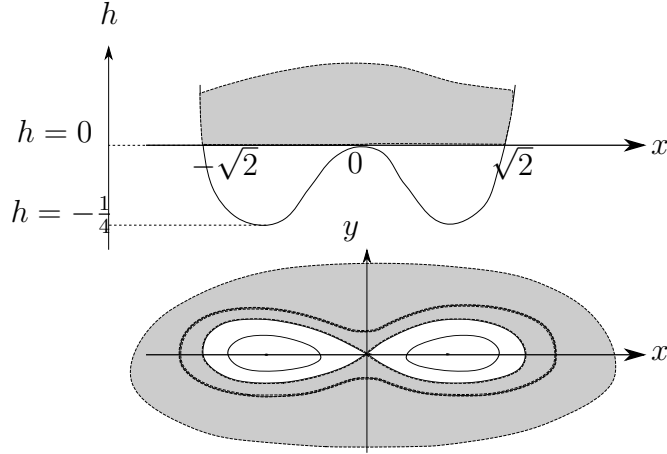


Figure 2.2: Phase portrait of X_0 on the (x, y) -plane and the graph of $h = -\frac{x^2}{2} + \frac{x^4}{4}$

From Fig. 2.2 we see that as h increases from h^c , $+\infty$ the schemas of ovals of the sextic algebraic curves defined by $H(x, y) = h$ will be varied as follows:

- (1) $h \in (h^c, h^s)$: there exist 2 periodic orbits $\Gamma_{int_i}^h$, $i = 1, 2$, enclosing the centers $(\pm 1, 0)$. When $h \rightarrow h^s$ $\Gamma_{int_i}^h$ approaches a saddle point an inner boundary of the period annulus consisting of a homoclinic loop;
- (2) $h = h^s$: there exist 2 symmetric homoclinic orbits $\Gamma_{int_i}^{h^s}$ connecting the saddle point $(0, 0)$, we have then the configuration of eight loop Γ_∞ ;
- (3) $h \in (h^s, +\infty)$: there is a global period annulus Γ_{ext}^h enclosing all 3 singular points.

Theorem 2.2.1 (Mardesic-Roussarie [40], Iliev-Perko [33]) *The maximal number of limit cycles, which bifurcate from the exterior period annulus of X_0 with respect to the perturbation $X_{\lambda, \nu}$ is equal to two.*

Theorem 2.2.2 [33, 40] *The cyclicity of the exterior period annulus $\{(x, y) \in \mathbb{R}^2 : H(x, y) > 0\}$ of $dH = 0$ with respect to the perturbation (2.1) equals two.*

Remark 2.2.3 *The above Theorem claims that from any compact, contained in the open exterior period annulus $\{(x, y) \in \mathbb{R}^2 : H(x, y) > 0\}$, bifurcate at most two limit cycles. It says nothing about the limit cycles bifurcating from the separatrix eight-loop or from infinity (i.e. the equator of the Poincaré sphere).*

Let $\{\gamma(h)\}_h$ be the continuous family of exterior ovals of the non-perturbed system, where

$$\gamma(h) \subset \{H = h\}$$

and consider the complete elliptic integrals

$$I_i = \oint_{\gamma(h)} x^i y dx. \quad (2.4)$$

It has been shown in [33], that if we restrict our attention to a one parameter deformation

$$\lambda_i = \lambda_i(\varepsilon), \nu = \nu(\varepsilon)$$

then the first non-vanishing Poincaré-Pontryagin-Melnikov function M_k (governing the bifurcation of limit cycles) is given by a linear combination of the complete elliptic integrals of first and second kind I_0, I_2, I_4'

$$M_k(h) = \lambda_{0k} I_0(h) + \lambda_{2k} I_2(h) + \lambda_{4k} I_4'(h). \quad (2.5)$$

We recall that if P_ε is the first return map of the perturbed vector field $X_{\lambda(\varepsilon), \nu(\varepsilon)}$, parametrized by the restriction h of the first integral $H(x, y)$ on a suitable cross-section, then for the displacement map $P_\varepsilon - id$ holds 1.12, we recall:

$$P_\varepsilon(h) - h = \varepsilon^k M_k(h) + O(\varepsilon^{k+1})$$

The above identity holds true uniformly in h on every given compact subset of the interval of definition $(0, \infty)$, and hence the zeros of the function M_k on $(0, \infty)$ approximate the limit cycles (fixed points of the displacement map) bifurcating from the exterior period annulus of X_0 .

It is shown, by making use of Picard-Fuchs equations combined with Rolle's theorem in a real domain, that the space of elliptic integrals of first and second kind I_0, I_1, I_4' satisfy the Chebyshev property. This means that each non-trivial linear combination of these three functions has at most two zeros counted with multiplicity, on the interval $(0, \infty)$. The method is described in details in [32, Iliev]. This result is further generalized for multi-parameter deformations. It turns out that the Bautin ideal associated to the deformation can be always principalized (this is a general fact), and that the leading term of the displacement map is given again by a function of the form (2.5), which completes the proof of Theorem 2.2.2, see [40].

The purpose of the present chapter is to study the number of the zeros of the family $\{I_0, I_1, I_4'\}$ in the complex domain $\mathcal{D} = \mathbb{C} \setminus (-\infty, 0]$. We use the well known Petrov method which is based on the argument principle. To find the exact number of zeros we construct the bifurcation diagram of zeros of M_k in \mathcal{D} in the spirit of [21, fig.4]. The result is summarized in Theorem 2.6.2 and Figure 2.6, which is the main result of this chapter. This gives an information on the complex limit cycles of the system, and implies in particular that the number of corresponding limit cycles can not exceed three. It can be also seen as a complex counterpart of Theorem 2.2.2.

Our primary motivation was that the complex methods we use, are necessary to understand the bifurcations from the separatrix eight-loop, see remark 2.2.3 above. Another reason is, that the complexity of the bifurcation set of M_k in a complex domain is directly related to the number of the zeros of M_k . This observation can be possibly generalized to higher genus curves.

This chapter is organized as follows. In section 2.3 we recall some known Picard-Fuchs equations, which will be used later. The monodromy of the Abelian integrals, based on the classical Picard-Lefschetz theory is described in section 2.4. The Petrov method is then applied in section 2.5. The main result is that the principal part of the displacement map can have at most four zeros in a complex domain, a result which is not optimal - see Lemma 2.5.2. The exact upper bound for the number of the zeros in a complex domain turns out to be three. This result, together with the bifurcation diagram of zeros in a complex domain is given in section 2.6.

2.3 Picard-Fuchs equations

The results of this section are known, or can be easily deduced, see [33, 34, 48].

First we note that the affine algebraic curve

$$\Gamma_h = \{(x, y) \in \mathbb{C} : H(x, y) = h\}$$

is smooth for $h \neq 0, -1/4$ and has the topological type of a torus with two removed points $\pm\infty$ (at "infinity"). Its homology group is therefore of rang three, the corresponding De Rham group has for generators the (restrictions of) polynomial differential one-forms

$$ydx, xydx, x^2ydx$$

which are also generators of the related Brieskorn-Petrov $\mathbb{C}[h]$ -module [19].

Because of the symmetry $(x, y) \rightarrow (\pm x, y)$ the Abelian integrals $I_{2k+1}(h)$ vanish identically, while I_{2k} , as well their derivatives can be expressed as linear combinations of I_0, I_2 , with coefficients in the field $\mathbb{C}(h)$.

Lemma 2.3.1

The integrals $I_i, i = 0, 2$, satisfy the following Picard-Fuchs system :

$$I_0(h) = \frac{4}{3}hI_0'(h) + \frac{1}{3}I_2'(h) \tag{2.6}$$

$$I_2(h) = \frac{4}{15}hI_0'(h) + \left(\frac{4}{5}h + \frac{4}{15}\right)I_2'(h) \tag{2.7}$$

$$(4h + 1)I_4'(h) = 4hI_0(h) + 5I_2(h) \tag{2.8}$$

$$4h(4h + 1)I_0''(h) = -3I_0(h). \tag{2.9}$$

Proof See proof of lemma5 of Petrov [44] to take an idea.

We have:

$$\begin{aligned} I_i(h) &= \oint_{\gamma(h)} x^i y dx \\ I'_i(h) &= \oint_{\gamma(h)} \frac{x^i}{y} dx \end{aligned}$$

★ Express $I_0(h)$ in function of $I'_0(h)$ and $I'_2(h)$.

$$\text{We have } I_0(h) = \oint_{\gamma(h)} y dx = \oint_{\gamma(h)} \frac{y^2}{y} dx = \oint_{\gamma(h)} \frac{2h+x^2-\frac{1}{2}x^4}{y} dx$$

$$I_0(h) = 2hI'_0(h) + I'_2(h) - \frac{1}{2}I'_4(h) \quad (2.10)$$

* Express x^4 in function of x^2 et x .

We have $d(xy^3) = y^3 dx + xdy^3$ or :

$$\bullet y^3 dx = (2yh + x^2y - \frac{1}{2}x^4y) dx$$

$$\bullet xdy^3 = xd(\sqrt{2h+x^2-\frac{1}{2}x^4})^3 = (3x^2y - 3x^4y) dx$$

$$\text{Then } d(xy^3) = (2yh + 4x^2y - \frac{7}{2}x^4y) dx$$

$$\text{Or } \oint_{\gamma(h)} d(xy^3) = 0 \Rightarrow 2hI_0(h) + 4I_2(h) - \frac{7}{2}I_4(h) = 0 \Rightarrow I_4(h) = \frac{4h}{7}I_0(h) + \frac{8}{7}I_2(h).$$

$$\text{Thus } I'_4(h) = \frac{4I_0(h)}{7} + \frac{4h}{7}I'_0(h) + \frac{8}{7}I'_2(h).$$

Expressing $I'_4(h)$ in (2.10) we find :

$$I_0(h) = \frac{4}{3}hI'_0(h) + \frac{1}{3}I'_2(h).$$

★ Express $I_2(h)$ in function of $I'_0(h)$ and $I'_2(h)$.

$$\text{We have } I_2(h) = \oint_{\gamma(h)} x^2 y dx = \oint_{\gamma(h)} x^2 \frac{y^2}{y} dx = \oint_{\gamma(h)} x^2 \frac{2h+x^2-\frac{1}{2}x^4}{y} dx$$

$$I_2(h) = 2hI'_2(h) + I'_4(h) - \frac{1}{2}I'_6(h) \quad (2.11)$$

* Express x^6 in function of x^4 and x^2 .

2.3 Picard-Fuchs equations

We have $d(x^3y^3) = 3x^2y^3dx + x^3dy^3$ or :

- $3x^2y^3dx = (6x^2yh + 3x^4y - \frac{3}{2}x^6y)dx$
- $x^3dy^3 = x^3d(\sqrt{2h + x^2 - \frac{1}{2}x^4})^3 = (3x^4y - 3x^6y)dx$

Then $d(xy^3) = (6hx^2y + 6x^4y - \frac{9}{2}x^6y)dx$

Or $\oint_{\gamma(h)} d(x^3y^3) = 0 \Rightarrow 6hI_2(h) + 6I_4(h) - \frac{9}{2}I_6(h) = 0$

Thus $I'_6(h) = \frac{4I_2(h)}{3} + \frac{4h}{3}I'_2(h) + \frac{4}{3}I'_4(h)$.

Expressing $I'_6(h)$ and $I'_4(h)$ in (2.11) we find :

$$I_2(h) = \frac{4}{15}hI'_0(h) + (\frac{4}{5}h + \frac{4}{15})I'_2(h).$$

By using (2.10) and the above equations of Picards-Fuchs we have:

$$I'_4(h) = \frac{1}{4(h+1)}(hI_0 - 5I_2)$$

By using the below Picard-Fuchs equations we have:

$$I'_0(h) = -4hI''_0(h) - 4I''_2(h) \quad (2.12)$$

$$I'_2(h) = -4hI''_0(h) + 4hI''_2(h) \quad (2.13)$$

and by using (2.10), we can have $4h(4h+1)I''_0(h) = -3I_0(h)$. \square

The above equations imply the following asymptotic expansions near $h = 0$ (they agree with the Picard-Lefschetz formula)

Lemma 2.3.2 *The integrals I_i , $i = 0, 2$, and I'_4 have the following asymptotic expansions in the neighborhood of $h = 0$:*

$$I_0(h) = (-h + \frac{3}{8}h^2 - \frac{35}{64}h^3 + \dots) \ln h + \frac{4}{3} + a_1h + a_2h^2 + \dots$$

$$I_2(h) = (\frac{1}{2}h^2 - \frac{5}{8}h^3 - \frac{315}{256}h^4 \dots) \ln h + \frac{16}{15} + 4h + b_2h^2 + \dots$$

$$I'_4(h) = (-\frac{3}{2}h^2 + \frac{35}{8}h^3 - \frac{471}{256}h^4 + \dots) \ln h + \frac{16}{3} + 4h + (4a_1 + 5b_2 - \frac{304}{3})h^2 + \dots$$

Proof For proof see [26].

We have $\oint_{\gamma(h)} w_i = \frac{\ln h}{2\pi k} \oint_{\delta(h)} w_i + P(h)$.

Proof If we take:

$$\oint_{\gamma(h)} w_i - \frac{\ln h}{2\pi k} \oint_{\delta(h)} w_i = P(h).$$

Or by applying the theories of Picard-Lefschetz for $\oint_{\gamma(h)} w_i$: we have

- $\gamma(h) \rightarrow \gamma(h) + \delta(h)$
- $\delta(h) \rightarrow \delta(h)$

and because of the monodromy we have $\ln h \rightarrow \ln h + 2\pi k$ (after a tour)

$$\oint_{\gamma(h)+\delta(h)} w_i - \frac{(\ln h + 2\pi k)}{2\pi k} \oint_{\delta(h)} w_i = \oint_{\gamma} w_i - \frac{\ln h}{2\pi k} \oint_{\delta(h)} w_i = P(h)$$

We arrive at the departure equation then $P(h)$ is uniform

for $i = 0$: $I_0(h) = \frac{\ln h}{2\pi k} \oint_{\delta(h)} y dx + P(h)$ the same for $i = 2$: $I_2(h) = \frac{\ln h}{2\pi k} \oint_{\delta(h)} x^2 y dx + P(h)$

- $\int_{\delta(h)} y dx = \int \int dx dy =$ the air of surface $\delta(h) = \pi r^2 = \pi h$ (for $|x| = \sqrt{h}$)

Then $\oint_{\delta(h)} y dx \simeq h$, thus the first coefficient of $\ln h$ in $I_0(h)$ starts with h .

- $\int_{\delta(h)} x^2 y dx = h \int_{\delta(h)} y dx \simeq h^2$, thus the first coefficient of $\ln h$ in $I_2(h)$ starts with h^2 .

Then:

$$\begin{aligned} I_0(h) &= [q_{0,0}h + q_{1,0}h^2 + q_{2,0}h^3 + \dots] \ln h + a_0 + a_1h + a_2h^2 + \dots \\ I_2(h) &= [q_{0,2}h^2 + q_{1,2}h^3 + q_{2,2}h^4 + \dots] \ln h + b_0 + b_1h + b_2h^2 + \dots \end{aligned}$$

* Compute a_0 :

$$a_0 = I_0(h)|_{h=0} = \text{Air} = \int \int_{\gamma(0)} dx dy.$$

We have for $H = 0$, $y = |x| \sqrt{1 - \frac{x^2}{2}}$

$$\text{Then } a_0 = \int_{\mu(0)} y dx = \int_{-\sqrt{2}}^{\sqrt{2}} y dx = 2 \int_0^{\sqrt{2}} y dx = \frac{4}{3}$$

2.3 Picard-Fuchs equations

* Compute b_0 :

$$b_0 = I_2(h)|_{h=0} = \int_{\gamma(0)} x^2 y dx = 2 \int_0^{\sqrt{2}} x^2 y dx = \frac{16}{15} \text{ (using integration by parts).}$$

* Compute b_1 :

$$b_1 = I_2'(h)|_{h=0} = \int_{\gamma(0)} \frac{x^2}{y} dx = 2 \int_0^{\sqrt{2}} \frac{x^2}{\sqrt{x^2 - \frac{x^4}{2}}} = 4.$$

* Compute $q_{0,0}$:

$$\text{We have } 4h(4h+1)I_0''(h) = -3I_0'(h) \Rightarrow 16h^2 I_0''(h) + 4h I_0''(h) = -3I_0'(h)|_{h=0} \Rightarrow q_{0,0} = -1$$

* Compute $q_{0,2}$, $q_{1,0}$, $q_{1,2}$, $q_{2,0}$ and $q_{2,2}$

$$\text{We have } I_0(h) = \frac{4}{3}hI_0'(h) + \frac{1}{3}I_2'(h)$$

Then

$$[q_{0,0}h + q_{1,0}h^2 + q_{2,0}h^3 + \dots] \ln h + a_0 + a_1h + a_2h^2 + \dots = [\frac{4}{3}q_{0,0}h + \frac{8}{3}q_{1,0}h^2 + 4q_{2,0}h^3 + \dots] \ln h + [\frac{4}{3}q_{0,0}h + \frac{4}{3}q_{1,0}h^2 + \dots] + \frac{4}{3}a_1h + \frac{8}{3}a_2h^2 + [\frac{2}{3}q_{0,2}h + q_{1,2}h^2 + \frac{4}{3}q_{2,2}h^3 + \dots] \ln h + \frac{1}{h}[\frac{q_{0,2}}{3}h^2 + \dots] + \frac{1}{3}b_1 + \frac{2}{3}b_2h$$

$$\text{By identification, we have: } q_{0,0} = \frac{4}{3}q_{0,0} + \frac{2}{3}q_{0,2} \Rightarrow q_{0,2} = \frac{1}{2}$$

we also have:

$$q_{2,0} = -\frac{4}{9}q_{2,2}. \quad (2.14)$$

$$q_{1,0} = \frac{8}{3}q_{1,0} + q_{1,2} \Rightarrow q_{1,2} = -\frac{5}{3}q_{1,0}$$

$$\text{Or we have } I_2(h) = \frac{4}{15}hI_0'(h) + (\frac{4}{5}h + \frac{4}{15})I_2'(h)$$

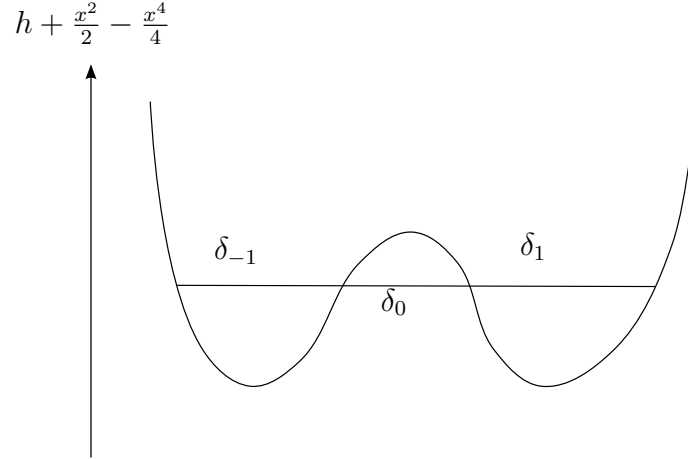
Then

$$[q_{0,2}h^2 + q_{1,2}h^3 + q_{2,2}h^4 + \dots] \ln h + b_0 + b_1h + b_2h^2 + \dots = [\frac{4}{15}q_{0,0}h + \frac{8}{15}q_{1,0}h^2 + \frac{12}{15}q_{2,0}h^3 + \dots] \ln h + [\frac{4}{15}q_{0,0}h + \frac{4}{15}q_{1,0}h^2 + \dots] + \frac{4}{15}a_1h + \frac{8}{15}a_2h^2 + [\frac{8}{5}q_{0,2}h^2 + \frac{12}{5}q_{1,2}h^3 + \frac{16}{5}q_{2,2}h^4 + \dots] \ln h + [\frac{8}{15}q_{0,2}h + \frac{12}{15}q_{1,2}h^2 + \frac{16}{15}q_{2,2}h^3 + \dots] \ln h + \frac{1}{h}[\frac{4q_{0,2}}{15}h^2 + \dots] + \frac{4}{15}b_1 + \frac{8}{15}b_2h$$

$$\text{By identification, we have: } q_{0,2} = \frac{8}{15}q_{1,0} + \frac{4}{5}q_{0,2} + \frac{12}{15}q_{1,2} \Rightarrow q_{1,0} = \frac{3}{8} \Rightarrow q_{1,2} = -\frac{5}{8}$$

We also have:

$$q_{1,2} = \frac{12}{15}q_{2,0} + \frac{12}{5}q_{1,2} + \frac{16}{15}q_{2,2}. \text{ Then By using (2.14) we have: } q_{2,0} = -\frac{35}{64} \Rightarrow q_{2,2} = -\frac{315}{256}$$


 Figure 2.3: The vanishing cycles $\delta_0(h), \delta_1(h), \delta_{-1}(h)$ for $-\frac{1}{4} < h < 0$
Conclusion 1

$$q_0 = \begin{pmatrix} q_{0,0} \\ 0 \end{pmatrix} = \begin{pmatrix} -1 \\ 0 \end{pmatrix}, \quad q_1 = \begin{pmatrix} q_{1,0} \\ q_{0,2} \end{pmatrix} = \begin{pmatrix} \frac{3}{8} \\ \frac{1}{2} \end{pmatrix}, \quad q_3 = \begin{pmatrix} q_{2,0} \\ q_{1,2} \end{pmatrix} = \begin{pmatrix} -\frac{35}{64} \\ -\frac{315}{256} \end{pmatrix}, \dots$$

* compute the asymptotic expansions of I'_4

$$\text{We have } I'_4 = \frac{1}{4(h+1)}(4hI_0 + 5I_2)$$

Conclusion 2

$$I'_4(h) = \left(-\frac{3}{2}h^2 + \frac{35}{8}h^3 - \frac{471}{256}h^4 + \dots\right) \ln h + \frac{16}{3} + 4h + (4a_1 + 5b_2 - \frac{304}{3})h^2 + \dots$$

□

2.4 The monodromy of Abelian integrals

The Abelian integrals $I(h)$ of the form (2.4) are multivalued functions in $h \in \mathbb{C}$ which become single-valued analytic functions in the complex domain

$$\mathcal{D} = \mathbb{C} \setminus (-\infty, 0].$$

Along the segment $(-\infty, 0]$ the integrals have a continuous limit when $h \in \mathcal{D}$ tends to a point $h_0 \in [0, -\infty)$, depending on the sign of the imaginary part of h . When $\text{Im}(h) > 0$ we denote the corresponding limit by $I^+(h)$, and when $\text{Im}(h) < 0$ by $I^-(h_0)$. We use a similar notation for the continuous limits of loops $\gamma(h)$ when h tends to the segment $[0, -\infty)$. We have therefore

$$I^\pm(h) = \int_{\gamma^\pm(h)} \omega$$

2.4 The monodromy of Abelian integrals

where ω is a polynomial one-form, and the monodromy $I^+(h) - I^-(h)$, $h \in [0, -\infty)$ depends on the homology class of $\gamma^+(h) - \gamma^-(h)$ which is expressed by the Picard-Lefschetz formula. Namely, for $h \in \mathcal{D}$, define the continuous families of closed loops

$$\delta_0(h), \delta_1(h), \delta_{-1}(h) \subset \{(x, y) \in \mathbb{C}^2 : H(x, y) = h\}, \quad H(x, y) = \frac{y^2}{2} - \frac{x^2}{2} + \frac{x^4}{4}$$

as follows. First, for $h \in (-1/4, 0)$ let $\delta_1^+(h), \delta_{-1}^+(h)$ be the real ovals of $\{(x, y) \in \mathbb{R}^2 : H(x, y) = h\}$, defined by

$$\{(x, y) \in \mathbb{R}^2 : y = \pm \sqrt{h + \frac{x^2}{2} - \frac{x^4}{4}}, x_1 \leq x \leq x_2, -x_2 \leq x \leq -x_1\}$$

where, $-x_2, -x_1, x_1, x_2$ are the four real roots of $h + \frac{x^2}{2} - \frac{x^4}{4}$, as it is shown on fig.2.3. To visualize the loop $\delta_0^+(h)$ we consider the substitution $y \rightarrow iy$, after which the loop $\delta_0^+(h)$ is transformed to the oval of the curve

$$\{(x, y) \in \mathbb{R}^2 : -\frac{y^2}{2} - \frac{x^2}{2} + \frac{x^4}{4} = h\}.$$

The three families of loops $\delta_0(h), \delta_1(h), \delta_{-1}(h)$ are obtained by continuous deformations of $\delta_0^+(h), \delta_1^+(h)$ and $\delta_{-1}^+(h)$ to the half plane $\{h \in \mathbb{C} : \text{Im } h \geq 0\}$, and finally to the domain $h \in \mathcal{D}$. The reader familiar with the Picard-Lefschetz theory will note that $\delta_0(h), \delta_1(h), \delta_{-1}(h)$ represent continuous families of one-cycles, vanishing at the singular points of H , when h tends to the singular values $h = 0$ and $h = -1/4$, along paths contained in the upper half-plane $\{h \in \mathbb{C} : \text{Im } h \geq 0\}$. Therefore they form a distinguished family of vanishing cycles, to which we are going to apply the Picard-Lefschetz formula, see [3] for details.

The above construction defines uniquely the homology classes of the vanishing loops, up to an orientation. From now on we suppose that the loop $\gamma(h) \subset \{(x, y) \in \mathbb{R}^2 : H(x, y) = h\}$ for $h > 0$ is oriented by the vector field X_0 , and that the orientation of $\delta_0(h), \delta_1(h), \delta_{-1}(h)$ are chosen in such a way that

$$\gamma(h) = \delta_0(h) + \delta_1(h) + \delta_{-1}(h), \quad h \in \mathcal{D}.$$

According to the definition of the vanishing cycles

$$\gamma^+(h) = \delta_0^+(h) + \delta_1^+(h) + \delta_{-1}^+(h), \quad h \in (-\infty, 0]. \quad (2.15)$$

and the Picard-Lefschetz formula [3] implies

$$\gamma^-(h) = -\delta_0^+(h) + \delta_1^+(h) + \delta_{-1}^+(h), \quad h \in [-1/4, 0] \quad (2.16)$$

and

$$\gamma^-(h) = -\delta_0^+(h), \quad h \in (-\infty, -1/4] \quad (2.17)$$

For a further use we note that

$$\delta_0^-(h) = \delta_0^+(h), \quad h \in (-1/4, +\infty) \quad (2.18)$$

$$\delta_1^-(h) = \delta_1^+(h), \quad \delta_{-1}^-(h) = \delta_{-1}^+(h), \quad h \in (-\infty, 0) \quad (2.19)$$

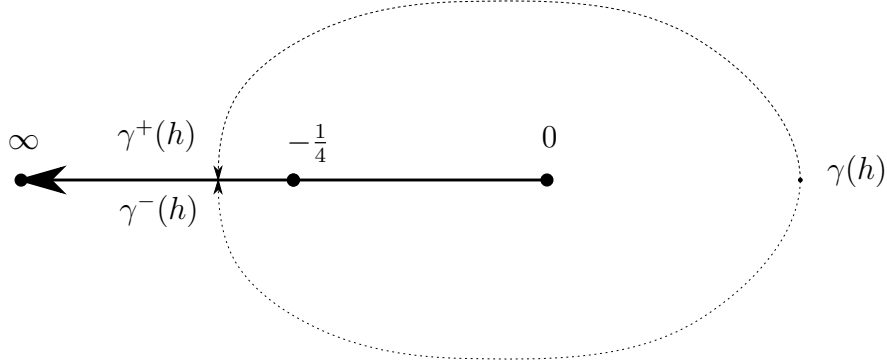


Figure 2.4: The analytic continuation of a cycle $\gamma(h_0)$ in the domain \mathcal{D}

2.5 The zeros of the principal part of the displacement map in a complex domain

If the first Poincaré-Pontryagin-Melnikov function $M_1(h)$ is not identically zero, then

$$M_1(h) = \lambda_0 I_0(h) + \lambda_2 I_2(h), \lambda_i \in \mathbb{R} \quad (2.20)$$

If $M_1 = 0$ the first non-vanishing Melnikov function M_k has the form [32], [33]

$$M_k(h) = \lambda_{0k} I_0(h) + \lambda_{2k} I_2(h) + \lambda_{4k} I_4'(h), \quad k \geq 2. \quad (2.21)$$

where the coefficients $\lambda_{0k}, \lambda_{2k}, \lambda_{4k}$ depend on the initial parameters $\lambda_0, \lambda_1, \lambda_2$. Following [40], we call the Abelian integral $M_k(h)$ *the principal part of the displacement map* of the system (2.1), associated to the exterior period annulus of X_0 .

Lemma 2.5.1 *If the first Poincaré-Pontryagin-Melnikov function M_1 given in (2.20) is not identically zero, then it has at most two zeros in the complex domain \mathcal{D} .*

Lemma 2.5.2 *The principal part (2.21) of the displacement map has at most four zeros in the complex domain \mathcal{D} .*

Lemma 2.5.3 *The Abelian integrals $I_0(h)$ and $I_0'(h)$ do not vanish in \mathcal{D} .*

Proof of Lemma 2.5.3 $I_0'(h)$ is a period of the holomorphic one-form $\frac{dx}{y}$ on the elliptic curve Γ_h , and therefore does not vanish. For real values of h $I_0'(h)$ represents the period of the orbit $\gamma(h)$ of $dH = 0$, while $I_0(h)$ equals the area of the interior of $\gamma(h)$. It is remarkable, that $I_0(h)$ does not vanish in a complex domain too. Indeed, consider the analytic function

$$F(h) = \frac{I_0(h)}{I_0'(h)}, h \in \mathcal{D}.$$

We shall count its zeros in \mathcal{D} by making use of the argument principle.

2.5 The zeros of the principal part of the displacement map in a complex domain

Let $\mathcal{D} \subset \mathbb{C}$ be a relatively compact domain, with a piece-wise smooth boundary. We suppose, that $f : \mathcal{D} \rightarrow \mathbb{C}$ is a continuous function, which is complex-analytic in D , except at a finite number of points on the border $\partial\mathcal{D}$. We suppose also that f does not vanish on ∂D . Denote by $Z_{\mathcal{D}}(f)$ the number of zeros of f in \mathcal{D} , counted with multiplicity. The increment of the argument $\text{Var}_{\partial\mathcal{D}}(\text{arg}f)$ of f along $\partial\mathcal{D}$ oriented counter-clockwise is well defined and equals the winding number of the curve $f(\partial\mathcal{D}) \subset \mathbb{C}$ about the origin, divided by 2π . The argument principle states then that

$$2\pi Z_{\mathcal{D}}(f) = \text{Var}_{\partial\mathcal{D}}(\text{arg}f) \quad (2.22)$$

Apply now the argument principle to the function F in the intersection of a big disc with a radius R and the complex domain \mathcal{D} . Along the circle of radius R , for R sufficiently big, the decrease of the argument of F is close to 2π , while along the branch cut $(-\infty, 0)$ we have

$$\begin{aligned} 2\sqrt{-1}\text{Im}(F(h) = F^+(h) - F^-(h)) &= \frac{I_0(h)}{I_0'(h)} - \frac{\overline{I_0(h)}}{\overline{I_0'(h)}} \\ &= \frac{\oint_{\gamma^+} y dx}{\oint_{\gamma^+} \frac{dx}{y}} - \frac{\oint_{\gamma^-} y dx}{\oint_{\gamma^-} \frac{dx}{y}} = \frac{W(h)}{|\oint_{\gamma^+} \frac{dx}{y}|^2}. \end{aligned}$$

where

$$W(h) = \det \begin{pmatrix} \oint_{\gamma^+} y dx & \oint_{\gamma^+} \frac{dx}{y} \\ \oint_{\gamma^-} y dx & \oint_{\gamma^-} \frac{dx}{y} \end{pmatrix}.$$

According to section 2.4, the function has two different determinations along $(-\infty, -1/4)$ and $(-1/4, 0)$, both of which have no monodromy, and hence are rational in h . In fact, (2.6) implies that in both of the cases $W(h)$ is a non-zero constant. If $W(h) = c$ in $(-\infty, -1/4)$, then it equals $2c$ in $(-1/4, 0)$. Therefore along the branch cut the argument of F^+ or F^- increases by at most π . Summing up the above information, we conclude that F has no zeros in \mathcal{D} .

Proof of Lemma 2.5.1 We denote

$$F(h) = \frac{M_1(h)}{I_0(h)} = \lambda_2 \frac{I_2(h)}{I_0(h)} + \lambda_0, h \in \mathcal{D}$$

and apply, as in the proof of Lemma 2.5.3, the argument principle to F . Along a big circle the increase of the argument of F is close to π . Along the branch cut $(-\infty, 0]$ we have

$$2\sqrt{-1}\text{Im}(F(h)) = F^+(h) - F^-(h) = \lambda_2 \frac{W(h)}{|I_0(h)|^2}$$

where

$$W(h) = \det \begin{pmatrix} \oint_{\gamma^+} yx^2 dx & \oint_{\gamma^+} y dx \\ \oint_{\gamma^-} yx^2 dx & \oint_{\gamma^-} y dx \end{pmatrix} = ch(4h + 1), c = \text{const.} \neq 0.$$

Therefore the imaginary part of $F(h)$ along the branch cut $(-\infty, 0)$ vanishes at most once, at $-1/4$. Summing up the above information, we get that F has at most two zeros in the complex domain \mathcal{D} .

Proof of Lemma 2.5.2 We denote

$$F(h) = (4h + 1) \frac{M_k(h)}{I_0(h)}, h \in \mathcal{D}$$

and apply, as in the proof of Lemma 3.4.8, the argument principle to F . By making use of (2.21) we have

$$F(h) = \alpha(h) \frac{I_2(h)}{I_0(h)} + \beta(h) \quad (2.23)$$

where

$$\alpha(h) = (4h + 1)\lambda_2 + 5\lambda_4, \quad \beta(h) = (4h + 1)\lambda_0 + 4h\lambda_4. \quad (2.24)$$

Along a big circle the increase of the argument of F is close to 3π . Along the branch cut $(-\infty, 0]$ we have as before

$$2\sqrt{-1} \text{Im}(F(h)) = F^+(h) - F^-(h) = \alpha(h) \frac{W(h)}{|I_0(h)|^2}$$

where

$$W(h) = \det \begin{pmatrix} \oint_{\gamma^+} yx^2 dx & \oint_{\gamma^+} y dx \\ \oint_{\gamma^-} yx^2 dx & \oint_{\gamma^-} y dx \end{pmatrix} = ch(4h + 1), c = \text{const.} \neq 0.$$

Therefore the imaginary part of $F(h)$ along the branch cut $(-\infty, 0)$ vanishes at most twice, at $-1/4$ and at the root of $\alpha(h)$. Summing up the above information, we get that F has at most four zeros in the complex domain \mathcal{D} .

2.6 The bifurcation diagram of the zeros of the Abelian integrals in a complex domain

2.6.1 The first Melnikov function M_1

Let $Z(M_1)$ be the number of the zeros of $M_1(h)$ in the domain \mathcal{D} , counted with multiplicity. It is a function of $[\lambda_0 : \lambda_2]$ seen as a point on the projective circle $S^1 = \mathbb{RP}^1$. The bifurcation

2.6 The bifurcation diagram of the zeros of the Abelian integrals in a complex domain

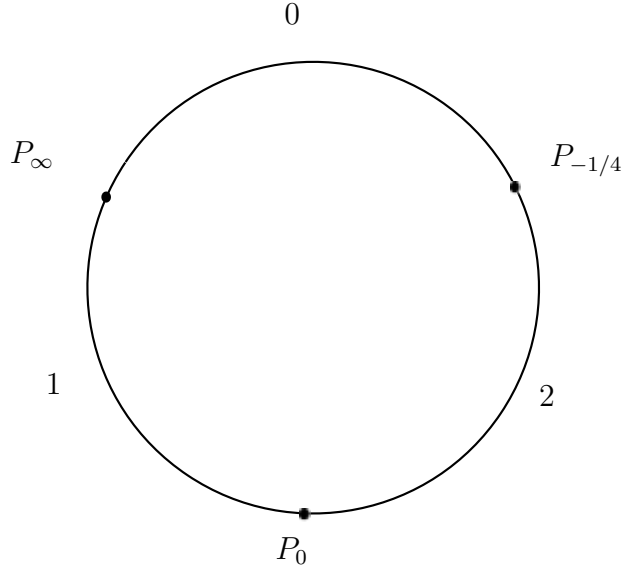


Figure 2.5: Bifurcation diagram of the zeros of the first Melnikov function M_1 in the complex domain \mathcal{D} .

set \mathbf{B} of $Z(M_1)$ is the set of points $[\lambda_0 : \lambda_2] \in \mathbb{RP}^1$ at which $Z(M_1)$ is not a locally constant function. It follows that if $\lambda = [\lambda_0 : \lambda_2]$ is a bifurcation point, then near λ a zero of $M_1(h)$ bifurcates from the border of the domain $\mathcal{D} \subset \mathbb{CP}^1$, see [21, Definition 2]. Therefore

$$\mathbf{B} = P_0 \cup P_{-1/4} \cup P_\infty \cup \Delta$$

where $P_0, P_{-1/4}, P_\infty \in S^1$ are the sets of parameter values λ , corresponding to bifurcations of zeros from $h = 0$, $h = -1/4$ and $h = \infty$ respectively. Finally, Δ is the set corresponding to bifurcations from the branch cut $(-\infty, 0)$. The results of the preceding section imply $\Delta = \emptyset$ while

$$P_0 = \{[\lambda_0 : \lambda_2] : \lambda_0 I_0(0) + \lambda_2 I_2(0) = 0\}, P_{-1/4} = \{[\lambda_0 : \lambda_2] : \lambda_0 I_0(-\frac{1}{4}) + \lambda_2 I_2(-\frac{1}{4}) = 0\}$$

and

$$P_\infty = \{[\lambda_0 : \lambda_2] : \lambda_2 = 0\}.$$

A local analysis shows that when the parameter $[\lambda_0 : \lambda_2]$ crosses P_0 or P_∞ , then a simple zero bifurcates from 0 or ∞ . Similarly, two complex conjugate zeros bifurcate from $h = -1/4$ when $[\lambda_0 : \lambda_2]$ crosses $P_{-1/4}$. This combined with Lemma 3.4.6 implies

Corollary 2.6.1 *The bifurcation diagram of $Z(M_1)$ together with the corresponding number of zeros of M_1 are shown on fig.2.5*

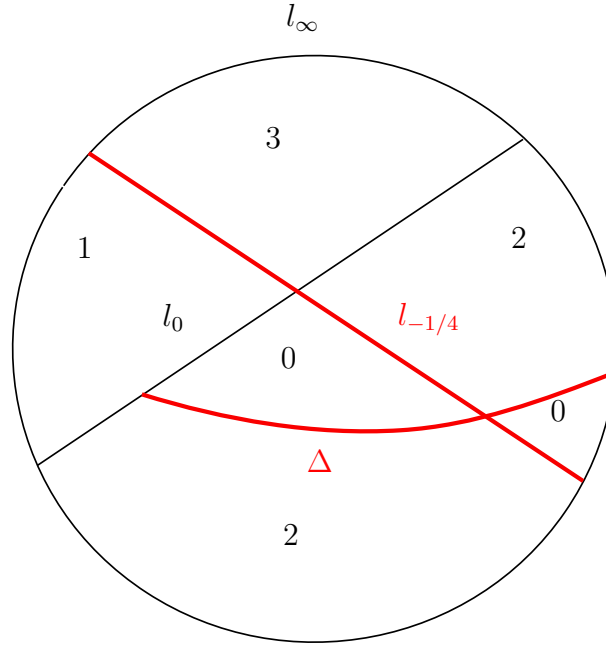


Figure 2.6: Bifurcation diagram of the zeros of M_k , $k \geq 2$, in the complex domain \mathcal{D} .

2.6.2 The principal part M_k of the displacement map

Let M_k , $k \geq 2$, be the first non-vanishing Melnikov function, see (2.5). Denote by $Z(M_k)$ the number of the zeros of $M_k(h)$ in the domain $\mathcal{D} = \mathbb{C} \setminus (-\infty, 0]$, counted with multiplicity. It is a function of $[\lambda_{0k} : \lambda_{2k} : \lambda_{4k}]$ seen as a point on the projective plane \mathbb{RP}^2 . The bifurcation set \mathbf{B} of $Z(M_k)$ is the set of points

$$[\lambda_{0k} : \lambda_{2k} : \lambda_{4k}] \in \mathbb{RP}^2$$

at which $Z(M_k)$ is not a locally constant function. It follows that if $\lambda = [\lambda_{0k} : \lambda_{2k} : \lambda_{4k}]$ is a bifurcation point, then near such a λ a zero of $M_k(h)$ bifurcates from the border of the domain $\mathcal{D} \subset \mathbb{CP}^1$, see [21, Definition 2]. Therefore

$$\mathbf{B} = l_0 \cup l_{-1/4} \cup l_\infty \cup \Delta$$

where $l_0, l_{-1/4}, l_\infty$ are the sets of parameter values λ , corresponding to bifurcations of zeros from $h = 0$, $h = -1/4$ and $h = \infty$ respectively. Finally, Δ is the set of parameter values λ , at which a bifurcation of zero of M_k from $(-\infty, -1/4) \cup (-1/4, 0)$ takes place. We are going to describe these sets explicitly. For convenience, we represent the projective plane \mathbb{RP}^2 by a closed disc as on fig. 2.6. The border of the disc is a circle with identified opposite points. The resulting quotient space is the projective plane \mathbb{RP}^2 .

As $I'_4(0) \neq 0$, then

$$l_0 = \{\lambda \in \mathbb{RP}^2 : \lambda_{0k}I_0(0) + \lambda_{2k}I_2(0) + \lambda_{4k}I'_4(0) = 0\}. \quad (2.25)$$

Similarly,

$$l_\infty = \{\lambda \in \mathbb{RP}^2 : \lambda_{2k} = 0\}. \quad (2.26)$$

A local analysis shows that $I'_4(h) \sim \text{const.} \times \log(4h + 1)$ near $-1/4$ which implies

$$l_{-1/4} = \{\lambda \in \mathbb{RP}^2 : \lambda_{4k} = 0\}. \quad (2.27)$$

Finally, to compute Δ we suppose that for some $h \in (-\infty, -1/4) \cup (-1/4, 0)$, $M_k(h) = \overline{M_k(h)} = 0$. The latter implies $\text{Im}(I(h)) = 0$, and hence $\alpha(h) = 0$ and $\beta(h) = 0$, see (3.27). The condition, that the polynomials $\alpha(h), \beta(h)$ have a common real root imply that either $\lambda_{4k} = 0$ in which case the root is $h = -1/4$, or

$$5(\lambda_{0k} + \lambda_{4k}) + \lambda_{2k} = 0 \quad (2.28)$$

in which case

$$(4h + 1)(\lambda_{0k}I_2(h) + \lambda_{2k}I_2(h) + \lambda_{4k}I'_4(h)) = (4h(\lambda_{0k} + \lambda_{4k}) + \lambda_{0k})(I_0(h) - 5I_2(h))$$

see (2.24). The Abelian integral $I_0(h) - 5I_2(h)$ vanishes at $h = -1/4$ and corresponds therefore to the point $P_{-1/4}$ on fig.2.5. In particular it has no zeros in the domain \mathcal{D} . Thus, in the case when the root of $4h(\lambda_{0k} + \lambda_{4k}) + \lambda_{0k}$ belongs to \mathcal{D} , the Abelian integral M_k has exactly one zero in \mathcal{D} , otherwise it has complex conjugate zeros on $(-\infty, 0)$. This implies from one hand that Δ is the segment of the line (2.28), connecting l_∞ and l_0 as on fig.2.6. On the other hand this implies that in one of the connected components of $\mathbb{RP}^2 \setminus \mathbf{B}$ the function M_k has exactly one zero, as shown on fig.2.6. To determine the number of the zeros of M_k in the remaining connected components of the complement to the bifurcation set in \mathbb{RP}^2 we note that

- when crossing Δ or $l_{-1/4}$ (in bold on the figure) two zeros are added or subtracted
- when crossing l_0 or l_∞ one simple zero is added or subtracted
- the total number of zeros of M_k is not bigger than three

The above considerations, combined with Lemma 2.5.2, determine uniquely the number of the zeros of M_k in each connected component. This is summarized in the following

Theorem 2.6.2 *The bifurcation set $\mathbf{B} \subset \mathbb{RP}^2$ of the zeros $Z(M_k)$ of the principal part of the displacement map, in the complex domain $\mathcal{D} \subset \mathbb{C}$ is the union of the projective lines $l_0, l_{-1/4}, l_\infty$ and the segment Δ connecting l_0 to l_∞ . Their mutual position, together with the corresponding number of zeros of M_k are shown on fig.2.6.*

The bound for the number of the zeros in the above Theorem in the complex domain \mathcal{D} is three, which, according to Theorem 2.2.2, is not optimal on the real interval $(0, \infty)$. It seems impossible to deduce Theorem 2.2.2 from Theorem 2.6.2 by making use of complex methods only.

Chapter 3

General Cubic Perturbations of $\ddot{x} = x - x^3$

We consider arbitrary one-parameter cubic deformations of the Duffing oscillator $x'' = x - x^3$. Our first result is to compute the first Melnikov function M_1 in the interior and exterior cases, next, according to the Iliev formula [32] we can compute M_2 in the case when M_1 vanishes and by using Picard-Fuchs equations. Our second result is an estimate for the number of its zeros in a suitable complex domain in the same way of Iliev and Gavrilov in [27] for the four asymmetric Hamiltonian $H = \frac{1}{2}y^2 + \frac{1}{2}x^2 - \frac{1}{2}x^3 + \frac{a}{4}x^4$, $a \neq 0, \frac{8}{9}$. From this we deduce the maximal cyclicity of the interior and exterior of the period annuli, when at least M_1 or M_2 does not vanish identically.

3.1 Introduction

Consider the perturbed Duffing oscillator

$$X_\epsilon : \begin{cases} \dot{x} &= H_y + \epsilon f(x, y, \epsilon) \\ \dot{y} &= -H_x + \epsilon g(x, y, \epsilon) \end{cases} \quad (3.1)$$

Where $f(x, y, \epsilon)$, $g(x, y, \epsilon)$ are arbitrary cubic polynomials:

$$\begin{aligned} f(x, y, \epsilon) &= \lambda_0 + \lambda_1 x + \lambda_2 y + \lambda_3 xy + \lambda_4 x^2 + \lambda_5 y^2 + \lambda_6 x^2 y + \lambda_7 xy^2 + \lambda_8 x^3 + \lambda_9 y^3 \\ g(x, y, \epsilon) &= \gamma_0 + \gamma_1 x + \gamma_2 y + \gamma_3 xy + \gamma_4 x^2 + \gamma_5 y^2 + \gamma_6 x^2 y + \gamma_7 xy^2 + \gamma_8 x^3 + \gamma_9 y^3 \end{aligned}$$

and the parameters $\lambda_i = \sum_{j \geq 0} \lambda_{i,j} \epsilon^j$, $\lambda_{i,j} \in \mathbb{R}$ and $\gamma_i = \sum_{j \geq 0} \gamma_{i,j} \epsilon^j$, $\gamma_{i,j} \in \mathbb{R}$ are analytic functions of the small parameter ϵ . For $\epsilon = 0$ the system is integrable, with the same first integral mentioned in chapter 2

$$\begin{aligned} H &= \frac{y^2}{2} - \frac{x^2}{2} + \frac{x^4}{4} \\ &= \frac{y^2}{2} - U(x); \text{ where } U(x) = \frac{x^2}{2} - \frac{x^4}{4} \end{aligned}$$

and its phase portrait is shown on fig.2.2. The exterior period annulus and the two interior period annuli on fig.2.2 give rise to three displacement maps of X_ϵ with power series expansions of the form

$$d(h, \epsilon) = \epsilon^k M_k(h) + \epsilon^{k+1} M_{k+1}(h) + \dots$$

(where as usual h is the restriction of H on a suitable cross-section to the period annulus). The number of the limit cycles bifurcating from each period annulus is bounded by the number of the zeros of the first non-vanishing Melnikov function M_k . According to the Poincaré-Pontryagin formula

$$M_1(h) = \int_{H=h} \omega_0 dx = \int_{H=h} g(x, y, 0) dx - f(x, y, 0) dy$$

is a complete elliptic integral. Its zeros correspond to limit cycles bifurcating from the corresponding period annulus. It is well known, that in our case the first non-vanishing Melnikov function M_k is a complete elliptic integral, see [25, Corollary 1], and [20, 22], and its general form has been established in formula (23) and Theorem 3 of [25], as a linear combination of complete elliptic integrals.

Our first result is an explicit formula for the second Melnikov function M_2 , under the hypothesis that M_1 is identically zero, see Proposition 3.2.2 and Proposition 3.2.3. The main tool is the Iliev formula for M_2 [32]. Our second result is an estimate for the number of the zeros of M_1 as well as M_2 , Lemma 3.4.2, 3.4.3, 3.4.6, 3.4.7. From this we deduce the maximal cyclicity of the period annuli, when at least M_1 or M_2 does not vanish identically.

This chapter is organized as follows. In section 3.2 we compute the Melnikov functions $M_1(h)$ and $M_2(h)$ (when $M_1(h) \equiv 0$) in the interior and exterior eight-loop case respectively. In section 3.3 we recall some known Picard-Fuchs equations of chapter 2, section 2.3, which will be used later. Finally, in section 3.4 we describe the monodromy of the Abelian integrals, based on the classical Picard-Lefschetz theory, and then apply the so called Petrov trick, to obtain estimates to the number of their zeros in a suitable complex domain.

3.2 Computation of Melnikov Functions

Let $\{\gamma(h)\}_h$ be the continuous family of ovals of the non-perturbed system, where

$$\gamma(h) \subset \{H = h\}$$

with $h \in \Sigma = (h_c, h_s)$ in the interior eight-loop case and $h \in \Sigma = (h_s, +\infty)$ in the exterior eight-loop case, where $h_s = 0$, $h_c = -1/4$ are the critical values of H .

3.2 Computation of Melnikov Functions

Consider the complete elliptic integrals

$$I_i(h) = \begin{cases} I_{\tilde{\omega}_i} = \oint_{\gamma(h)} x^i y dx & \text{if } \Sigma = (h_c, h_s) \\ I_{\tilde{\omega}_i} = \oint_{\gamma(h)} x^i y dx & \text{if } \Sigma = (h_s, +\infty) \end{cases} \quad (3.2)$$

The Abelian integrals I_k , $k \geq 0$, can be expressed as linear combinations of I_0, I_1, I_2 , with coefficients in the field $\mathbb{R}(h)$. In the exterior eight-loop case the symmetry $(x, y) \rightarrow (\pm x, y)$ transforms the oval $\gamma(h)$ to $-\gamma(h)$ which implies that $I_k(h) \equiv 0$ for odd k .

As well known, if we parameterize the displacement map by the Hamiltonian level h , then the following power series expansion holds

$$d(h, \epsilon) = P(h, \epsilon) - h = \epsilon M_1(h) + \epsilon^2 M_2(h) + \dots, h \in \Sigma \quad (3.3)$$

Where $P(h, \epsilon)$ is the first return map, Σ is an open interval depending on the case under consideration. Our first goal will be to calculate explicitly the first Melnikov function M_1 and then M_2 in (3.3). We use the Iliev formula [32].

We denote:

$$f(x, y, 0) = \lambda_{0,1} + \lambda_{1,1}x + \lambda_{2,1}y + \lambda_{3,1}xy + \lambda_{4,1}x^2 + \lambda_{5,1}y^2 + \lambda_{6,1}x^2y + \lambda_{7,1}xy^2 + \lambda_{8,1}x^3 + \lambda_{9,1}y^3 \quad (3.4)$$

$$g(x, y, 0) = \gamma_{0,1} + \gamma_{1,1}x + \gamma_{2,1}y + \gamma_{3,1}xy + \gamma_{4,1}x^2 + \gamma_{5,1}y^2 + \gamma_{6,1}x^2y + \gamma_{7,1}xy^2 + \gamma_{8,1}x^3 + \gamma_{9,1}y^3 \quad (3.5)$$

$$f_\epsilon(x, y, 0) = \lambda_{0,2} + \lambda_{1,2}x + \lambda_{2,2}y + \lambda_{3,2}xy + \lambda_{4,2}x^2 + \lambda_{5,2}y^2 + \lambda_{6,2}x^2y + \lambda_{7,2}xy^2 + \lambda_{8,2}x^3 + \lambda_{9,2}y^3 \quad (3.6)$$

$$g_\epsilon(x, y, 0) = \gamma_{0,2} + \gamma_{1,2}x + \gamma_{2,2}y + \gamma_{3,2}xy + \gamma_{4,2}x^2 + \gamma_{5,2}y^2 + \gamma_{6,2}x^2y + \gamma_{7,2}xy^2 + \gamma_{8,2}x^3 + \gamma_{9,2}y^3 \quad (3.7)$$

We recall, that non-perturbed Hamiltonian system has two bounded (interior) period annuli and one unbounded (exterior) period annulus.

3.2.1 Computation of M_1

3.2.1.1 The interior Duffing oscillator

Proposition 1 *The first Melnikov functions M_1 for the perturbed interior Duffing oscillator have the form*

$$M_1(h) = \alpha_0(h)I_0 + \alpha_1 I_1 + \alpha_2 I_2 \quad (3.8)$$

where

$$\alpha_0(h) = c_0 + c_1 h, \alpha_1 = 2\lambda_{4,1} + \gamma_{3,1}, \alpha_2 = c_2,$$

and

$$c_0 = \lambda_{1,1} + \gamma_{2,1}, c_1 = \frac{4}{7}(\lambda_{7,1} + 3\gamma_{9,1}), c_2 = \gamma_{6,1} + 3\lambda_{8,1} + \frac{1}{7}\lambda_{7,1} + \frac{3}{7}\gamma_{9,1}.$$

Proof It is well known that :

$$M_1(h) = \int_{H=h} \omega_0 = \int_{H=h} g(x, y, 0)dx - f(x, y, 0)dy$$

where

$$\begin{aligned} \int_{H=h} g(x, y, 0)dx &= \int_{H=h} [y(\gamma_{2,1} + \gamma_{3,1}x + \gamma_{6,1}x^2) + y^2(\gamma_{5,1} + \gamma_{7,1}x) + \gamma_{9,1}y^3]dx \\ - \int_{H=h} f(x, y, 0)dy &= - \int_{H=h} [\lambda_{1,1}x + \lambda_{3,1}xy + \lambda_{4,1}x^2 + \lambda_{6,1}x^2y + \lambda_{7,1}xy^2 + \lambda_{8,1}x^3]dy \end{aligned}$$

Or

$$xdy = d(xy) - ydx, \quad xydy = d(x\frac{y^2}{2}) - \frac{y^2}{2}dx, \quad x^2dy = d(x^2y) - 2xydx$$

$$x^2ydy = d(x^2\frac{y^2}{2}) - xy^2dx, \quad xy^2dy = d(x\frac{y^3}{3}) - \frac{y^3}{3}dx, \quad x^3dy = d(x^3y) - 3x^2ydx$$

Therefore we can rewrite $\int_{H=h} \omega$ in the form $\int_{H=h} \omega = \int dQ(x, y, 0) + yq(x, y, 0)dx$ with

$$Q(x, y, 0) = \gamma_{0,1}x + \frac{\gamma_{1,1}}{2}x^2 + \frac{\gamma_{4,1}}{3}x^3 + \frac{\gamma_{8,1}}{4}x^4$$

and

$$\begin{aligned} yq(x, y, 0) &= [(\lambda_{1,1} + \gamma_{2,1}) + (\gamma_{3,1} + 2\lambda_{4,1})x + (\gamma_{6,1} + 3\lambda_{8,1})x^2]y \\ &+ [(\gamma_{5,1} + \frac{\lambda_{3,1}}{2}) + (\lambda_{6,1} + \gamma_{7,1})x]y^2 + (\gamma_{9,1} + \frac{\lambda_{7,1}}{3})y^3. \end{aligned}$$

Then

$$M_1(h) = (\gamma_{2,1} + \lambda_{1,1})I_0 + (\gamma_{3,1} + 2\lambda_{4,1})I_1 + (\gamma_{6,1} + 3\lambda_{8,1})I_2 + (\frac{\lambda_{7,1}}{3} + \gamma_{9,1}) \int_{H=h} y^3 dx.$$

and

$$\int_{H=h} y^3 dx = \int_{H=h} y(2h + x^2 - \frac{x^4}{2})dx = 2hI_0 + I_2 - \frac{I_4}{2} = \frac{12h}{7}I_0 + \frac{3}{7}I_2$$

implies (3.8) \square

3.2.1.2 The exterior Duffing oscillator

Property 3.2.1 *The first Melnikov functions M_1 for the perturbed exterior Duffing oscillator have the form*

$$M_1(h) = \alpha_0(h)I_0 + \alpha_2 I_2 \quad (3.9)$$

where

$$\alpha_0(h) = c_0 + c_1 h, \alpha_2 = c_2$$

$$c_0 = \lambda_{1,1} + \gamma_{2,1}, c_1 = \frac{4}{7}(\lambda_{7,1} + 3\gamma_{9,1}), c_2 = \gamma_{6,1} + 3\lambda_{8,1} + \frac{1}{7}\lambda_{7,1} + \frac{3}{7}\gamma_{9,1}.$$

Proof It is similar to the proof in the exterior case, with the only exception that $I_1 = 0$.

3.2.2 Computation of M_2

If $M_1 = 0$, the Iliev formula [32] for the second Melnikov function $M_2(h)$ reads

$$M_2(h) = \int_{H=h} [G_{1h}(x, y)p_2(x, h) - G_1(x, y)p_{2h}(x, h)]dx$$

$$- \int_{H=h} \frac{F(x, y)}{y} (f_x(x, y, 0) + g_y(x, y, 0))dx$$

$$+ \int_{H=h} g_\epsilon(x, y, 0)dx - f_\epsilon(x, y, 0)dy$$

where

$$F(x, y) = \int_0^y f(x, s, 0)ds - \int_0^x g(s, 0, 0)ds, \quad G(x, y) = g(x, y, 0) + F_x(x, y)$$

and $G_1(x, y)$, $G_2(x, y)$ are the odd and even parts of $G(x, y)$ with respect to y . Thus if

$$G(x, y) = y[(\lambda_{1,1} + \gamma_{2,1}) + (\gamma_{3,1} + 2\lambda_{4,1})x + (\gamma_{6,1} + 3\lambda_{8,1})x^2 + y^2(\gamma_{9,1} + \frac{\lambda_{7,1}}{3})] + y^2[(\gamma_{5,1} + \frac{\lambda_{3,1}}{2}) + (\gamma_{7,1} + \lambda_{6,1})x]$$

then

$$G(x, y) = G_1(x, y) + G_2(x, y), \quad G_1(x, y) = yp_1(x, y^2), \quad G_2(x, y) = p_2(x, y^2)$$

with

$$p_1(x, y^2) = (\lambda_{1,1} + \gamma_{2,1}) + (\gamma_{3,1} + 2\lambda_{4,1})x + (\gamma_{6,1} + 3\lambda_{8,1})x^2 + y^2(\gamma_{9,1} + \frac{\lambda_{7,1}}{3})$$

and

$$p_2(x, y^2) = y^2[(\gamma_{5,1} + \frac{\lambda_{3,1}}{2}) + (\gamma_{7,1} + \lambda_{6,1})x]$$

• $p_2(x, h)$ is the polynomial $p_2(x, h) = \int_0^x p_2(s, 2h + 2U(s))ds = 2hx(\gamma_{5,1} + \frac{\lambda_{3,1}}{2}) + hx^2(\gamma_{7,1} + \lambda_{6,1})$

$$+ \frac{x^3}{3}(\gamma_{5,1} + \frac{\lambda_{3,1}}{2}) + \frac{x^4}{4}(\gamma_{7,1} + \lambda_{6,1}) - \frac{x^5}{10}(\gamma_{5,1} + \frac{\lambda_{3,1}}{2}) - \frac{x^6}{12}(\gamma_{7,1} + \lambda_{6,1})$$

- We note that

$$G_{1h}(x, y) = G_{1y}(x, y)/y = (\lambda_{1,1} + \gamma_{2,1})\frac{1}{y} + (\gamma_{3,1} + 2\lambda_{4,1})\frac{x}{y} + (\gamma_{6,1} + 3\lambda_{8,1})\frac{x^2}{y} + 3y(\gamma_{9,1} + \frac{\lambda_{7,1}}{3}). \quad (3.10)$$

- $g(x, y, 0) = \gamma_{0,1} + \gamma_{1,1}x + \gamma_{4,1}x^2 + \gamma_{8,1}x^3 + y(\gamma_{2,1} + \gamma_{3,1}x + \gamma_{6,1}x^2) + y^2(\gamma_{5,1} + \gamma_{7,1}x) + \gamma_{9,1}y^3$
- $F(x, y) = \int_0^y f(x, s, 0)ds - \int_0^x g(s, 0, 0)ds = \lambda_{0,1}y + \lambda_{1,1}xy - \gamma_{0,1}x + \frac{\lambda_{2,1}}{2}y^2 - \frac{\gamma_{1,1}}{2}x^2 + \frac{\lambda_{3,1}}{2}xy^2 + \lambda_{4,1}x^2y - \frac{\gamma_{4,1}}{3}x^3 + \frac{\lambda_{5,1}}{3}y^3 + \frac{\lambda_{6,1}}{2}x^2y^2 + \frac{\lambda_{7,1}}{3}xy^3 + \lambda_{8,1}x^3y + \frac{\lambda_{9,1}}{4}y^4 - \frac{\gamma_{8,1}}{4}x^4.$

- Then

$$-\frac{F(x,y)}{y} = -\frac{1}{y}(\int_0^y f(x, s, 0)ds - \int_0^x g(s, 0, 0)ds) = -\lambda_{0,1} - \lambda_{1,1}x + \gamma_{0,1}\frac{x}{y} - \frac{\lambda_{2,1}}{2}y + \frac{\gamma_{1,1}}{2}\frac{x^2}{y} - \frac{\lambda_{3,1}}{2}xy - \lambda_{4,1}x^2 + \frac{\gamma_{4,1}}{3}\frac{x^3}{y} - \frac{\lambda_{5,1}}{3}y^2 - \frac{\lambda_{6,1}}{2}x^2y - \frac{\lambda_{7,1}}{3}xy^2 - \lambda_{8,1}x^3 - \frac{\lambda_{9,1}}{4}y^3 + \frac{\gamma_{8,1}}{4}\frac{x^4}{y}.$$

In fact:

$$\int_0^y f(x, s, 0)ds = \lambda_{0,1}y + \lambda_{1,1}xy + \lambda_{2,1}\frac{y^2}{2} + \lambda_{3,1}x\frac{y^2}{2} + \lambda_{4,1}x^2y + \lambda_{5,1}\frac{y^3}{3} + \lambda_{6,1}x^2\frac{y^2}{2} + \lambda_{7,1}\frac{xy^3}{3} + \lambda_{8,1}x^3y + \lambda_{9,1}\frac{y^4}{4}$$

$$\int_0^x g(s, 0, 0)ds = \gamma_{0,1}x + \gamma_{1,1}\frac{x^2}{2} + \gamma_{4,1}\frac{x^3}{3} + \gamma_{8,1}\frac{x^4}{4}$$

3.2.2.1 The interior Duffing oscillator

Lemma 2.3.2 implies easily the linear independence of the functions $I_0(h)$, $hI_0(h)$, $I_1(h)$ and $I_2(h)$. As $I_1 = c(4h - 3)$ then $M_1 = 0$ implies

$$\lambda_{1,1} + \gamma_{2,1} = 0 \quad (3.11)$$

$$\lambda_{7,1} + 3\gamma_{9,1} = 0 \quad (3.12)$$

$$2\lambda_{4,1} + \gamma_{3,1} = 0 \quad (3.13)$$

$$\gamma_{6,1} + 3\lambda_{8,1} = 0 \quad (3.14)$$

Property 3.2.2 *The function $M_2(h)$ has the follows form:*

$$M_2(h) = (\alpha_0 + 4\alpha_1h)I_0 + (\beta_0 + 4h\beta_1)I_1 + \rho I_2 \quad (3.15)$$

where

$$\alpha_0 = -\lambda_{0,1}(\lambda_{3,1} + 2\gamma_{5,1}) + \lambda_{1,2} + \gamma_{2,2}$$

3.2 Computation of Melnikov Functions

$$\alpha_1 = (\lambda_{3,1} + 2\gamma_{5,1})\left(-\frac{1}{7}\lambda_{8,1} - \lambda_{5,1}\right)$$

$$\beta_0 = -(\lambda_{3,1} + 2\gamma_{5,1})(\lambda_{1,1} - \frac{1}{8}\lambda_{7,1}) + 2(\lambda_{6,1} + \gamma_{7,1})(\lambda_{0,1} + 2\lambda_{4,1} - 2\lambda_{7,1}) + 2\lambda_{4,2} + \gamma_{3,2}$$

$$\beta_1 = -\frac{1}{2}\lambda_{7,1}(\lambda_{3,1} + 2\gamma_{5,1}) + 3\lambda_{7,1}(\lambda_{6,1} + \gamma_{7,1})$$

$$\rho = (\lambda_{3,1} + 2\gamma_{5,1})(\lambda_{4,1} - \frac{1}{7}\lambda_{5,1} - \frac{8}{7}\lambda_{8,1}) - 2\lambda_{1,1}(\lambda_{6,1} + \gamma_{7,1}) + \gamma_{6,2} + 3\lambda_{8,2} + \frac{1}{7}\lambda_{7,2} + \frac{3}{7}\gamma_{9,2}.$$

Proof According to the Iliev formula

$$\begin{aligned} M_2 &= \int_{H=h} [G_{1h}(x, y)p_2(x, h) - G_1(x, y)p_{2h}(x, h)]dx \\ &\quad - \int_{H=h} \frac{F(x, y)}{y} (f_x(x, y, 0) + g_y(x, y, 0))dx \\ &\quad + \int_{H=h} g_\epsilon(x, y, 0)dx - f_\epsilon(x, y, 0)dy \end{aligned}$$

where

$$\int_{H=h} g_\epsilon dx - f_\epsilon dy = [\lambda_{1,2} + \gamma_{2,2} + \frac{4}{7}(\lambda_{7,2} + 3\gamma_{9,2})h]I_0 + (2\lambda_{4,2} + \gamma_{3,2})I_1 + [\gamma_{6,2} + 3\lambda_{8,2} + \frac{1}{7}\lambda_{7,2} + \frac{3}{7}\gamma_{9,2}]I_2.$$

By using (3.11), (3.13), (3.14) and (3.15) we have: $p_1(x, y^2) = 0$ then $G_1(x, y) = 0$ and (3.10) becomes zero.

Thus

$$\begin{aligned} M_2(h) &= - \int_{H=h} \frac{F(x, y)}{y} (f_x + g_y)dx + \oint_{H=h} g_\epsilon dx - f_\epsilon dy \\ &= [-\lambda_{0,1}(\lambda_{3,1} + 2\gamma_{5,1}) + \lambda_{1,2} + \gamma_{2,2}]I_0 + [(\lambda_{3,1} + 2\gamma_{5,1})\left(-\frac{1}{7}\lambda_{8,1} - \lambda_{5,1}\right)]4hI_0 \end{aligned}$$

$$+ [-(\lambda_{3,1} + 2\gamma_{5,1})(\lambda_{1,1} - \frac{1}{8}\lambda_{7,1}) + 2(\lambda_{6,1} + \gamma_{7,1})(\lambda_{0,1} + 2\lambda_{4,1} - 2\lambda_{7,1}) + 2\lambda_{4,2} + \gamma_{3,2}]I_1$$

$$+ [-\frac{1}{2}\lambda_{7,1}(\lambda_{3,1} + 2\gamma_{5,1}) + 3\lambda_{7,1}(\lambda_{6,1} + \gamma_{7,1})]hI_1$$

$$+ [(\lambda_{3,1} + 2\gamma_{5,1})(\lambda_{4,1} - \frac{1}{7}\lambda_{5,1} - \frac{8}{7}\lambda_{8,1}) - 2\lambda_{1,1}(\lambda_{6,1} + \gamma_{7,1}) + \gamma_{6,2} + 3\lambda_{8,2} + \frac{1}{7}\lambda_{7,2} + \frac{3}{7}\gamma_{9,2}]I_2. \quad \square$$

3.2.2.2 The exterior Duffing oscillator

In a way similar to the interior Duffing oscillator, we conclude that if $M_1 = 0$ then

$$\lambda_{1,1} + \gamma_{2,1} = 0 \tag{3.16}$$

$$\lambda_{7,1} + 3\gamma_{9,1} = 0 \tag{3.17}$$

$$\gamma_{6,1} + 3\lambda_{8,1} = 0 \tag{3.18}$$

Property 3.2.3 *The function $M_2(h)$ has the follows form:*

$$M_2(h) = (4h + 1)^{-1}[(\alpha_0 + 4\alpha_1 h + \alpha_2 h^2)I_0 + (\beta_0 + 4h\beta_1)I_2] \quad (3.19)$$

where

$$\begin{aligned} \alpha_0 &= -\lambda_{0,1}(\lambda_{3,1} + 2\gamma_{5,1}) + \lambda_{1,2} + \gamma_{2,2} - \gamma_{0,1}(2\lambda_{4,1} + \gamma_{3,1}) \\ \alpha_1 &= -\lambda_{0,1}(\lambda_{3,1} + 2\gamma_{5,1}) + \lambda_{1,2} + \gamma_{2,2} - \frac{4}{7}(\lambda_{5,1}(\lambda_{3,1} + 2\gamma_{5,1})) + \frac{4}{7}(\lambda_{7,2} + 3\gamma_{9,2}) - \frac{8}{7}(\lambda_{8,1}(\lambda_{6,1} + \gamma_{7,1})) + \frac{\gamma_{4,1}}{3}(2\lambda_{4,1} + \gamma_{3,1}) \\ &\quad + \frac{8}{15}(\gamma_{3,1} + 2\lambda_{4,1})(\gamma_{5,1} + \frac{\lambda_{3,1}}{2}) \\ \alpha_2 &= -\frac{4}{7}(\lambda_{5,1}(\lambda_{3,1} + 2\gamma_{5,1})) + \frac{4}{7}(\lambda_{7,2} + 3\gamma_{9,2}) - \frac{8}{7}(\lambda_{8,1}(\lambda_{6,1} + \gamma_{7,1})) \end{aligned}$$

$$\begin{aligned} \beta_0 &= -[2\lambda_{4,1}\lambda_{3,1} + \frac{\lambda_{3,1}\gamma_{3,1}}{2} + 2\lambda_{4,1}\gamma_{5,1} + 2\lambda_{1,1}\lambda_{6,1} + 2\lambda_{1,1}\gamma_{7,1} - \gamma_{6,2} - 3\lambda_{8,2} - \frac{1}{7}\lambda_{7,2} - \frac{3}{7}\gamma_{9,2} \\ &\quad + \frac{\lambda_{5,1}}{7}(\lambda_{3,1} + 2\gamma_{5,1}) + \frac{16}{7}(\lambda_{8,1}(\lambda_{6,1} + \gamma_{7,1})) - 5(2\lambda_{4,1} + \gamma_{3,1})(\frac{\gamma_{4,1}}{3} + \gamma_{0,1}) + \frac{17}{15}(\gamma_{3,1} + 2\lambda_{4,1})(\gamma_{5,1} + \frac{\lambda_{3,1}}{2})] \end{aligned}$$

$$\begin{aligned} \beta_1 &= -[2\lambda_{4,1}\lambda_{3,1} + \frac{\lambda_{3,1}\gamma_{3,1}}{2} + 2\lambda_{4,1}\gamma_{5,1} + 2\lambda_{1,1}\lambda_{6,1} + 2\lambda_{1,1}\gamma_{7,1} - \gamma_{6,2} - 3\lambda_{8,2} - \frac{1}{7}\lambda_{7,2} - \frac{3}{7}\gamma_{9,2} \\ &\quad + \frac{\lambda_{5,1}}{7}(\lambda_{3,1} + 2\gamma_{5,1}) + \frac{16}{7}(\lambda_{8,1}(\lambda_{6,1} + \gamma_{7,1})) - \frac{1}{5}(\gamma_{3,1} + 2\lambda_{4,1})(\gamma_{5,1} + \frac{\lambda_{3,1}}{2})] \end{aligned}$$

Proof The same way of proof of property 3, We use also the formula of Iliev [32]:

$$\begin{aligned} M_2(h) &= \int_{H=h} [G_{1h}(x, y)p_2(x, h) - G_1(x, y)p_{2h}(x, h)]dx \\ &\quad - \int_{H=h} \frac{F(x, y)}{y} (f_x(x, y, 0) + g_y(x, y, 0))dx \\ &\quad + \int_{H=h} g_\epsilon(x, y, 0)dx - f_\epsilon(x, y, 0)dy \end{aligned}$$

By using (3.16), (3.18) and (3.19) we have $p_1(x, y^2) = (\gamma_{3,1} + 2\lambda_{4,1})x$ and (3.10) becomes

$$G_{1h}(x, y) = (\gamma_{3,1} + 2\lambda_{4,1})\frac{x}{y}$$

Then

$$\begin{aligned} \bullet \int_{H=h} [G_{1h}(x, y)p_2(x, h) - G_1(x, y)p_{2h}(x, h)]dx &= -2(\gamma_{3,1} + 2\lambda_{4,1})(\gamma_{5,1} + \frac{\lambda_{3,1}}{2})I_2 \\ + 2h(\gamma_{3,1} + 2\lambda_{4,1})(\gamma_{5,1} + \frac{\lambda_{3,1}}{2})I_2' &+ \frac{1}{3}(\gamma_{3,1} + 2\lambda_{4,1})(\gamma_{5,1} + \frac{\lambda_{3,1}}{2})I_4' - \frac{1}{10}(\gamma_{3,1} + 2\lambda_{4,1})(\gamma_{5,1} + \frac{\lambda_{3,1}}{2})I_6' \end{aligned}$$

3.2 Computation of Melnikov Functions

and by using the Picards-Fuchs equations of chapter 2, section 2.3 (see for instance [16], for more detail) we have

$$\begin{aligned} I_2' &= (4h+1)^{-1}(5I_2 - I_0) \\ I_4' &= (4h+1)^{-1}(4hI_0 + 5I_2) \\ I_6' &= (4h+1)^{-1}\left[\frac{4}{3}(4h+1)I_2 + \frac{4}{3}h(5I_2 - I_0) + \frac{4}{3}(4hI_0 + 5I_2)\right] \end{aligned}$$

Then

$$\begin{aligned} &\int_{H=h} [G_{1h}(x, y)p_2(x, h) - G_1(x, y)p_{2h}(x, h)]dx \\ &= (4h+1)^{-1}(\gamma_{3,1} + 2\lambda_{4,1})(\gamma_{5,1} + \frac{\lambda_{3,1}}{2})\left[\left(\frac{4}{5}h - \frac{17}{15}\right)I_2 - \frac{32}{15}hI_0\right] \end{aligned}$$

$$\int_{H=h} g_\epsilon dx - f_\epsilon dy = [\lambda_{1,2} + \gamma_{2,2} + \frac{4}{7}(\lambda_{7,2} + 3\gamma_{9,2})h]I_0 + [\gamma_{6,2} + 3\lambda_{8,2} + \frac{1}{7}\lambda_{7,2} + \frac{3}{7}\gamma_{9,2}]I_2$$

By using (3.16) we have also

$$(f_x + g_y) = (2\lambda_{4,1} + \gamma_{3,1})x + (\lambda_{3,1} + 2\gamma_{5,1})y + 2(\lambda_{6,1} + \gamma_{7,1})xy$$

Then

$$\begin{aligned} &\bullet - \int_{H=h} \frac{F(x,y)}{y} (f_x + g_y)dx + \oint_{H=h} g_\epsilon dx - f_\epsilon dy \\ &= [-\lambda_{0,1}(\lambda_{3,1} + 2\gamma_{5,1}) + \lambda_{1,2} + \gamma_{2,2}]I_0 \\ &+ \left[-\frac{4}{7}(\lambda_{5,1}(\lambda_{3,1} + 2\gamma_{5,1})) + \frac{4}{7}(\lambda_{7,2} + 3\gamma_{9,2}) - \frac{8}{7}(\lambda_{8,1}(\lambda_{6,1} + \gamma_{7,1}))\right]hI_0 \\ &- \left[2\lambda_{4,1}\lambda_{3,1} + \frac{\lambda_{3,1}\gamma_{3,1}}{2} + 2\lambda_{4,1}\gamma_{5,1} + 2\lambda_{1,1}\lambda_{6,1} + 2\lambda_{1,1}\gamma_{7,1} - \gamma_{6,2} - 3\lambda_{8,2} - \frac{1}{7}\lambda_{7,2} - \frac{3}{7}\gamma_{9,2} + \frac{\lambda_{5,1}}{7}(\lambda_{3,1} + 2\gamma_{5,1})\right. \\ &\left. + \frac{16}{7}(\lambda_{8,1}(\lambda_{6,1} + \gamma_{7,1}))\right]I_2 \\ &+ \gamma_{0,1}(2\lambda_{4,1} + \gamma_{3,1})I_2' + \frac{\gamma_{4,1}}{3}(2\lambda_{4,1} + \gamma_{3,1})I_4' \end{aligned}$$

Or we have $I_2' = (4h+1)^{-1}(5I_2 - I_0)$ and $I_4' = (4h+1)^{-1}(4hI_0 + 5I_2)$.

Then we can obtain by using the above information proposition 2. \square

3.3 Picards-Fuchs equations

We recall the results of chapter 2, section 2.3.

Lemma 3.3.1

The integrals I_i , $i = 0, 2$, satisfy the following system of Picard-Fuchs:

$$I_0(h) = \frac{4}{3}hI_0'(h) + \frac{1}{3}I_2'(h) \tag{3.20}$$

$$I_2(h) = \frac{4}{15}hI_0'(h) + \left(\frac{4}{5}h + \frac{4}{15}\right) I_2'(h) \tag{3.21}$$

Proof See proof of lemma 2.3.1 in chapter 2 for details.

The above equations imply the following asymptotic expansions near $h = 0$ (they agree with the Picard-Lefschetz formula)

Lemma 3.3.2 The integrals I_i , $i = 0, 2$, have the following asymptotic expansions in the neighborhood of $h = 0$:

$$\begin{aligned} I_0(h) &= \left(-h + \frac{3}{8}h^2 - \frac{35}{64}h^3 + \dots\right) \ln h + \frac{4}{3} + a_1h + a_2h^2 + \dots \\ I_2(h) &= \left(\frac{1}{2}h^2 - \frac{5}{8}h^3 - \frac{315}{256}h^4 + \dots\right) \ln h + \frac{16}{15} + 4h + b_2h^2 + \dots \end{aligned}$$

Proof See proof of lemma 2.3.2 in the previous chapter.

3.4 Zeros of Abelian integrals in a complex domain

Our goal will be to find the upper bounds number of the zeroes of the Abelian integrals defined in (3.8) and (3.19) on the interval of existence of the ovals $\{\gamma(h)\}$.

All families of cycles will depend continuously on a parameter h and will be defined without ambiguity in the complex half-plane $h : \text{Im}(h) > 0$. This will allow a continuation on \mathbb{C} along any curve avoiding the real critical values of H .

We use the well known Petrov method which is based on the argument principle. This gives an information on the complex limit cycles of the system in the interior and exterior eight-loop, see later the lemmas 3.4.2, 3.4.6 and 3.4.7, respectively .

Our primary motivation was that the complex methods we use, are necessary to understand the bifurcations from the separatrix eight-loop. Another reason is, that the complexity of the bifurcation set of M_1, M_2 in a complex domain is directly related to the number of the zeros of M_1, M_2 . This observation can be possibly generalized to higher genus curves.

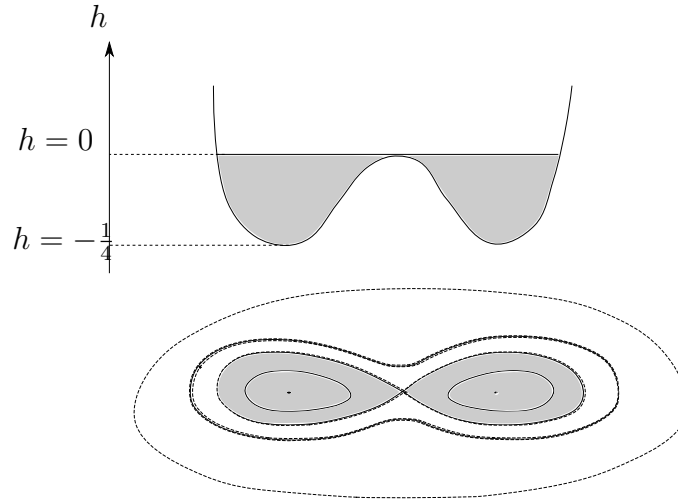


Figure 3.1: Phase portrait of X_h where $-\frac{1}{4} < h < 0$; and the graph of $-\frac{x^2}{2} + \frac{x^4}{4}$

3.4.1 The interior eight-loop case

In this section, we consider the interior eight-loop case, with period annulus as shown in fig.3.1 (hatched part). Let $\gamma(h) \subset \{H = h\}$ be the continuous family of ovals of the non-perturbed system defined on the maximal open interval $\Sigma = (h_c, h_s)$, where for $h = h_c = -\frac{1}{4}$ the oval degenerates into two centers δ_{-1}, δ_1 respectively at the singular point $(-1, 0), (1, 0)$ and for $h = h_s = 0$ every oval δ_{-1} or δ_1 becomes a homoclinic loop of the Hamiltonian $dH = 0$.

The family δ_h represents a continuous family of cycles vanishing at the centers δ_{-1} and δ_1

Theorem 3.4.1 *The maximal cyclicity of the interior period annulus $\{(x, y) \in \mathbb{R}^2 : -\frac{1}{4} < H(x, y) < 0\}$ of $dH = 0$ with respect to one-parameter analytic deformation (3.1) is*

- (i) *three, if $M_1 \neq 0$*
- (ii) *four, if $M_1 = 0$ but $M_2 \neq 0$.*

3.4.1.1 The monodromy of Abelian integrals

The Abelian integrals $I(h)$ of the form (3.2) are multivalued functions in $h \in \mathbb{C}$ which become single-valued analytic functions in the complex domain

$$\mathcal{D} = \mathbb{C} \setminus [0, +\infty).$$

Moreover, along the segment $[0, +\infty)$ the integral $I(h)$ has a continuous limit when $h \in \mathcal{D}$ tends to a point $h_0 \in [0, +\infty)$. Namely, for $h \in \mathcal{D}$, let $\{\gamma(h)\}_h$ be a continuous family of cycles, vanishing at the saddle point as h tends to $h_s = 0$.

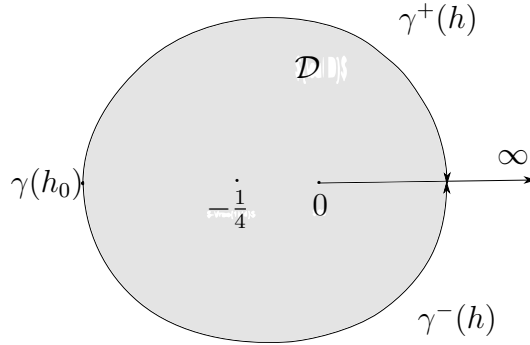


Figure 3.2: The analytic continuation of a cycle $\gamma(h)$ in the domain $\mathcal{D} = \mathbb{C} \setminus [0, +\infty)$

The family $\{\gamma(h)\}_h$ has two analytic complex-conjugate continuations on $(-\infty, 0)$, depending on the way in which the h approaches this segment $[0, +\infty)$. For $h \in (0, +\infty)$ denote $\gamma(h) = \gamma^+(h)$ the limit obtained when $Im(h) > 0$. The cycle $\gamma^-(h)$ is defined in a similar way. It is important to note, the as $I(h)$ is real-analytic on $(-\infty, 0)$, then $\gamma^-(h) = \overline{\gamma^+(\overline{h})}$ for $h \in (0, +\infty)$ (as follows also from the Schwarz reflection principle). Finally, the Picard-Lefschetz formula implies

$$\gamma^+(h) = \gamma^-(h) + \delta_0(h)$$

where $\delta_0(h)$ is a continuous family of cycles vanishing at the saddle point as $h \rightarrow 0$.

3.4.1.2 Zeros of the first return map in a complex domain

Lemma 3.4.2 *The first non-vanishing Poincaré-Pontryagin-Melnikov function (3.8) has at most three zeros in the complex domain \mathcal{D} .*

Lemma 3.4.3 *The second Poincaré-Pontryagin-Melnikov function (3.15) of the first return map has at most four zeros in the complex domain \mathcal{D} .*

3.4 Zeros of Abelian integrals in a complex domain

Proof of lemma 3.4.2 It follows from theorem of Petrov [44]. We sketch the proof:

We denote

$$M_1(h) = \alpha_0(h)I_0(h) + \alpha_1 I_1(h) + \alpha_2 I_2(h) = \oint_{\gamma(h)} \omega = I_\omega(h), h \in \mathcal{D}$$

The monodormy of I_1 is I_1 on the ray $\{0 < h\}$ (because of symmetry). Then $I_1(h) = a + bh = c(4h + 1)$, where $c \in \mathbb{R}$. Indeed, $I_1(h)$ is univalued, of moderate growth, has no poles, vanishes at $h = -1/4$, and grows no faster than h as h tends to infinity. It follows that

$$M_1(h) = \alpha_0(h)I_0(h) + \alpha_2 I_2(h) + c(4h + 1).$$

We shall use the argument principle for analytic functions in the domain

$$\mathcal{D}_R = \mathcal{D} \cap \{|h| \leq R\}$$

as follows. Consider a contour encircling \mathcal{D}_R . The number of zeros of the integral $M_1(h)$ in this domain is the number of rotations of the curve described by $M_1(h)$ about the origin as h describes the contour.

- As h describes the circle $\{|h| = R\}$, for some fixed sufficiently big $R > 0$, the integral $M_1(h)$ behaves as $h^{\frac{7}{4}}$. Thus the increase of the argument of $M_1(h)$ is close to $\frac{7\pi}{2} < 4\pi$.
- Along the cut $[0, \mathbb{R}]$, the number of zeros of $M_1(h)$ about the origin is bounded by the number of zeros of the imaginary part of M_1 , and

$$\text{Im } M_1(h) = \int_{\delta_0(h)} \omega, \text{ where } \delta_0 = \gamma^+ - \gamma^-.$$

Therefore

$$\text{Im } M_1(h) = \alpha_0(h) \oint_{\delta_0(h)} y dx + \alpha_2 \oint_{\delta_0(h)} x^2 y dx, \quad h \in [0, R]$$

and by lemmas 7 and 8 of Petrov[44] cannot exceed 1. We conclude that the total increase of the argument of M_1 along the border of \mathcal{D}_R can not exceed three, which proves Lemma 3.4.2.

□

Proof of Lemma 3.4.3 We denote

$$M_2(h) = (\alpha_0 + 4\alpha_1 h)I_0 + (\beta_0 + 4h\beta_1)I_1 + \rho I_2 = \oint_{\gamma(h)} w = I_w(h), h \in \mathcal{D},$$

where α_i, β_i and ρ are defined in (3.15).

By making use the expression of $I_1 = c(4h - 3)$ Then

$$M_2(h) = \mu(h) + \alpha_0(h)I_0(h) + \alpha_2 I_2(h) + \rho I_2$$

where

$$\alpha_0(h) = \alpha_0 + 4\alpha_1 h$$

$$\begin{aligned} \mu(h) = & 16ch^2\left(-\frac{1}{2}\lambda_{7,1}(\lambda_{3,1} + 2\gamma_{5,1}) + 3\lambda_{7,1}(\lambda_{6,1} + \gamma_{7,1})\right) \\ & + h\left[-12c\left(-\frac{1}{2}\lambda_{7,1}(\lambda_{3,1} + 2\gamma_{5,1}) + 3\lambda_{7,1}(\lambda_{6,1} + \gamma_{7,1})\right) + 4\beta_0\right] - 3\beta_0 \end{aligned}$$

and apply, as in the proof of Lemma 3.4.2, the argument principle to M_2 . The number of zeros of the integral in this domain is the number of rotations of the curve described by $M_2(h)$ about the origin as h describes the border of \mathcal{D}_R .

- As h describes the circle $\{|h| = R\}$; the integral $M_2(h)$ behaves as h^2 and the increase of the argument of $M_2(h)$ is close to 4π .
- Along the cut $(0, R]$, the number of zeros of $M_2(h)$ about the origin is bounded by the number of zeros of the imaginary part of $M_2(h)$ and

$$\text{Im } M_2(h) = \alpha_0(h) \oint_{\delta_0(h)} y dx + (\alpha_2 + \rho) \oint_{\delta_0(h)} x^2 y dx, \quad h \in [0, R].$$

Lemmas 7 and 8 of Petrov[44] imply that the number of the zeros of $\text{Im } M_2(h)$ cannot exceed 1.

Consequently, the total number of circuits cannot exceed three, which implies Lemma 3.4.3 and hence Theorem 3.4.1. \square

3.4.2 The exterior eight-loop case

In this section we consider the exterior eight-loop case, with period annulus as shown in fig.2.2. Let $\gamma(h)_h$ be the continuous family of exterior ovals of the non-perturbed system defined on the maximal open interval $\Sigma = (0, +\infty)$, where

$$\gamma(h) \subset \{H = h\}$$

.

Theorem 3.4.4 *The maximal cyclicity of the exterior period annulus $\{(x, y) \in \mathbb{R}^2 : H(x, y) > 0\}$ of $dH = 0$ with respect to one-parameter analytic deformation (3.1) is*

- (i) two, if $M_1 \neq 0$

3.4 Zeros of Abelian integrals in a complex domain

(ii) four, if $M_1 = 0$ but $M_2 \neq 0$.

Remark 3.4.5 *The above Theorem claims that from any compact, contained in the open exterior period annulus $\{(x, y) \in \mathbb{R}^2 : H(x, y) > 0\}$, bifurcate at most four limit cycles (if $M_2 \neq 0$). It says nothing about the limit cycles bifurcating from the separatrix eight-loop or from infinity (i.e. the equator of the Poincaré sphere).*

3.4.2.1 The monodromy of Abelian integrals

The Abelian integrals $I(h)$ of the form (3.2) are multivalued functions in $h \in \mathbb{C}$ which become single-valued analytic functions in the complex domain

$$\mathcal{D} = \mathbb{C} \setminus [0, -\infty).$$

Along the segment $[0, -\infty)$ the integrals have a continuous limit when $h \in \mathcal{D}$ tends to a point $h_0 \in [0, -\infty)$, depending on the sign of the imaginary part of h . Namely, if $\text{Im}(h) > 0$ we denote the corresponding limit by $I^+(h)$, and when $\text{Im}(h) < 0$ by $I^-(h_0)$. We use a similar notation for the continuous limits of loops $\gamma(h)$ when h tends to the segment $[0, -\infty)$. We have therefore

$$I^\pm(h) = \int_{\gamma^\pm(h)} \omega$$

where ω is a polynomial one-form. The monodromy $I^+(h) - I^-(h)$, $h \in [0, -\infty)$ depends therefore on the monodromy of $\gamma(h)$ which is expressed by the Picard-Lefschetz formula. Namely, for $h \in \mathcal{D}$, define the continuous families of closed loops

$$\delta_0(h), \delta_1(h), \delta_{-1}(h)$$

which vanish at the singular points $(0, 0)$, $(0, 1)$, $(0, -1)$ when h tends to 0 or $-1/4$ respectively, and in such a way that $\text{Im}(h) > 0$, see fig.2.3 (chapter 2). This defines uniquely the homology classes of the loops, up to an orientation. From now on we suppose that the loop $\gamma(h)$ for $h > 0$ is oriented by the vector field X_0 , and that the orientation of $\delta_0(h), \delta_1(h), \delta_{-1}(h)$ are chosen in such a way that

$$\gamma(h) = \delta_0(h) + \delta_1(h) + \delta_{-1}(h), \quad h \in \mathcal{D}.$$

According to the definition of the vanishing cycles

$$\gamma^+(h) = \delta_0^+(h) + \delta_1^+(h) + \delta_{-1}^+(h), \quad h \in (-\infty, 0]. \quad (3.22)$$

and the Picard-Lefschetz formula implies

$$\gamma^-(h) = -\delta_0^+(h) + \delta_1^+(h) + \delta_{-1}^+(h), \quad h \in [-1/4, 0] \quad (3.23)$$

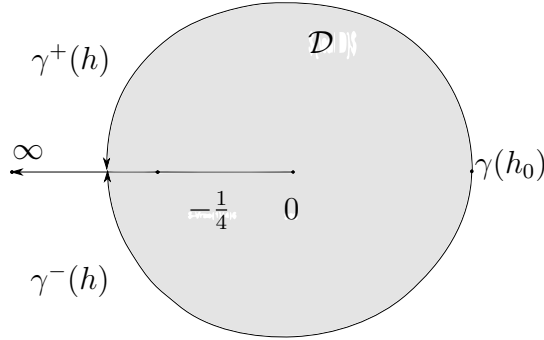


Figure 3.3: The analytic continuation of a cycle $\gamma(h)$ in the domain $\mathcal{D} = \mathbb{C} \setminus [0, -\infty)$

and

$$\gamma^-(h) = -\delta_0^+(h), h \in (-\infty, -1/4] \quad (3.24)$$

For a further use we note that

$$\delta_0^-(h) = \delta_0^+(h), h \in (-1/4, +\infty) \quad (3.25)$$

$$\delta_1^-(h) = \delta_1^+(h), \delta_{-1}^-(h) = \delta_{-1}^+(h), h \in (-\infty, 0) \quad (3.26)$$

Lemma 3.4.6 *The first non-vanishing Poincaré-Pontryagin-Melnikov function (3.8) has at most two zeros in the complex domain \mathcal{D} .*

Lemma 3.4.7 *The second Poincaré-Pontryagin-Melnikov function (3.19) of the first return map has at most four zeros in the complex domain \mathcal{D} .*

Lemma 3.4.8 *The Abelian integrals $I_0(h)$ and $I'_0(h)$ do not vanish in \mathcal{D} .*

Proof of Lemma 3.4.8 $I'_0(h)$ is a period of the holomorphic one-form $\frac{dx}{y}$ on the elliptic curve Γ_h , and therefore does not vanish. For real values of h , $I'_0(h)$ represents the period of the orbit

3.4 Zeros of Abelian integrals in a complex domain

$\gamma(h)$ of $dH = 0$, while $I_0(h)$ equals the area of the interior of $\gamma(h)$. It is remarkable, that $I_0(h)$ does not vanish in a complex domain too. Indeed, consider the analytic function

$$F(h) = \frac{I_0(h)}{I_0'(h)}, h \in \mathcal{D}.$$

We shall count its zeros in \mathcal{D} by making use of the argument principle as the proof of previous lemma (see subsection 3.4.1.2). We recall then the equation 2.22 in which the principle of the argument states that:

$$2\pi Z_D(f) = \text{Var}_{\partial D}(\arg f)$$

Apply now the above formula to the function F in the intersection of a big disc with a radius R and the complex domain \mathcal{D} . Along the circle of radius R , for R sufficiently big, the decrease of the argument of F is close to 2π , while along the branch cut $(-\infty, 0)$ we have

$$\begin{aligned} 2\sqrt{-1}\text{Im}(F(h)) &= F^+(h) - F^-(h) = \frac{I_0(h)}{I_0'(h)} - \frac{\overline{I_0(h)}}{\overline{I_0'(h)}} \\ &= \frac{\oint_{\gamma^+} y dx}{\oint_{\gamma^+} \frac{dx}{y}} - \frac{\oint_{\gamma^-} y dx}{\oint_{\gamma^-} \frac{dx}{y}} = \frac{W(h)}{|\oint_{\gamma^+} \frac{dx}{y}|^2}. \end{aligned}$$

where

$$W(h) = \det \begin{pmatrix} \oint_{\gamma^+} y dx & \oint_{\gamma^+} \frac{dx}{y} \\ \oint_{\gamma^-} y dx & \oint_{\gamma^-} \frac{dx}{y} \end{pmatrix}.$$

According to subsection 3.4.2.1, the function has two different determinations along $(-\infty, -1/4)$ and $(-1/4, 0)$, both of which have no monodromy, and hence are rational in h . In fact, (3.20) implies that $W(h)$ is a non-zero constant. If $W(h) = c$ in $(-\infty, -1/4)$, then it equals $2c$ in $(-1/4, 0)$. Therefore along the branch cut the argument of F^+ or F^- increases by at most π . Summing up the above information, we conclude that F has no zeros in \mathcal{D} . \square

Proof of Lemma 3.4.6 We denote

$$F(h) = \frac{M_1(h)}{I_0(h)} = M_1(h) = \alpha_0(h) + \alpha_2 \frac{I_2(h)}{I_0(h)}, h \in \mathcal{D}$$

We apply, as in the proof of Lemma 3.4.8, the argument principle to F . Along a big circle the increase of the argument of F is close to π . Along the branch cut $(-\infty, 0]$ we have

$$2\sqrt{-1}\text{Im}(F(h)) = F^+(h) - F^-(h) = \alpha_2 \frac{W(h)}{|I_0(h)|^2}$$

where

$$W(h) = \det \begin{pmatrix} \oint_{\gamma^+} y x^2 dx & \oint_{\gamma^+} y dx \\ \oint_{\gamma^-} y x^2 dx & \oint_{\gamma^-} y dx \end{pmatrix} = ch(4h + 1), c = \text{const.} \neq 0.$$

Therefore the imaginary part of $F(h)$ along the branch cut $(-\infty, 0)$ vanishes at most once, at $-1/4$. Summing up the above information, we get that F has at most two zeros in the complex domain \mathcal{D} . \square

Proof of Lemma 3.4.7 We denote

$$F(h) = (4h + 1) \frac{M_2(h)}{I_0(h)}, h \in \mathcal{D},$$

and apply, as in the proof of Lemma 3.4.8, the argument principle to F . By making use of (3.19) we have

$$F(h) = \mu(h) \frac{I_2(h)}{I_0(h)} + \lambda(h) \quad (3.27)$$

where

$$\lambda(h) = \alpha_0 + 4\alpha_1 h + 4\alpha_2 h^2, \quad \mu(h) = \beta_0 + 4\beta_1 h. \quad (3.28)$$

Along a big circle the increase of the argument of F is close to 4π . Along the branch cut $(-\infty, 0]$ we have as before

$$2\sqrt{-1} \operatorname{Im}(F(h)) = F^+(h) - F^-(h) = \mu(h) \frac{W(h)}{|I_0(h)|^2}$$

where

$$W(h) = \det \begin{pmatrix} \oint_{\gamma^+} yx^2 dx & \oint_{\gamma^+} y dx \\ \oint_{\gamma^-} yx^2 dx & \oint_{\gamma^-} y dx \end{pmatrix} = ch(4h + 1), c = \text{const.} \neq 0.$$

Therefore the imaginary part of $F(h)$ along the branch cut $(-\infty, 0)$ vanishes at most two, at $-1/4$ and at the root of $\mu(h)$. Summing up the above information, we get that F has at most four zeros in the complex domain \mathcal{D} . \square

Chapter 4

Study of the Duffing oscillator near a eight-loop

This chapter, studies the cyclicity of eight loop as on fig 4.1 in the spirit of Gavrilov and Iliev [26]. Our main result is that at most two limit cycle can bifurcate from double homoclinic loop (Theorem 4.1.1), although we did not succeed to prove that this bound is exact. It is interesting to note, that even for a generic perturbation (4.1), two limit cycle can appear near a eight-loop, while at the same time the first Melnikov function exhibits only one zero. Hence there is a limit cycle that is not covered by a zero of the related Abelian integral such a limit cycle is called an "alien" limit cycle.

4.1 Introduction

Consider the perturbed Duffing oscillator, which has the following form:

$$X_{\nu,\epsilon} : \begin{cases} \dot{x} = y \\ \dot{y} = x - x^3 + \nu x^2 + \lambda_0 y + \lambda_2 x^2 y \end{cases} \quad (4.1)$$

in which $\lambda_0 = \epsilon \tilde{\lambda}_0$ and $\lambda_2 = \epsilon \tilde{\lambda}_2$; where $\epsilon \ll 1$ and the parameters $\nu, \tilde{\lambda}_0, \tilde{\lambda}_2$ are small reals parameters.

For $\epsilon = \nu = 0$ the system 4.1 is integrable, with the same first integral 2.2 mentioned in the previous chapters

$$H(x, y) = \frac{y^2}{2} - \frac{x^2}{2} + \frac{x^4}{4}$$

We recall that the system 4.1 $|_{\epsilon=0}$ has 2 centers symmetric at $(1, 0)$, $(-1, 0)$ and saddle point at $(0, 0)$.

We get from (2.2) that:

$h_0^s = H(0, 0) = 0$, $h_1^c = H(1, 0) = -\frac{1}{4}$, $h_2^c = h_1^c = H(-1, 0) = -\frac{1}{4}$ and its phase portrait is shown on fig. 2.2.

From Fig. 2.2 (chapter 2)

When $h = h^s$: there exist 2 symmetric homoclinic orbits $\Gamma_{int_i}^{h^s}$ connecting the saddle point $(0, 0)$, we have then the configuration of eight loop Γ_∞ ;

Our main result is the following:

Theorem 4.1.1 *The cyclicity of the eight-loop $\{(x, y) \in \mathbb{R}^2 : H(x, y) = 0\}$ of $dH = 0$ with respect to the perturbation (4.1) is at most equals to two.*

The result will be proved by making use of complex methods, as explained in chapter 2 (see section 2.5), combined with the precise computation of the first or the higher order Poincaré-Pontryagin (or Melnikov) functions, which can be found in chapter 2 (see the equations (2.20) and (2.21)). (see also M. A. Jebrane and A. Mourtada [35]).

4.2 The Petrov trick and the Dulac map

The limit cycles of X_ϵ are the fixed points of P_ϵ . We are going to study these fixed points in a complex domain, where they correspond to complex limit cycles. P_ϵ is obviously a composition of two Dulac maps d_ϵ^\pm as on Fig. 4.1

$$P_\epsilon = d_\epsilon^+ o (d_\epsilon^-)^{-1}$$

Not forgetting that, the power series expansion of the first return map P_ϵ takes for every fixed h the form (1.12)

$$P_\epsilon(h) = h + \epsilon^k M_k(h) + O(\epsilon^{k+1})$$

So the fixed points h of P_ϵ are the zeros of the displacement map $d_\epsilon^+ - d_\epsilon^-$. In a complex domain this map has two singular points corresponding to the saddles S_ϵ^\pm and we shall study its zeros in the complex domain \mathcal{D}_ϵ , shown on Fig. 4.2. This domain is bounded by a circle, by the segment $(S_\epsilon^+, S_\epsilon^-)$, and by the zero locus of the imaginary part of d_ϵ^+ . The number of the zeros of $d_\epsilon^+ - d_\epsilon^-$ in \mathcal{D}_ϵ is computed according to the argument principle: it equals the increase of the argument along the boundary of \mathcal{D}_ϵ .

4.2 The Petrov trick and the Dulac map

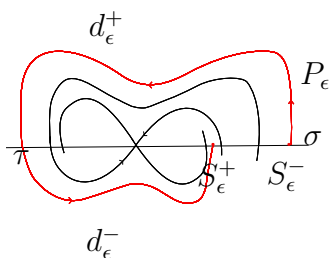


Figure 4.1: Monodromic eight-loop and the Dulac map d_ϵ^\pm

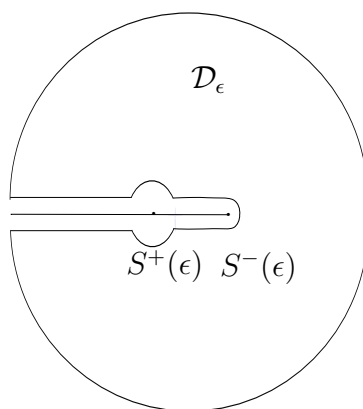


Figure 4.2: The domain \mathcal{D}_ϵ

- Along the circle and far from the critical points, the displacement function is "well" approximated by $\epsilon^k M_k(h)$ which allows one to estimate the increase of the argument.
- Along the segment $(S_\epsilon^+, S_\epsilon^-)$ the zeros of the imaginary part of the displacement function coincide with the fixed points of the holomorphic holonomy map along the separatrix through S_ϵ^- . The zeros are therefore well approximated, similarly to (1.12), by an Abelian integral along the cycle $\delta^-(h)$ in the fibers of H , vanishing at $S^-(0) = (0, 0)$. This observation may be seen as a far going generalization of the so called Petrov trick, see [23] for details.
- Along the zero locus of the imaginary part of d_ϵ^+ , the zeros of imaginary part of the displacement map coincide with the fixed points of the composition of the holonomies associated to the separatrices through S_ϵ^- and S_ϵ^+ . As this map is holomorphic, it is similarly approximated by the zeros of an Abelian integral along $\delta(h)$, where $\delta(h)$ is a cycle in the fibers of H , vanishing at $S(0) = (0, 0)$. Thus, to count the number of the limit cycles, it is enough to recall the Melnikov functions 2.20, 2.21 and see lemma 2.3.2.

4.3 Cyclicity of eight-loop

In this section we prove Theorem 4.1.1.

Let $\delta(h)$ be a continuous family of cycles, vanishing at the saddle point $S(0) = (0, 0)$, with orientations chosen in the same way of d_ϵ^\pm respectively.

The involution $(x, y) \rightarrow (-x, -y)$ leaves the level set $\{H = h\}$ invariant, reversing its orientation. Therefore $\delta^+ = \delta^-$.

We recall that the complete elliptic integrals

$$I_i(h) = \int_{\gamma(h)} \omega_i = \frac{\ln h}{2\pi k} \int_{\delta(h)} \omega_i + P(h)$$

where $\omega_i = x^i y$.

Then the expansion near the critical saddle value $h = 0$ of the complete Abelian integrals $M_1(h)$ (2.20) or $M_k(h)$ (2.20); $k \geq 2$, have by using lemma 2.3.2 (chapter 2) the following form

$$M_k(h) = c_0 + c_1 h \ln h + c_2 h + c_3 h^2 \ln h + \dots \quad (4.2)$$

Let $\mathbf{h}_{\delta^\pm}^\epsilon$ be the two holonomy maps associated to the separatrices of the perturbed foliation, intersecting the cross-section σ . There are two-possible orientations for the loop defining the holonomy, this corresponds to a choice of orientation of δ^\pm . Similarly to (1.12) we have :

4.3 Cyclicity of eight-loop

$$\mathbf{h}_{\delta^+}^\epsilon = h + \epsilon^k M_k^+(h) + O(\epsilon^{k+1}) \quad (4.3)$$

$$\mathbf{h}_{\delta^-}^\epsilon = h + \epsilon^k M_k^-(h) + O(\epsilon^{k+1}) \quad (4.4)$$

$$\mathbf{h}_{\delta^+}^\epsilon \circ \mathbf{h}_{\delta^-}^\epsilon = h + \epsilon^k (M_k^+(h) + M_k^-(h)) + O(\epsilon^{k+1}) \quad (4.5)$$

$$\mathbf{h}_{\delta^-}^\epsilon \circ \mathbf{h}_{\delta^+}^\epsilon = h + \epsilon^k (M_k^-(h) + M_k^+(h)) + O(\epsilon^{k+1}) \quad (4.6)$$

where $M_1(h) = \int_{\delta(h)} \omega|_{\epsilon=0} = \int_{\delta(h)} (\lambda_0 y + \lambda_2 x^2 y) dx$ and $M_k(h) = \int_{\delta(h)} (\lambda_{0k} y + \lambda_{2k} x^2 y + \lambda_{4k} \frac{x^4}{y}) dx$; $k \geq 2$

Property 4.3.1 *If the first Melnikov function is not identically zero, then at most two limit cycles bifurcate from γ .*

Property 4.3.2 *If the first Melnikov function is identically zero:*

- if $\lambda_{0k} \neq 0$, then at most two limit cycles bifurcate from γ
- If $\lambda_{0k} = \lambda_{2k} = 0$ and $\lambda_{4k} \neq 0$ or $\lambda_{0k} = \lambda_{4k} = 0$ and $\lambda_{2k} \neq 0$ then at most four limit cycles bifurcate from γ .

To the end of this section we shall prove property and .

Consider the Dulac maps d_ϵ^+ , d_ϵ^- associated to the perturbed foliation, and to the cross sections σ and τ , see Fig. 4.1. We parameterize each cross-section by the restriction of the first integral f on it, and denote $h = f|_\sigma$. Each function d_ϵ^\pm is multivalued and has a critical point at $S_\epsilon^\pm \in \mathbb{R}$, $S_\epsilon^\pm(0) = 0$. The points S^+ , S^- depend analytically on ϵ . Without loss of generality we shall suppose that $\epsilon > 0$ and $S_\epsilon^- > S_\epsilon^+$, see Fig. 4.2. A limit cycle intersects the cross-section σ at h if and only if $d_\epsilon^+(h) = d_\epsilon^-(h)$. Therefore zeros of the displacement map

$$d_\epsilon^+ - d_\epsilon^- = (d_\epsilon^+ \circ (d_\epsilon^-)^{-1} - id) \circ d_\epsilon^- = (P_\epsilon - id) \circ d_\epsilon^- = \epsilon^k M_k(h) + \epsilon^{k+1} M_{k+1}(h) + \dots \quad (4.7)$$

correspond to limit cycles. Our aim is to bound the number of those zeros. For this, we consider an appropriate complex domain \mathcal{D}_ϵ of the universal covering of $\mathbb{C} \setminus S_\epsilon^\pm$ and compute the number of the zeros of the displacement map, by making use of the argument principle 2.22(chapter 2). The crucial fact is that, roughly speaking, the monodromy of the Dulac map is the holonomy of its separatrix. The analytical counter-part of this statement is that the zero

locus H_ϵ^\pm of the imaginary part of the Dulac map d_ϵ^\pm for $R(h) < S^\pm$ is a real-analytic curve in $\{\mathbb{R}^2 = \mathbb{C}\} \cap \mathcal{D}_\epsilon$, defined in terms of the holonomies of the separatrices. It follows from [[24], section 4] that

$$\begin{aligned} H_\epsilon^+ &= \{z \in \mathbb{C}^2 : \mathbf{h}_{\delta^+}^\epsilon(z) = \bar{z}\} \\ H_\epsilon^- &= \{z \in \mathbb{C}^2 : \mathbf{h}_{\delta^-}^\epsilon(\bar{z}) = z\} \end{aligned}$$

.

Note that the above describes, strictly speaking, only one connected component of H_ϵ^\pm , the second one is "complex conjugate" and defined by a similar formula

$$H_\epsilon^+ = \{z \in \mathbb{C}^2 : \mathbf{h}_{\delta^+}^\epsilon(\bar{z}) = z\}, H_\epsilon^- = \{z \in \mathbb{C}^2 : \mathbf{h}_{\delta^-}^\epsilon(z) = \bar{z}\}.$$

By abuse of notation we use H_ϵ^\pm to denote only the first connected component (the second corresponds to the opposite orientation of δ^\pm).

The analyticity of the above curves is crucial in computing the complex zeros of the transcendental Dulac maps. For instance, to compute the number of intersection points of H_ϵ^\pm with the real axis $\{z = \bar{z}\}$ we have to solve the equation

$$\mathbf{h}_{\delta^\pm}^\epsilon(z) = z \tag{4.8}$$

and to compute the number of the intersection point of H_ϵ^- with H_ϵ^+ , we have to solve the equation

$$\mathbf{h}_{\delta^-}^\epsilon \circ \mathbf{h}_{\delta^+}^\epsilon(z) = z. \tag{4.9}$$

Let us define first the complex domain \mathcal{D}_ϵ in which the computation will take place: it is bounded by the circle

$$S_R = \{h : |h| = R\}$$

by the interval $[S^+(\epsilon), S^-(\epsilon)]$, and by the zero locus H_ϵ^+ , as it is shown on Fig. 4.2.

We wish to bound the number of the zeros of the displacement map in the domain \mathcal{D}_ϵ . If the map were an analytic function in a neighborhood of the closure of the domain, and non-vanishing on its border, we could apply the argument principle (see 2.22) :

The number of the zeros (counted with multiplicity) in the complex domain \mathcal{D}_ϵ equals the increment of the argument of this function along the border of \mathcal{D}_ϵ , divided by 2π .

4.3 Cyclicity of eight-loop

The above principle holds true with the analyticity condition relaxed: it is enough that the map allows a continuation on the closure of the domain \mathcal{D}_ϵ , considered as a subset of the universal covering of

$$\mathbb{C} \setminus [S^+(\epsilon), S^-(\epsilon)]$$

This is indeed the case, and it remains to assure finally the non-vanishing property. Along S_R the displacement map has a known asymptotic behavior and hence does not vanish. Along the remaining part of the border, including $S^\pm(\epsilon)$ the displacement map can have isolated zeros. For this we may add to the displacement map a small real constant $c > 0$, sufficiently smaller with respect to ϵ . The new function $d_\epsilon^+ - d_\epsilon^- + c$ which we obtain in this way has at least so many zeros in \mathcal{D}_ϵ , as the original displacement map, but is non-vanishing on the border of the domain. The increase of the argument of $d_\epsilon^+ - d_\epsilon^- + c$ along S_R will be close to the increase of the argument of $d_\epsilon^+ - d_\epsilon^-$ (because $c \ll \epsilon$). At last, the imaginary parts $d_\epsilon^+ - d_\epsilon^-$ and $d_\epsilon^+ - d_\epsilon^- + c$ are the same. The intuitive content of this is that when the displacement map has zeros on the border of the domain, it will have less zeros in the interior of the domain.

To resume, according to the argument principle, to evaluate the number of the zeros of the displacement map in the domain \mathcal{D}_ϵ , it is enough to evaluate:

- The increase of the argument of the displacement map, along the circle S_R .
- The number of the zeros of the imaginary part of the displacement map, along the interval $[S^+(\epsilon), S^-(\epsilon)]$.
- The number of the zeros of the imaginary part of the displacement map, along the real analytic curve H_ϵ^+ .

4.3.1 The case $M_1 \neq 0$

According to the above we conclude that:

- The displacement map along the circle S_R is approximated by ϵM_1 which has as a leading term $h \ln h$ (because if $c_0 = 0$ then $c_1 \neq 0$). The increase of the argument of $h \ln h$, and hence of the displacement map, along the circle S_R is close to 2π but strictly less than 2π .

Then the number of the zeros of ϵM_1 is at most equals to once .

- The imaginary part of the displacement map, along the interval $[S^+(\epsilon), S^-(\epsilon)]$ equals the imaginary part of $d_\epsilon^-(h)$. Its zeros equal the number of intersection points of H_ϵ^+ with the real axes, which amounts to solve $\mathbf{h}_{\delta^-}^\epsilon(z) = z$, see(4.8).

By (4.4) the number of the zeros is bounded by the multiplicity of the holomorphic Abelian integral $M_1^-(h) = \int_{\delta^-(h)} \omega_0$ having a simple zero at the origin. Note, however, that the holonomy map $\mathbf{h}_{\delta^-}^\epsilon$ has $S^-(\epsilon)$ as a fixed point (a zero). Therefore the imaginary part of the displacement map does not vanish along the open interval $[S^+(\epsilon), S^-(\epsilon)]$.

- The number of the zeros of the imaginary part of the displacement map, along the real analytic curve H_ϵ^+ equals the number of the zeros of the imaginary part of $d_\epsilon^-(h)$ along this curve, that is to say the number of intersection points of this curve with H_ϵ^- . According to (4.9), (4.6), this number is bounded by the multiplicity of the holomorphic Abelian integral $M_1(h) = \int_{\delta^+(h)} \omega_0 + \int_{\delta^-(h)} \omega_0 =^\infty 2 \int_{\delta^+(h)} \omega_0 = c_1 h + c_3 h^2 + \dots$. Then this number is one .

We conclude that the displacement map can have at most two zeros in the domain \mathcal{D}_ϵ .

This completes the proof of Property 4.3. \square

4.3.2 The case $M_1 = 0$

In this section we suppose that the Melnikov function $M_1(h)$ vanishes identically.

Following the method of the preceding subsection, we evaluate the number of the zeros of the displacement map 4.7 in the domain \mathcal{D}_ϵ .

- Along the circle S_R

- If $\lambda_{0k} \neq 0$

The displacement map is approximated by $\epsilon^k M_k$ which has as a leading term: $h \ln h$ as (because if $c_0 = 0$ then $c_1 \neq 0$) in the expansion of the first Melnikov function 4.2, see Lemma2.3.2. The increase of the argument of $h \ln h$, and hence of the displacement map, along the circle S_R is close to 2π but strictly less than 2π .

Then the number of the zeros of $\epsilon^k M_k$ is at most equals to once .

- If $\lambda_{0k} = \lambda_{2k} = 0$ and $\lambda_{4k} \neq 0$ or $\lambda_{0k} = \lambda_{4k} = 0$ and $\lambda_{2k} \neq 0$

The displacement map is approximated by $\epsilon^k M_k$ which has as a leading term $h^2 \ln h$ (as $c_1 \neq 0$ and $c_3 \neq 0$) in the expansion of the first Melnikov function 4.2, see Lemma2.3.2. The increase of the argument of $h^2 \ln h$, and hence of the displacement map, along the

4.4 Detecting alien limit cycles near a eight-loop

circle S_R is close to $2 * 2\pi$ but strictly less than 4π .

Then the number of the zeros of $\epsilon^k M_k$ is at most equals to two.

- The imaginary part of the displacement map, along the interval $[S^+(\epsilon), S^-(\epsilon)]$ equals the imaginary part of $d_\epsilon^-(h)$. Its zeros equal the number of intersection points of H_ϵ^+ with the real axes, which amounts to solve $\mathbf{h}_{\delta^-}^\epsilon(z) = z$, see(4.8). By (4.4) the number of the zeros is bounded by the multiplicity of the holomorphic Abelian integral $M_d^-(h) = \int_{\delta^-(h)} \omega_k$ having a zero at the origin. Note, however, that the holonomy map $\mathbf{h}_{\delta^-}^\epsilon$ has $S^-(\epsilon)$ as a fixed point (a zero), and hence the cyclicity of the saddle point is zero. We conclude that the imaginary part of the displacement map does not vanish along the open interval $[S^+(\epsilon), S^-(\epsilon)]$.

- The number of the zeros of the imaginary part of the displacement map, along the real analytic curve H_ϵ^+ equals the number of the zeros of the imaginary part of $d_\epsilon^-(h)$ along this curve, that is to say the number of intersection points of this curve with H_ϵ^- . According to (4.9), (4.6)

this number is bounded by:

- If $\lambda_{0k} \neq 0$

This number is bounded by the cyclicity of $c_1 h + c_3 h^2 + \dots$

Then this number is one .

- If $\lambda_{0k} = \lambda_{2k} = 0$ and $\lambda_{4k} \neq 0$ or $\lambda_{0k} = \lambda_{4k} = 0$ and $\lambda_{2k} \neq 0$

This number is bounded by the cyclicity of $c_3 h^2 + \dots$

Then this number is two .

If the first non-vanishing Melnikov function $M_k(h)$, $k \geq 2$ is as 2.21, we conclude that:

- If $\lambda_{0k} \neq 0$

The displacement map can have at most two zeros in the domain \mathcal{D}_ϵ .

- If $\lambda_{0k} = \lambda_{2k} = 0$ and $\lambda_{4k} \neq 0$ or $\lambda_{0k} = \lambda_{4k} = 0$ and $\lambda_{2k} \neq 0$

The displacement map can have at most four zeros in the domain \mathcal{D}_ϵ .

This completes the proof of Property 4.3. \square

4.4 Detecting alien limit cycles near a eight-loop

The first return map of $X_{0,\epsilon}$ takes the form

$$h \mapsto h + \epsilon \int_{\gamma(h)} P(x, y, \lambda) dx + O(\epsilon^2)$$

where $\int_{\gamma(h)} P(x, y, \lambda)dx$ is the first return Poincaré-Pontryagin function associated to $X_{0,\epsilon}$, we have by using the lemma 3.3.2

$$\int_{\gamma(h)} P(x, y, \lambda)dx = d_0(\lambda) + d_1(\lambda_0)h \ln h + d_2(\lambda)h^2 \ln h + O(h)$$

where $d_0(0) = 0$, $d_1(0) \neq 0$. It follows that for sufficiently small $\|\lambda\|$, $|h|$, the Poincaré-Pontryagin function $\int_{\gamma(h)} P(x, y, \lambda)dx$ has at most one zero. The purpose of this section is to show that the number of the limit cycles, which bifurcate from Γ , exceeds the number of the zeros of $\int_{\gamma(h)} P(x, y, \lambda)dx$ near $h = 0$. The "missing" second limit cycle, which does not correspond to a zero is an alien limit cycle. This is a new unexpected phenomenon in the bifurcation theory of vector fields, discovered recently by Caubergh, Dumortier and Roussarie [10, 17].

Property 4.4.1 *The cyclicity of the eight-loop $Cycl(\Gamma, X_{0,\epsilon})$ with respect to the deformed vector field $X_{\nu,\epsilon}$ (4.1) is equals to two .*

Note that, according to proposition 4.3, the cyclicity is at most two.

Proof We shall follow closely [17].section 6.2. The trace σ of the vector field $X_{0,\epsilon}$ at the saddle point determine "is stability". As the coordinates of the saddle point satisfy

$$x = O(\epsilon), y = O(\epsilon)$$

then for the trace σ at the saddle point we get

$$\sigma = \lambda_0\epsilon + O(\epsilon^2)$$

For small ϵ and a general perturbation (non symmetric perturbation), the connections of the eight-loop $\Gamma_{1,2}$ will be broken. The distance between the two branches (stable and unstable separatrix) of the broken connection can be measured on a segment, transverse to Γ_1 or Γ_2 . Let us denote these distances (or shift functions) by $b_{1,2}$. It is well known that the shift functions are analytic functions in ϵ , λ , and if we use the restriction of H to the transverse segments as a local parameter h , then

$$b_i(\epsilon, \lambda) = \epsilon \int_{\Gamma_i} w_\lambda + O(\epsilon^2), i = 1, 2$$

With the notations above we compute

$$\int_{\Gamma_1} ydx = c_1 \neq 0$$

$$\int_{\Gamma_2} ydx = d_1 \neq 0$$

4.4 Detecting alien limit cycles near a eight-loop

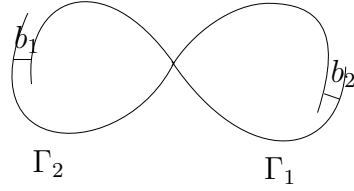


Figure 4.3: Non symmetric perturbation of the eight-loop.

$$\int_{\Gamma_1} x^2 y dx = c_2$$

$$\int_{\Gamma_2} x^2 y dx = d_2$$

i.e. (In case of non symmetric perturbation)

$$c_1 \neq d_1$$

$$c_2 \neq d_2$$

and therefore

$$\int_{\Gamma_1} w_\lambda = \lambda_0 c_1 + \lambda_2 c_2$$

$$\int_{\Gamma_2} w_\lambda = \lambda_0 d_1 + \lambda_2 d_2$$

It is immediately seen that

- for every sufficiently small $\epsilon \neq 0$ and $\|\lambda\|$

$$\det \begin{pmatrix} c_1 & c_2 \\ d_1 & d_2 \end{pmatrix} \neq 0.$$

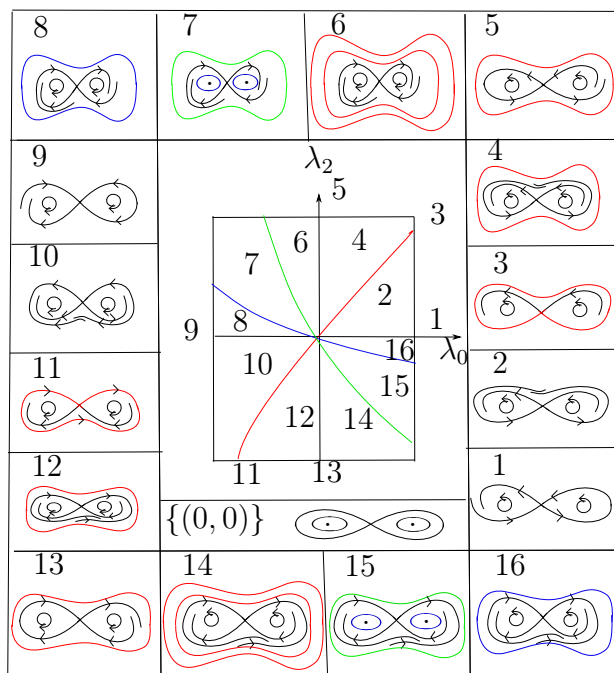


Figure 4.4: Bifurcation diagram of the first Melnikov function, containing an eight-loop. The domain 14 has two limit cycles.

Under these conditions, the bifurcation diagram of limit cycles near the eight loop $\Gamma = \Gamma_1 \cup \Gamma_2$ was computed, see fig. 4.4. It follows that the cyclicity of the eight-loop Γ under the perturbation (4.1) is equals to two. \square

Remark 4.4.2 *The proof of this proposition can be deduced by used the Hopf Poincaré-Bendixon theorem, which is illustrated on fig. 4.4*

Bibliography

- [1] V.I. Arnold, Loss of stability of self-oscillations close to resonance and versal deformations of equivariant vector fields, *Functional Anal. Appl.* **11**, 85–92 (1977).
- [2] V.I. Arnold, Geometric Methods in the Theory of Ordinary Differential Equations. *Springer, New York* (1983).
- [3] V.I. Arnold, S.M. Gusein-Zade, A.N. Varchenko, *Singularities of Differentiable Maps*, vols. **1** and **2**, Monographs in mathematics, Birkhäuser, Boston, (1985) and (1988).
- [4] J. C. Artés, J. Libre and D. Schlomiuk, The geometry of quadratic differential systems with a weak focus of second order. *Inter. J. Bifur. and Chaos.* **16**, 3127–3194 (2006).
- [5] N.N. Bautin, On the number of limit cycles which appear with the variation of coefficients from an equilibrium position of focus or center type. *Mat. Sb. (N. S.)* **30**(72), 181–196 (1952).
- [6] B. Ben Hamed, A. Gargouri, L. Gavrilov, Cubic Perturbations of Symmetric elliptic Hamiltonians of degree four in a Complex domain. Accepted in *Bull. Sci. Math.* (2015).
- [7] B. Ben Hamed, A. Gargouri, L. Gavrilov, Perturbations of symmetric elliptic Hamiltonians of degree four in a complex domain, *J. Math. Anal. Appl.* **424**, 774–784 (2015).
- [8] G.I Binyamini, D. Novikov, S. Yakovenko. On the number of zeros of abelian integrals. *Invent. Math.* **181**(2), 227–289 (2010).
- [9] M. Bobiński, P. Mardesic, D. Novikov, Pseudo-Abelian integrals: unfolding generic exponential. *J. Differential Equations.*, **247**(12) , 3357–3376, (2009).
- [10] M. Caubergh, F. Dumortier, R. Roussarie, Alien limit cycle near a Hamiltonian 2-saddle cycle. *C. R. Math. Acad. Sci. Paris.* **340**(8) , 587–592 (2005).
- [11] L.S. Chen, M.S. Wang, The relative position, and the number, of limit cycles of a quadratic differential system. *Acta Math. Sin.* **22**, 751–758 (1979).
- [12] F. Chen, C. Li, J. libre, Z. Zhang, A unified proof on the weak Hilbert 16th problem for $n = 2$. *J. Diff. Eqns.* **221**, 309–342 (2006).

- [13] C.J. Christopher, N.G. Lloyd, Polynomial systems: a lower bound for the Hilbert numbers. *Proc. R. Soc. Lond. A* **450**, 219–224 (1995).
- [14] S.-N. Chow, C. Li, Y. Yi, The cyclicity of period annulus of degenerate quadratic Hamiltonian system with elliptic segment. *Ergod. Theory Dyn. Syst.* **22(4)**, 1233–1261 (2002).
- [15] B. Coll, C. Li, R. Prohens, Quadratic Perturbations of a class of Quadratic Reversible Systems with two Centers. *Discrete and Continuous Dynamical Systems.* **24**, Number **3**, July (2009).
- [16] P. Deligne, Équations différentielles à point singuliers réguliers. *Lect. Notes Maths.* **163**, Springer-verlag (1970).
- [17] F. Dumortier, R. Roussarie, Abelian integrals and limit cycles. *J. Differential Equations.* **227(1)**, 116–165, (2006).
- [18] J.P. Françoise, Successive derivatives of a first return map, application to the study of quadratic vector field. *Ergodic Theo. Dyn. Syst.* **16**, 87–96 (1996).
- [19] L. Gavrilov, Petrov modules and zeros of Abelian integrals. *Bull. Sci. Math.*, **122** (8), 571–584, (1998).
- [20] L. Gavrilov, Abelian integrals related to Morse polynomials and perturbations of plane Hamiltonian vector fields. *Ann. Inst. Fourier (Grenoble)*, **49(2)**, 611–652, (1999).
- [21] L. Gavrilov, The infinitesimal 16th Hilbert problem in the quadratic case. *Invent. Math.* **143** (3), 449–497 (2001).
- [22] L. Gavrilov, Higher order Poincaré-Pontryagin functions and iterated path integrals, *Ann. Fac. Sci. Toulouse Math. (6)*, **14(4)** 663–682, (2005).
- [23] L. Gavrilov, On the number of limit cycles which appear by perturbation of two-saddle cycles of planar vector fields, arXiv:1106.0857 [math.DS], (2011).
- [24] L. Gavrilov, On the number of limit cycles which appear by perturbation of Hamiltonian two-saddle cycles of planar vector fields, *Bull. Braz. Math. Soc.(N.S.)*, **42(1)**:1-23, (2011).
- [25] L. Gavrilov, I.D. Iliev, The displacement map associated to polynomial unfoldings of planar Hamiltonian vector fields. *Amer. J. Math.* **127**, 1153–1190 (2005).
- [26] L. Gavrilov, I.D. Iliev, Perturbations of quadratic Hamiltonian two-saddle cycles. *Ann. I. H. Poincaré - AN* **32**, 307–324 (2015).

BIBLIOGRAPHY

- [27] L. Gavrilov, I.D. Iliev, Cubic perturbations of elliptic Hamiltonian vector fields of degree three. <http://arxiv.org/abs/1406.0208>, Submitted on 1 Jun 2014.
- [28] M. Han, D. Shang, Z. Wang, P. Yu, Bifurcation of limit cycles in a 4th-order near-Hamiltonian systems. *Int. J. Bifurc. Chaos* **17**(11) (2007).
- [29] D. Hilbert. Mathematical problems. *Bull. A. M. S.*, **8**, 437–479 (1902).
- [30] D. Hilbert, Mathematical problems (M. Newton, transl.). *Bull. Am. Math. Soc.* **8**, 437–479 (1902), reprinted in *Bull. Am. Math. Soc. (N. S.)*, **37**, 407–436 (2000).
- [31] E. Horzov, I.D. Iliev, On the number of limit cycles in perturbations of quadratic Hamiltonian systems. *Proc. London Math. Soc.* **69**, 198–224 (1994).
- [32] I.D. Iliev, On second order bifurcations of limit cycles. *J. London Math. Soc.* **58** (2), 353–366 (1998).
- [33] I.D. Iliev, L.M. Perko, Higher order bifurcations of limit cycles. *J. Differential Eq.* **154**, 339–363 (1999).
- [34] J. M. Jebrane, H. Żoładek, Abelian integrals in nonsymmetric perturbation of symmetric Hamiltonian vector field. *Adv. in Appl. Math.*, **15**(1), 1–12, (1994).
- [35] M. A. Jebrane, A. Mourtada, Cyclicité finie des lacets double non triviaux. *Non linearity* **7**, 1349–1365, (1994).
- [36] A. G. Khovansky, Real analytic manifolds with tiniteness properties and complex abelian integrals, *Functional Anal. Appl.* **18**, 119–128 (1984).
- [37] J. Li, C.F. Li, Planar cubic Hamiltonian systems and distribution of limit cycles of (E3). *Acta Math. Sin.* **28**, 509–521 (1985).
- [38] C. Li, Estimate of the number of zeros of Abelian integrals for an elliptic Hamiltonian with figure-of-eight loop. *Nonlinearity*. **16**, 1151–1163 (2003).
- [39] J. Li, M.Q. Zhang, Bifurcations of limit cycles in a Z_8 -equivariant planar vector field of degree 7. *J. Differ. Equ. Dyn. Syst.* **16**(4), 1123–1139 (2004).
- [40] C. Li, P. Mardešić, R. Roussarie, Perturbations of symmetric elliptic Hamiltonians of degree four. *J. Differential Eq.* **231**, 78–91 (2006).
- [41] C. Li, L. Liu, J. Yang, A cubic system with thirteen limit cycles. *J. Differ. Equ.* **246**, 3609–3619 (2009).

- [42] J. Llibre, G. Rodríguez, Configurations of limit cycles and planar polynomial vector fields. *J. Differ. Equ.* **198**(2), 374–380 (2004).
- [43] L. Perko, *Differential equations and dynamical systems*. Second Edition. Springer-Verlag, New York, Berlin, Heidelberg, (2001).
- [44] G.S. Petrov, Complex zeros of an elliptic integral. *Funct. Anal. Appl.* **18-23**, 87–128 (1984-1987).
- [45] G.S. Petrov, Elliptic integrals and their non-oscillatoriness. *Funct. Anal. Appl.* **20**, 46–49 (1986).
- [46] G.S. Petrov, Nonoscillatoriness of elliptic integrals. *Funct. Anal. Appl.* **24**, 45–50 (1990).
- [47] H. Poincaré, *Les Méthodes Nouvelles de la Mécanique Céleste* (1892–1899).
- [48] C. Rousseau, H. Żołądek, Zeroes of complete elliptic integrals for 1 : 2 resonance. *J. Differential Eq.* **94**, 41–54 (1991).
- [49] S. Shi, A concrete example of the existence of four limit cycles for plane quadratic systems. *Sci. Sin.* **11**, 1051–1056 (1979) (in Chinese); **23**, 153–158 (1980) (in English).
- [50] A. N. Varchenko, Estimate of the number of zeroes of abelian integrals depending on parameters and limit cycles. *Functional Anal. Appl.* **18**, 98–108 (1984).
- [51] A.N. Varchenko, V.I. Arnold, S.M. Gusein-Zade, Singularities of Differentiable Maps. *Monogr.Math.Birkhuser, Bosten.* volume **II Monodromy and Asymptotic Integrals** (1988).
- [52] S. Wang, P. Yu, Bifurcation of limit cycles in a quintic Hamiltonian system under sixth-order perturbation. *Chaos Solitons Fractals* **26**(5), 1317–1335 (2005).
- [53] S. Wang, P. Yu, Existence of 121 limit cycles in a perturbed planar polynomial Hamiltonian vector field of degree 11. *Chaos Solitons Fractals.* **30**(3), 606–621 (2006).
- [54] S.Wang, P. Yu, J. Li, Bifurcation of limit cycles in Z_{10} -equivariant vector fields of degree 9. *Int.J. Bifurc. Chaos* **16**(8), 2309–2324 (2006).
- [55] W. Yao, P. Yu, Bifurcation of small limit cycles in Z_5 -equivariant planar vector fields of order 5. *J. Math. Anal. Appl.* **328**(1), 400–413 (2007).
- [56] Z. Zhang, C. li, On the number of limit cycles of a class of quadratic Hamiltonian systems under quadratic perturbations. *Adv.Math.* **26**, 445–460 (1997).